

UCSF

UC San Francisco Previously Published Works

Title

A SARS-CoV-2 protein interaction map reveals targets for drug repurposing

Permalink

<https://escholarship.org/uc/item/1ch8v2qc>

Journal

Nature, 583(7816)

ISSN

0028-0836

Authors

Gordon, David E
Jang, Gwendolyn M
Bouhaddou, Mehdi
[et al.](#)

Publication Date

2020-07-16

DOI

10.1038/s41586-020-2286-9

Peer reviewed

A SARS-CoV-2-Human Protein-Protein Interaction Map Reveals Drug Targets and Potential Drug-Repurposing

David E. Gordon^{1,2,3,4}, Gwendolyn M. Jang^{1,2,3,4}, Mehdi Bouhaddou^{1,2,3,4}, Jiewei Xu^{1,2,3,4}, Kirsten Obernier^{1,2,3,4}, Matthew J. O'Meara⁵, Jeffrey Z. Guo^{1,2,3,4}, Danielle L. Swaney^{1,2,3,4}, Tia A. Tummino^{1,2,6}, Ruth Huettenhain^{1,2,3,4}, Robyn Kaake^{1,2,3,4}, Alicia L. Richards^{1,2,3,4}, Beril Tutuncuoglu^{1,2,3,4}, Helene Foussard^{1,2,3,4}, Jyoti Batra^{1,2,3,4}, Kelsey Haas^{1,2,3,4}, Maya Modak^{1,2,3,4}, Minkyu Kim^{1,2,3,4}, Paige Haas^{1,2,3,4}, Benjamin J. Polacco^{1,2,3,4}, Hannes Braberg^{1,2,3,4}, Jacqueline M. Fabius^{1,2,3,4}, Manon Eckhardt^{1,2,3,4}, Margaret Soucheray^{1,2,3,4}, Melanie J. Bennett^{1,2,3,4}, Merve Cakir^{1,2,3,4}, Michael J. McGregor^{1,2,3,4}, Qiongyu Li^{1,2,3,4}, Zun Zar Chi Naing^{1,2,3,4}, Yuan Zhou^{1,2,3,4}, Shiming Peng^{1,2,6}, Ilsa T. Kirby^{1,4,7}, James E. Melnyk^{1,4,7}, John S. Chorba^{1,4,7}, Kevin Lou^{1,4,7}, Shizhong A. Dai^{1,4,7}, Wenqi Shen^{1,4,7}, Ying Shi^{1,4,7}, Ziyang Zhang^{1,4,7}, Inigo Barrio-Hernandez⁸, Danish Memon⁸, Claudia Hernandez-Armenta⁸, Christopher J.P. Mathy^{1,9,10,2}, Tina Perica^{1,2,9}, Kala B. Pilla^{1,2,9}, Sai J. Ganesan^{1,2,9}, Daniel J. Saltzberg^{1,2,9}, Rakesh Ramachandran^{1,2,9}, Xi Liu^{1,2,6}, Sara B. Rosenthal¹¹, Lorenzo Calviello¹², Srivats Venkataraman¹², Jose Liboy-Lugo¹², Yizhu Lin¹², Stephanie A. Wankowicz^{1,13,9}, Markus Bohn⁶, Phillip P. Sharp^{1,2,4}, Raphael Trenker¹⁴, Janet M. Young¹⁵, Devin A. Cavero³, Joseph Hiatt^{16,3}, Theodore L. Roth^{16,3}, Ujjwal Rathore³, Advait Subramanian^{1,17}, Julia Noack^{1,17}, Mathieu Hubert¹⁸, Ferdinand Roesch¹⁹, Thomas Vallet¹⁹, Björn Meyer¹⁹, Kris M. White²⁰, Lisa Miorin²⁰, Oren S. Rosenberg^{21,22,23}, Kliment A Verba^{1,2,6}, David Agard^{1,24}, Melanie Ott^{3,21}, Michael Emerman²⁵, Davide Ruggero^{26,27,4}, Adolfo García-Sastre²⁰, Natalia Jura^{1,14,4}, Mark von Zastrow^{1,1,4,28}, Jack Taunton^{1,2,4}, Alan Ashworth^{1,27}, Olivier Schwartz¹⁸, Marco Vignuzzi¹⁹, Christophe d'Enfert²⁹, Shaeri Mukherjee^{1,17}, Matt Jacobson⁶, Harmit S. Malik¹⁵, Danica G. Fujimori^{1,4,6}, Trey Ideker³⁰, Charles S. Craik^{6,27}, Stephen Floor^{12,27}, James S. Fraser^{1,2,9}, John Gross^{1,2,6}, Andrej Sali^{1,2,6,9}, Tanja Kortemme^{1,9,10,2}, Pedro Beltrao⁸, Kevan Shokat^{1,4,7}, Brian K. Shoichet^{1,2,6}, Nevan J. Krogan^{1,2,3,4}

¹QBI COVID-19 Research Group (QCRG), San Francisco, CA, 94158, USA

²University of California San Francisco, Quantitative Biosciences Institute (QBI), San Francisco, CA, 94158, USA

³J. David Gladstone Institutes, San Francisco, CA 94158, USA

⁴University of California San Francisco, Department of Cellular and Molecular Pharmacology, San Francisco, CA, 94158, USA

⁵Department of Computational Medicine and Bioinformatics, University of Michigan, Ann Arbor, MI, 48109, USA

⁶Department of Pharmaceutical Chemistry, University of California, San Francisco

⁷Howard Hughes Medical Institute

⁸European Molecular Biology Laboratory (EMBL), European Bioinformatics Institute, Wellcome Genome Campus, Hinxton, Cambridge, UK.

⁹Department of Bioengineering and Therapeutic Sciences, University of California, San Francisco

¹⁰The UC Berkeley-UCSF Graduate Program in Bioengineering, University of California San Francisco, San Francisco, CA, USA

¹¹Center for Computational Biology and Bioinformatics, Department of Medicine, University of California San Diego

¹²Department of Cell and Tissue Biology, University of California, San Francisco

¹³Biophysics Graduate Program, University of California, San Francisco

- ¹⁴Cardiovascular Research Institute, University of California San Francisco, San Francisco, CA, 94158, USA.
- ¹⁵Division of Basic Sciences, Fred Hutchinson Cancer Research Center
- ¹⁶Medical Scientist Training Program, University of California, San Francisco, CA 94143, USA
- ¹⁷George William Hooper Foundation, Department of Microbiology and Immunology, UC San Francisco.
- ¹⁸Virus and Immunity Unit, Institut Pasteur, 28 rue du Dr Roux, 75724 Paris Cedex 15, France
- ¹⁹Viral Populations and Pathogenesis Unit, CNRS UMR 3569, Institut Pasteur, 28 rue du Dr Roux, 75724 Paris cedex 15, France
- ²⁰Department for Microbiology, Icahn School of Medicine at Mount Sinai, New York, NY
- ²¹Department of Medicine, University of California San Francisco, San Francisco, CA, USA
- ²²Department of Biochemistry and Biophysics, University of California San Francisco, San Francisco, CA, USA
- ²³Chan-Zuckerberg Biohub
- ²⁴Biochemistry & Biophysics and Quantitative Biosciences Institute UCSF 600 16th St San Francisco, CA 94143
- ²⁵Division of Human Biology, Fred Hutchinson Cancer Research Center, Seattle, WA 98103
- ²⁶Department of Urology, University of California, San Francisco, San Francisco, CA, USA.
- ²⁷Helen Diller Family Comprehensive Cancer Center, University of California, San Francisco, CA, 94158, USA
- ²⁸University of California San Francisco, Department of Psychiatry, San Francisco, CA, 94158, USA
- ²⁹Direction Scientifique, Institut Pasteur, 28 rue du Dr Roux, 75724 Paris cedex 15, France
- ³⁰Division of Genetics, Department of Medicine, University of California San Diego

Abbreviations:

HC-PPIs: High confidence protein-protein interactions

PPIs: protein-protein interaction

AP-MS: affinity purification-mass spectrometry

COVID-19: Coronavirus Disease-2019

ACE2: angiotensin converting enzyme 2

Orf: open reading frame

Nsp3: papain-like protease

Nsp5: main protease

Nsp: nonstructural protein

TPM: transcripts per million

Conflicts:

The **Krogan** Laboratory has received research support from Vir Biotechnology and F. Hoffmann-La Roche. **Kevan Shokat** has consulting agreements for the following companies involving cash and/or stock compensation: Black Diamond Therapeutics, BridGene Biosciences, Denali Therapeutics, Dice Molecules, eFFECTOR Therapeutics, Erasca, Genentech/Roche, Janssen Pharmaceuticals, Kumquat Biosciences, Kura Oncology, Merck, Mitokinin, Petra Pharma, Qulab Inc. Revolution Medicines, Type6 Therapeutics, Venthera, Wellspring Biosciences (Araxes Pharma). **Jack Taunton** is a cofounder and shareholder of Global Blood Therapeutics, Principia Biopharma, Kezar Life Sciences, and Cedilla Therapeutics. Jack Taunton and Phillip P. Sharp are listed as inventors on a provisional patent application describing PS3061.

ABSTRACT

An outbreak of the novel coronavirus SARS-CoV-2, the causative agent of COVID-19 respiratory disease, has infected over 290,000 people since the end of 2019, killed over 12,000, and caused worldwide social and economic disruption^{1,2}. There are currently no antiviral drugs with proven efficacy nor are there vaccines for its prevention. Unfortunately, the scientific community has little knowledge of the molecular details of SARS-CoV-2 infection. To illuminate this, we cloned, tagged and expressed 26 of the 29 viral proteins in human cells and identified the human proteins physically associated with each using affinity-purification mass spectrometry (AP-MS), which identified 332 high confidence SARS-CoV-2-human protein-protein interactions (PPIs). Among these, we identify 67 druggable human proteins or host factors targeted by 69 existing FDA-approved drugs, drugs in clinical trials and/or preclinical compounds, that we are currently evaluating for efficacy in live SARS-CoV-2 infection assays. The identification of host dependency factors mediating virus infection may provide key insights into effective molecular targets for developing broadly acting antiviral therapeutics against SARS-CoV-2 and other deadly coronavirus strains.

MAIN

The current pandemic of COVID-19 (Coronavirus Disease-2019), a respiratory disease that has led to over 290,000 confirmed cases and 12,000 fatalities in over 100 countries since its emergence in late 2019^{3,4}, is caused by a novel virus strain, SARS-CoV-2, an enveloped, positive-sense, single-stranded RNA betacoronavirus of the family *Coronaviridae*. Coronaviruses infecting humans historically included several mild common cold viruses e.g. hCoV-OC43, HKU, 229E⁵. However, over the past two decades, highly pathogenic human coronaviruses have emerged, including SARS-CoV in 2002 and 2003 with 8,000 cases worldwide and a death rate of ~10%, and MERS-CoV in 2012, which caused 2,500 confirmed cases and a fatality rate of 36%⁶. Infection with these highly pathogenic coronaviruses can result in Acute Respiratory Distress Syndrome (ARDS), which may lead to long-term reduction in lung function, arrhythmia, and death. Compared to MERS or SARS^{7,8}, SARS-CoV-2 appears to spread more efficiently, making it difficult to contain and increasing its pandemic potential. To devise therapeutic strategies to counteract SARS-CoV-2 infection, it is crucial to develop a comprehensive understanding of how this coronavirus hijacks the host during the course of infection, and to apply this knowledge towards developing both new drugs and repurposing existing ones.

So far, no clinically available antiviral drugs have been developed for SARS-CoV, SARS-CoV-2 or MERS-CoV. Clinical trials are ongoing for treatment of COVID-19 with the nucleotide analog RNA-dependent RNA

Polymerase (RdRP) inhibitor remdesivir⁹⁻¹¹, and recent data suggests a new nucleotide analog may be effective against SARS-CoV-2 infection in laboratory animals¹². Clinical trials on several vaccine candidates are also underway¹³, as well as trials of repurposed host-directed compounds inhibiting the human protease TMPRSS2¹⁴. We believe there is great potential in systematically exploring the host dependencies of the SARS-CoV-2 virus to identify other host proteins already targeted with existing drugs. Therapies targeting the host-virus interface, where mutational resistance is arguably less likely, could potentially present durable, broad-spectrum treatment modalities¹⁵. Unfortunately, our minimal knowledge of the molecular details of SARS-CoV-2 infection precludes a comprehensive evaluation of small molecule candidates for host-directed therapies. We sought to address this knowledge gap by systematically mapping the interaction landscape between SARS-CoV-2 proteins and human proteins.

Cloning and expression of predicted SARS-CoV-2 proteins

Sequence analysis of SARS-CoV-2 isolates suggests that the 30kb genome encodes as many as 14 open reading frames (Orfs). The 5' Orf1a / Orf1ab encodes polyproteins, which are auto-proteolytically processed into 16 non-structural proteins (Nsp1-16) which form the replicase / transcriptase complex (RTC). The RTC consists of multiple enzymes, including the papain-like protease (Nsp3), the main protease (Nsp5), the Nsp7-Nsp8 primase complex, the primary RNA-dependent RNA polymerase (Nsp12), a helicase/triphosphatase (Nsp13), an exoribonuclease (Nsp14), an endonuclease (Nsp15), and N7- and 2'O-methyltransferases (Nsp10/Nsp16)^{1,16,17}. At the 3' end of the viral genome, as many as 13 Orfs are expressed from nine predicted sub-genomic RNAs. These include four structural proteins: Spike (S), Envelope (E), Membrane (M) and Nucleocapsid (N)¹⁷, and nine putative accessory factors (Fig. 1a)^{1,16}. In genetic composition, the SARS-CoV-2 genome is very similar to SARS-CoV: each has an Orf1ab encoding 16 predicted Nsps and each has the four typical coronavirus structural proteins. However, they differ in their complement of 3' open reading frames: SARS-CoV-2 possesses an Orf3b and Orf10 with limited detectable protein homology to SARS-CoV¹⁶, and its Orf8 is intact while SARS-CoV encodes Orf8a and Orf8b (Fig. 1b)^{1,16,18}.

Mature Nsps and all predicted proteins expressed from other SARS-CoV-2 Orfs (27 proteins plus one mutant) were codon optimized and cloned into a mammalian expression vector with a 2xStrep tag fused to either the N- or C-terminus¹⁹. Protein expression plasmids were transfected into human HEK293T cells, which were incubated for 40 hours before lysis in a mild detergent buffer. Viral proteins were affinity purified using MagStrep beads. Beads were washed, on-bead digestion was performed overnight, and peptides were desalted and analyzed by protein mass spectrometry. High confidence interactors were identified using SAINTexpress and the MiST algorithm^{19,20}.

To verify viral protein expression, we performed an anti-Strep western blot on input cell lysate, and with the exception of Nsp4, Nsp6, Nsp11, and Orf3b, we observed bands consistent with predicted protein sizes (24 of 28 constructs). Despite the lack of detection via western blot we were able to detect expression of viral peptides Nsp4, Nsp6, and Orf3b in the proteomic analysis. The fourth construct not confirmed by western blot, the small peptide Nsp11, had a predicted molecular mass of 4.8 kDa (including tag) but an apparent mass of approximately 30 kDa (Fig. 1c). SARS-CoV-2 Orf3b has limited homology to SARS-CoV Orf3b¹⁶, and its restricted expression as measured by both western blot and AP-MS may indicate that it is either not a bonafide protein coding gene or that it requires co-expression of other SARS-CoV-2 proteins for robust expression. Ultimately we proceeded with analysis of protein interaction data from 27 baits, and excluded Orf7b, which had high prey detection background (Fig. 1d).

Global analysis of SARS-CoV-2 host interacting proteins

Our affinity purification-mass spectrometry analysis identified 332 protein interactions between SARS-CoV-2 proteins and human proteins (Extended Data Fig. 1, Supplementary Tables 1, 2; also see Fig. 3). We studied the interacting human proteins in regards to their cell biology, anatomical expression patterns, expression changes during SARS-CoV-2 infection²¹ and in relation to other maps of pathogen interacting proteins^{19,22–30} (Fig. 2a). For each of the viral proteins, we performed Gene Ontology enrichment analysis (Fig. 2b, Extended Data Fig. 2), identifying the major cell biological processes of the interacting proteins, including lipoprotein metabolism (S), nuclear transport (Nsp7), and biogenesis of ribonucleoprotein (Nsp8). To discover potential binding interfaces, we performed an enrichment for domain families within the interacting proteins of each viral bait (Extended Data Fig. 3). As examples, we note the enrichment of DNA polymerase domains in the interactors of Nsp1 and the enrichment of bromodomains and extra-terminal domain (BET) family for interactors of E (see also Figs. 3, 4). In line with the latter, the interactors of E are also enriched in genes annotated for binding to acetylated histones (Fig. 2b).

While the cells used for these AP-MS experiments, HEK-293T kidney cells, are permissive to SARS-CoV-2 infection³¹, they do not represent the primary physiological site of infection. Therefore, we asked whether the host proteins bound by SARS-CoV-2 might be specifically relevant to the virus's typical environment, lung tissue. We tested if the interacting human proteins were preferentially highly expressed, at the protein level, in any of 29 human tissues³², which identified the lung as the tissue with the highest expression of the prey proteins relative to the average proteome (Fig. 2c). In accordance to this, when compared to overall RefSeq gene expression in the lung (median=3.198 TPM), the interacting proteins were more highly expressed (median=25.52 TPM, $p=0.0007$; t-test, Extended Data Fig. 4) and were also specifically enriched in lung expression relative to other tissues (Extended Data Fig. 5). These data support the hypothesis that SARS-CoV-2 preferentially hijacks proteins available in lung tissue and the degree of tissue specific expression may facilitate the drug targeting of host factors with fewer systemic side-effects; this observation is particularly compelling given its derivation from HEK293 cells, which are themselves not lung derived. To further study the relevance of our map, we analyzed the recently reported protein abundance changes during SARS-CoV-2 infection³³. We calculated, when possible, the correlation between changes in abundance of viral proteins and their human interaction partners across the 4 timepoints reported. Interacting pairs tended to have stronger correlated changes than other pairs of viral-human proteins (Fig. 2d, KS test $p\text{-value}=4.8e-05$), arguing that the AP-MS derived interactions are of high relevance for the target tissue and the infection context. We compared our SARS-CoV-2 interaction map with those derived for 10 other pathogens (Fig. 2e), identifying West Nile Virus (WNV)²³ and *Mycobacterium tuberculosis* (Mtb)²⁷ as having the most similar host protein interaction partners. The association with Mtb is particularly interesting considering it also infects lung tissue.

Finally, we studied the evolutionary properties of the host proteins. Successful virus spread in a diverse population in theory could be facilitated by a reliance on conserved host molecular components, therefore we analyzed the conservation of the human proteins identified in the SARS-CoV-2 interactome. Relative to a control sample of genes, the 332 SARS-CoV-2 interacting human proteins had depleted missense and premature stop mutations in gnomAD³⁴, indicating that they have reduced genetic variation in human populations (Extended Data Fig. 6).

The SARS-CoV-2 interactome reveals novel aspects of SARS-CoV-2 biology

Our study highlighted interactions between SARS-CoV-2 proteins and human proteins with a range of functions including DNA replication (Nsp1), epigenetic and gene expression regulators (Nsp5, Nsp8, Nsp13, E), vesicle trafficking (Nsp6, Nsp7, Nsp10, Nsp13, Nsp15, Orf3a, E, M, Orf8), lipid modification (Spike), RNA processing and regulation (Nsp8, N), ubiquitin ligases (Orf10), signaling (Nsp8, Nsp13, N, Orf9b), nuclear transport machinery (Nsp9, Nsp15, Orf6), cytoskeleton (Nsp1, Nsp13), mitochondria (Nsp4, Nsp8, Orf9c), and extracellular matrix (Nsp9) (Fig. 3).

A prominent number of interactions were related to lipid modifications and vesicle trafficking. Interestingly, the Spike protein (S) interacts with the GOLGA7-ZDHHC5 acyl-transferase complex, which likely mediates palmitoylation on its cytosolic tail (see also Appendix)³⁵. Palmitoylation has been reported to facilitate membrane fusion by SARS-CoV Spike and suggests a potential target for therapeutic inhibition³⁶. Interestingly, ZDHHC5 also has a published role in allowing anthrax toxin to enter cells, suggesting that inhibition of this enzyme could have broad utility³⁷. Host interactions of Nsp8 (signal recognition particle), Orf8 (endoplasmic reticulum quality control), M (ER structural morphology proteins), Nsp13 (golgins) may facilitate the dramatic reconfiguration of ER/Golgi trafficking during coronavirus infection, and interactions in peripheral compartments by Nsp6 and M (vacuolar ATPase), Nsp7 (Rabs), Nsp10 (AP2), E (AP3), and Orf3a (HOPS) may also modify endomembrane compartments to favor coronavirus replication.

We identified protein-protein interactions with the main protease Nsp5, using both wild-type and catalytic dead (C145A) constructs. For wild-type Nsp5, we identified one high-confidence interaction, the epigenetic regulator histone deacetylase 2 (HDAC2), and predicted a cleavage site between the HDAC domain and the nuclear localization sequence, suggesting that Nsp5 may inhibit HDAC2 transport into the nucleus (Extended Data Fig. 7), potentially impacting the published functions of HDAC2 in mediating inflammation and interferon response^{38,39}. We also identified an interaction of Nsp5 (C145A) with tRNA methyltransferase 1 (TRMT1), which is responsible for synthesis of the dimethylguanosine (m²,2G) base modification on both nuclear and mitochondrial tRNAs⁴⁰. We predict TRMT1 is also cleaved by Nsp5, removing its zinc finger and nuclear localization signal and likely resulting in an exclusively mitochondrial localization (Extended Data Fig. 7).

SARS-CoV-2 interacts with multiple innate immune pathways

We identified a number of cellular proteins implicated in innate immune signaling that are targeted by several SARS-CoV-2 viral proteins. Interestingly, we found that Nsp13 interacts with two key players of IFN signaling pathway including TANK-binding kinase 1 (TBK1) and TANK-binding kinase 1-binding protein 1 (TBKBP1/SINTBAD). SINTBAD acts as a critical adaptor protein between TBK1 and IKKi and therefore mediates induction of IRF-dependent transcription⁴¹. Further, Nsp13 interacts with multiple proteins of the TLE family, which are known to modulate NF- κ B inflammatory response⁴²⁻⁴⁴. RNF41/Nrdp1, an E3 ubiquitin ligase is targeted by Nsp15 protein which promotes activation of TBK1 and IRF3 and therefore increases type I interferon production⁴⁵. Two other E3 ubiquitin ligases, TRIM59 and MIB1 regulate antiviral innate immune signaling and are usurped by Orf3a and Nsp9, respectively^{46,47}. Orf9c protein was found to interact with multiple proteins that modulate I κ B kinase and NF- κ B signaling pathway including NLRX1, F2RL1, NDFIP2⁴⁸⁻⁵⁰. We also found that Orf9b interacts with a mitochondrial import receptor, Tom70, which acts as an essential adaptor linking MAVS to TBK1/IRF3, resulting in the activation of IRF-3⁵¹.

N targets stress granule protein G3BP1, an essential antiviral protein which is known to induce innate immune response through multiple mechanisms⁵²⁻⁵⁴. Common among *coronaviridae* is the manipulation of stress granules (SG) and related RNA biology, possibly leading to suppression of stress granules and host translation shutoff⁵⁵. This functionality seems to benefit viral replication, as stress granules are inhibitory to replication of MERS-CoV⁵⁶ and other viruses⁵⁷. The SARS-CoV-2 nucleocapsid (N) interactome includes many host mRNA

binding proteins, including the SG related factors G3BP1/2, the mTOR translational repressors LARP1, and the protein kinases CK2 (Fig. 4a). SGs are induced by protein kinase R (PKR)-mediated phosphorylation of eIF2 α upon viral dsRNA recognition⁵⁷. Promoting G3BP aggregation via the eIF4A inhibitor Zotatafin^{58,59} or reducing SG disassembly by Silitasertib inhibition of CK2⁶⁰ warrant investigation for treatment of SARS-CoV-2. The mTOR inhibitor rapamycin disrupts the binding of LARP1 to mTORC1⁶¹ and has been shown to reduce MERS infection by ~60% *in vitro*⁶², another drug that could be tested for repurposing.

Orf6 of SARS-CoV has been shown to play a role in antagonizing host interferon signaling⁶³; we identified a novel, high-confidence interaction between SARS-CoV-2 Orf6 and NUP98-RAE1, an interferon-inducible mRNA nuclear export complex⁶⁴ that is hijacked or degraded by multiple viruses, including VSV, Influenza-A, KSHV, and Polio, and is a restriction factor for Influenza-A infection^{58,60,62,65}. The X-ray structure of VSV M protein complexed with NUP98-RAE1⁶⁶ reveals key binding interactions that include a buried methionine residue on the M-protein packing into a hydrophobic pocket in RAE1, as well as neighboring acidic residues interacting with a basic patch on the NUP98-RAE1 complex (Fig 4b). These binding features are also present in a conserved motif in the C-terminal region of SARS-CoV-2 Orf6 (Fig. 4b, Extended Data Fig. 8), providing a structural hypothesis for the observed SARS-CoV-2–NUP98-RAE1 interaction. Moreover, a peptide containing the binding region of the VSV M protein was previously shown to outcompete RNA binding to NUP98-RAE1, suggesting a role in interfering with mRNA export⁶⁶. These observations suggest a viral strategy to target the RNA nuclear export activity of RAE1, potentially revealing a mode of interferon antagonism by SARS-CoV-2.

The novel Orf10 of SARS-CoV-2 interacts with a Cullin ubiquitin ligase complex

Viruses commonly hijack ubiquitination pathways for replication and pathogenesis⁶⁷. The novel Orf10 of SARS-CoV-2 interacts with multiple members of a Cullin 2 (CUL2) RING E3 ligase complex (Fig. 4c), specifically the CUL2^{ZYG11B} complex. ZYG11B, a substrate adapter of CUL2 that targets substrates with exposed N-terminal glycines for degradation⁶⁵, is the highest scoring protein in the Orf10 interactome suggesting its direct interaction with Orf10. Orf10 may bind to the CUL2^{ZYG11B} complex and hijack it for ubiquitination and degradation of restriction factors. The ubiquitin transfer to a substrate requires neddylation of CUL2 via NEDD8-activating enzyme (NAE), a druggable target that can be inhibited by the small molecule Pevonedistat⁶⁸ (Fig. 4c).

SARS-CoV-2 envelope interacts with bromodomain proteins

Surprisingly, we find that the transmembrane protein E binds to the bromodomain-containing proteins BRD2 and BRD4 (Fig. 4d, Extended Data Fig. 9), potentially disrupting BRD-histone binding by mimicking histone structure. BRD2 is a member of the bromodomain and extra-terminal (BET) domain family whose members bind acetylated histones to regulate gene transcription⁶⁹. The N-terminus of histone 2A shares local sequence similarity over an alpha-helix of approximately 15 residues, some of which are in a transmembrane segment, of Protein E (Fig. 4d). Moreover, this matching region of the histone is spanned by acetylated lysine residues shown to bind BRD2⁷⁰. This analysis may suggest that Protein E mimics the histone to disrupt its interaction with BRD2, thus inducing changes in host's protein expression that are beneficial to the virus.

For a more comprehensive overview of the virus-host interactions we detected, see Supplemental Discussion.

Identification of existing drugs targeting SARS-CoV-2 human host factors.

To identify small molecules targeting human proteins in the SARS-CoV-2 interactome, we sought ligands known to interact with the human proteins, often directly but also by pathway and complexes, drawing on cheminformatics databases and analyses (Methods). Molecules were prioritized by the statistical significance of the interaction between the human and viral proteins; by their status as approved drugs, investigational new drugs (INDs, “clinical” in Table 1a,b), or as preclinical candidates; by their apparent selectivity; and by their

availability (for purchase availability notes, see Supplemental Tables 3 and 4). Cheminformatics searches yielded 15 approved drugs, four investigational new drugs (clinical), and 18 pre-clinical candidates (Table 1a), while specialist knowledge revealed 12 approved drugs, 10 investigational new drugs (clinical), and 10 preclinical candidates (Table 1b). Of the 332 human targets that interact with the viral bait proteins with high significance, 63 have drugs/INDs/preclinical molecules that modulate them (Fig. 3). If we reduce our protein interaction score threshold slightly, we find an additional four human targets, revealing a total of 67 human targets (Supplementary Tables 3 and 4). The drug-human protein associations may be overlaid on top of our protein interaction network, highlighting potentially druggable host interactions (Fig. 5a).

There are several mechanistically interesting, and potentially disease-relevant drug-target interactions revealed in the cheminformatic network (Fig. 5a). Among them, the well-known chemical probe, Bafilomycin A1, is a potent inhibitor of the V1-ATPase, subunits of which interact with Nsp6 and M. Bafilomycin's inhibition of this cotransporter acts to prevent the acidification of the lysosome, inhibiting autophagy and endosome trafficking pathways, which may impact the viral life-cycle. Similarly, drugs exist to target several well-known epigenetic regulators prominent among the human interactors, including HDAC2, BRD2 and BRD4, which interact with viral proteins nsp5 and E, respectively (Figs. 3 and 5a). The approved drug Valproic acid (an anticonvulsant) and the pre-clinical candidate Apicidin inhibit HDAC2 with affinities of 62 μ M and 120 nM, respectively. Clinical compounds ABBV-744 and CPI-0610 act on BRD2/4, with an affinity of 2 nM or 39 nM, respectively -- several preclinical compounds also target bromodomain-containing proteins (Table 1a,b). As a final example, we were intrigued to observe that the SARS-CoV-2 Nsp6 protein interacts with the Sigma receptor, which is thought to regulate ER stress response⁷¹. Similarly, the Sigma2 receptor interacted with the viral protein orf9. Both Sigma1 and Sigma2 are promiscuous receptors that interact with many non-polar, cationic drugs. We prioritized several of these drugs based on potency or potential disease relevance, including the antipsychotic Haloperidol, which binds in the low nM range to both receptors⁷², and Chloroquine, which is currently in clinical trials for COVID-19 and has mid-nM activity vs the Sigma1 receptor, and low μ M activity against the Sigma2 receptor. Because many patients are already treated with drugs that have off-target impact on Sigma receptors, associating clinical outcomes accompanying treatment with these drugs may merit investigation, a point to which we return. Finally, in addition to the druggable host factors, a few of which we have highlighted here, the SARS-CoV-2-human interactome reveals many traditionally "undruggable" targets. Among these, for instance, are components of the centriole such as CEP250, which interacts with the viral Nsp13. Intriguingly, a very recent patent disclosure revealed a natural product, WDB002, that directly and specifically targets CEP250. As a natural product, WDB002 would likely be harder to source than the molecules on which we have focused on here, but may well merit investigation. Similarly, other "undruggable" targets may be revealed to have compounds that could usefully perturb the viral-human interaction network, and act as leads to therapeutics.

Beyond direct interactions, several drug-pathway interactions seemed noteworthy. The human purine biosynthesis enzyme Inosine-5'-monophosphate dehydrogenase (IMPDH2) interacts with the viral protein nsp14. Several chemically diverse compounds inhibit IMPDH2, including the clinically approved mycophenolic acid (20 nM), the approved antiviral drug ribavirin (200 nM), and the investigational new drug Merimepodib (10 nM) (Table 1a). Intriguingly, the preclinical molecule Sanglifehrin A (Table 1b) is known to act as a molecular glue linking IMPDH with cyclophilin A (Fig. 5b)⁷³, which itself is implicated in viral capsid packaging, even though it itself is not a human "prey" in the viral-human protein interactome. Similarly, direct viral-human interactions with proteins regulated by the mTORC1 pathway, such as LARP1, and FKBP7, which interact with the viral N and Orf8 proteins, led us to inhibitors of mTORC1, even though that kinase itself is not found to directly interact with a viral protein (Fig. 5c). Sapanisertib and rapamycin are low nM inhibitors of mTORC1, while metformin is an indirect modulator of this protein complex.

Discussion

We have used affinity purification-mass spectrometry to identify 332 high-confidence SARS-CoV-2-human PPIs. We find the viral proteins connected to a wide array of biological processes, including protein trafficking, translation, transcription and ubiquitination regulation. Using a combination of a systematic chemoinformatic drug search with a pathway centric analysis, we uncovered close to 70 different drugs and compounds, including FDA approved drugs, compounds in clinical trials as well as preclinical compounds, targeting parts of the resulting network. We are currently testing these compounds for antiviral activity and encourage others to do the same as well as extract insights from the map that could have therapeutic value.

More generally, this proteomic/chemoinformatic analysis is not only identifying drug and clinical molecules that might perturb the viral-human interactome, it gives these potentially therapeutic perturbations a mechanistic context. Among those that may be infection relevant are the inhibition of lysosomal acidification and trafficking with Bafilomycin A1, via inhibition of V-ATPase⁷⁴, and modulation of the ER stress and the protein unfolding response pathway by targeting the Sigma1 and Sigma2 receptor by drugs like haloperidol (Fig. 5a, Tables 1a,b). Indeed, several of the human proteins in the interactome are targeted by drugs that have emerged phenotypically as candidate therapeutics for treating COVID-19, such as chloroquine^{75,76}. While we do not pretend to have identified the molecular basis of chloroquine's putative activity, we do note that this drug targets the Sigma1 and Sigma2 receptors at mid-nM and low μ M concentrations, respectively. Similarly, antibiotics like azithromycin have also been mooted as treatments for COVID-19. While this too remains to be demonstrated, we note that Azithromycin has off-target activity against human mitochondrial ribosomes, components of which interact with the SARS-CoV-2 Nsp8 protein (MRPS5, MRPS27, MRPS2, and MRPS25). Other antibiotics that also have an off-target effect on mitochondrial ribosomes, such as chloramphenicol, tigecycline, and Linezolid^{77,78} may also merit study for efficacy. Indeed, this logic may be extended. Many COVID-19 patients will be on the drugs identified here, treating pre-existing conditions. It may be useful to correlate clinical outcomes with the taking of these drugs, cross-referencing with the networks described here. In some senses, this is already occurring phenomenologically, leading to concerns about ACE inhibitors such as captopril and enalapril, and for NSAIDs. What this study provides is a systematic schema for clinical/drug associations going forward, giving them a mechanistic context that allows investigators to seek them directly.

Systematic validation using genetic-based approaches^{79,80} will be key to determine the functional relevance of these interactions and if the human proteins are being used by the virus or are fighting off infection, information that would inform future pharmacological studies. *It is important to note that pharmacological intervention with the agents we identified in this study could be either detrimental or beneficial for infection.* For instance, the HDAC2 inhibitors may compound the potential action of the Nsp5 protease to hydrolyze this human protein. Future work will involve generation of protein-protein interaction maps in different human cell types, as well as bat cells, and the study of related coronaviruses including SARS-CoV, MERS-CoV and the less virulent OC43⁵, data that will allow for valuable cross-species and viral evolution studies. Targeted biochemical and structural studies will also be crucial for a deeper understanding of the viral-host complexes, which will inform more targeted drug design.

Along with SARS-CoV-2, we have previously utilized global affinity purification-mass spectrometry (AP-MS) analysis to map the host-pathogen interfaces of a number of human pathogens including Ebola²², Dengue³⁰, Zika³⁰, Herpesvirus²⁹, Hepatitis C²⁸, Tuberculosis²⁷, Chlamydia²⁶, Enteroviruses²⁵, HIV¹⁹, HPV²⁴, and West Nile Fever²³. Excitingly, we have uncovered both shared and unique mechanisms in which these pathogens co-opt the host machinery during the course of infection. Although host-directed therapy is often not explored for

combatting pathogenic infections, it would be interesting to use this information to identify host factors that could serve as targets that would harbor pan-pathogenic activity so that when the next virus undergoes zoonosis, we will have treatment options available.

Supplementary Information is available for this paper.

Correspondence and requests for materials should be addressed to nevan.krogan@ucsf.edu

Reprints and permissions information is available at www.nature.com/reprints

The authors have not filed for patent protection on the SARS-CoV-2 host interactions or the use of predicted drugs for treating COVID-19 to ensure all the information is freely available to accelerate the discovery of a treatment.

FIGURE LEGENDS

Figure 1: AP-MS Workflow for Identification of SARS-CoV-2 Host Protein-Protein Interactions. (a) SARS-CoV-2 genome annotation. (b) Table of the SARS-CoV-2 proteins, including molecular weight, sequence

similarity with the SARS-CoV homolog, and inferred function based on the SARS-CoV homolog. (c) Immunoblot detection of 2xStrep tag demonstrates expression of each bait in input samples, as indicated by red arrowhead. (d) Experimental workflow for expressing each 2xStrep tagged SARS-CoV-2 fusion protein in biological triplicate in HEK293T cells, followed by affinity purification-mass spectrometry, and PPI scoring to identify 332 high confidence protein-protein interactions.

Figure 2: Global Analysis of SARS-CoV-2 Protein Interactions. (a) Overview of global analyses performed. (b) Gene Ontology (GO) enrichment analysis performed on the human interacting proteins of each viral protein (Methods). The top GO term of each viral protein was selected for visualization. (c) Degree of differential protein expression for the human interacting proteins across human tissues. We obtained protein abundance values for the proteome in 29 human tissues and calculated the median level of abundance for the set of human interacting proteins (top 16 tissues shown). This median value was then compared with the distribution of abundance values for the full proteome in each tissue and summarized as a Z-score from which a p-value was calculated and adjusted for multiple tests. (d) Distribution of correlation of protein level changes during SARS-CoV-2 infection for pairs of viral-human proteins. (e) Significance of the overlap of human interacting proteins between SARS-CoV-2 and other pathogens.

Figure 3: SARS-CoV-2 Protein-Protein Interaction Network. In total, 332 high confidence interactions are represented between 26 SARS-CoV-2 proteins and their human interactors. Red diamonds represent a SARS-CoV-2 viral protein, interacting human host proteins are represented with circles, with drug targets in orange. Edge color is proportional to MiST score and edge thickness proportional to spectral counts. Physical interactions among host proteins are noted as thin black lines, protein complexes are highlighted in yellow, and proteins sharing the same biological process are highlighted in blue.

Figure 4: The SARS-CoV-2 interactome reveals novel aspects of SARS-CoV-2 biology that can be targeted pharmacologically. (a) Protein N targets stress granule proteins. (i) Protein N interactome. (ii) Model for therapeutic targeting of N interactions in the formation of stress granules (SGs). SGs are known to exhibit antiviral activity, with the integrative stress response (ISR) inducing eIF2 α phosphorylation and SG formation, and Casein kinase II (CK2) disrupting and preventing the formation of SGs. By activating SG formation, or inhibiting CK2, the cellular environment could potentially shift to a more antiviral state. (b) Orf6 interacts with an interferon-inducible mRNA nuclear export complex. (i) Orf6 interactome including small molecule inhibitors for RAE. (ii) Annotated C-terminal sequence of SARS-CoV-2 Orf6, highlighting previously described trafficking motifs and the putative NUP98-RAE1 binding sequence. Colors indicate chemical properties of amino acids: polar (G,S,T,Y,C, green), neutral (Q,N, purple), basic (K, R, H, blue), acidic (D, E, red), and hydrophobic (A, V, L, I, P, W, F, M, black). (iii) SARS-CoV-2 Orf6 carboxy-terminal peptide modeled into the binding site of the VSV M protein-NUP98-RAE1 complex (PDB ID: 4OWR). Orf6 shown in dark purple, M protein in yellow, NUP98 in green, and RAE1 in light purple. Orf6 and M protein residues labeled. RAE1 hydrophobic residues contacting the key methionine and basic patch residues of RAE1 and NUP98 are shown. (iv) Putative NUP98-RAE1 interaction motifs present in proteins from several viral species. The consensus motif consists of negatively charged residues (red) surrounding a conserved methionine (yellow). (c) Orf10 interacts with the CUL2^{ZYG11B} complex. (i) Orf10 interactome. (ii) The secondary structure of Orf10 contains an alpha helix motif. (iii) Surface representation of the homology model for CUL2^{ZYG11B} complex, residues that are conserved amongst ZYG11B orthologues from various species are indicated in red are likely protein interaction surfaces for binding substrates and other proteins. (iv) A possible model of how Orf10 binds to the CUL2^{ZYG11B} complex to hijack the complex for ubiquitination or viral restriction factors and how it can be targeted pharmacologically. (d) Envelope (E) interacts with bromodomain proteins. (i) E interactome. (ii) Sequence alignment of highlighted regions of E and Histone 2A (H2A). The positions with identical and similar amino acid residues are highlighted in red and yellow, respectively. Note the greater hydrophobicity of E may indicate a part of the alignment represents a

transmembrane segment. (iii) Model of how E might mimic the BRD2 native interaction partner Histone 2A and how BRD2 can be targeted pharmacologically.

Figure 5: Drug-human target network. (a) Significant interactions identified by AP-MS between SARS-CoV-2 baits (red diamonds) and human prey proteins (orange circles) are shown as in **Fig 3**. Chemoinformatic and expert analysis identified FDA approved drugs (green), clinical candidates (yellow), and preclinical candidates (purple) with experimental activities against the host proteins and processes, with representative chemicals shown. (b) Inosine Monophosphate Dehydrogenase 2 (IMPDH2) regulates de novo nucleic acid biosynthesis. It is a target for proliferative diseases including cancer⁸¹ and autoimmune disorders, for instance by the approved drug mycophenolic acid⁸², and as a broad spectrum antiviral by Ribavirin⁸³. While Ribavirin has activity against SARS in vitro⁸⁴, it has low tolerability, something that might be addressed by the more selective Merimepodib, which is in phase II clinical trials⁸⁵. (c) The mammalian target of Rapamycin (mTOR) pathway is a master regulator of cell proliferation and autophagy, which viruses including Influenza A are known to modulate^{86,87}. Several proteins that interact with SARS-CoV-2 baits, including components of the Respiratory complex 1 by Nsp7, Nsp12, and Orf9c, the leucine importer B(0)AT2 (SLC6A15)^{88,89} by Nsp6 and LARP1 by N (not shown). In addition to Rapamycin, the mTOR pathway can be indirectly modulated by metformin, a widely prescribed diabetes drug, and by Sapanisertib, a drug in clinical trials for solid tumors⁶¹.

ACKNOWLEDGEMENTS

We thank Joshua Sarlo for his artistic contributions to the manuscript.

This research was funded by grants from the National Institutes of Health (P50AI150476, U19AI135990, U19AI135972, R01AI143292, R01AI120694, P01A1063302, and R01AI122747 to N.J.K.; R35GM122481 to B.K.S.; 1R01CA221969 and 1R01CA244550 to K.M.S.; K08HL124068 to J.S.C.; 1F32CA236347-01 to J.E.M.); funding from F. Hoffmann-La Roche and Vir Biotechnology and gifts from The Ron Conway Family. K.M.S is an investigator of the Howard Hughes Medical Institute.

MATERIALS AND METHODS

Genome annotation. The genbank sequence for SARS-CoV-2 isolate 2019-nCoV/USA-WA1/2020, accession MN985325, was downloaded on January 24, 2020. In total, we identified 29 open reading frames and proteolytically mature proteins encoded by SARS-CoV-2^{1,16}. Proteolytic products resulting from Nsp3 and Nsp5-mediated cleavage of the Orf1a / Orf1ab polyprotein were predicted based on the protease specificity of SARS-CoV proteases⁹⁰, and 16 predicted nonstructural proteins (Nsps) were subsequently cloned (Nsp1-Nsp16). For the proteases Nsp3 (papain-like / Plpro) and Nsp5 (3Cl-like / 3CLpro), we also designed catalytic dyad/triad mutants: Nsp3 C857A⁹¹ and Nsp5 C145A^{92,93}. Open reading frames at the 3' end of the viral genome annotated in the original genbank file included 4 Structural proteins: S, E, M, N, and the additional open reading frames Orf3a, Orf6, Orf7a, Orf8, and Orf10. Based on analysis of open reading frames in the genome and comparisons with other annotated SARS-CoV open reading frames, we annotated a further four open reading frames: Orf3b, Orf7b, Orf9b, and Orf9c.

Cell culture. HEK293T cells were cultured in Dulbecco's Modified Eagle's Medium (Corning) supplemented with 10% Fetal Bovine Serum (Gibco, Life Technologies) and 1% Penicillin-Streptomycin (Corning) and maintained at 37°C in a humidified atmosphere of 5% CO₂.

Transfection. For each affinity purification, ten million HEK293T cells were plated per 15-cm dish and transfected with up to 15 µg of individual Strep-tagged expression constructs after 20-24 hours. Total plasmid was normalized to 15 µg with empty vector and complexed with PolyJet Transfection Reagent (SignaGen Laboratories) at a 1:3 µg:µl ratio of plasmid to transfection reagent based on manufacturer's recommendations. After more than 38 hours, cells were dissociated at room temperature using 10 ml Dulbecco's Phosphate Buffered Saline without calcium and magnesium (D-PBS) supplemented with 10 mM EDTA for at least 5 minutes and subsequently washed with 10 ml D-PBS. Each step was followed by centrifugation at 200 xg, 4°C for 5 minutes. Cell pellets were frozen on dry ice and stored at - 80°C. At least three biological replicates were independently prepared for affinity purification.

Affinity purification. Frozen cell pellets were thawed on ice for 15-20 minutes and suspended in 1 ml Lysis Buffer [IP Buffer (50 mM Tris-HCl, pH 7.4 at 4°C, 150 mM NaCl, 1 mM EDTA) supplemented with 0.5% Nonidet P 40 Substitute (NP40; Fluka Analytical) and cOmplete mini EDTA-free protease and PhosSTOP phosphatase inhibitor cocktails (Roche)]. Samples were then frozen on dry ice for 10-20 minutes and partially thawed at 37°C before incubation on a tube rotator for 30 minutes at 4°C and centrifugation at 13,000 xg, 4°C for 15 minutes to pellet debris. After reserving 50 µl lysate, up to 48 samples were arrayed into a 96-well Deepwell plate for affinity purification on the KingFisher Flex Purification System (Thermo Scientific) as follows: MagStrep "type3" beads (30 µl; IBA Lifesciences) were equilibrated twice with 1 ml Wash Buffer (IP Buffer supplemented with 0.05% NP40) and incubated with 0.95 ml lysate for 2 hours. Beads were washed three times with 1 ml Wash Buffer and then once with 1 ml IP Buffer. To directly digest bead-bound proteins as well as elute proteins with biotin, beads were manually suspended in IP Buffer and divided in half before transferring to 50 µl Denaturation-Reduction Buffer (2 M urea, 50 mM Tris-HCl pH 8.0, 1 mM DTT) and 50 µl 1x Buffer BXT (IBA Lifesciences) dispensed into a single 96-well KF microtiter plate, respectively. Purified proteins were first eluted at room temperature for 30 minutes with constant shaking at 1,100 rpm on a ThermoMixer C incubator. After removing eluates, on-bead digestion proceeded (below). Strep-tagged protein expression in lysates and enrichment in eluates were assessed by western blot and silver stain, respectively. The KingFisher Flex Purification System was placed in the cold room and allowed to equilibrate to 4°C overnight before use. All automated protocol steps were performed using the slow mix speed and the following mix times: 30 seconds for equilibration/wash steps, 2 hours for binding, and 1 minute for final bead release. Three 10 second bead collection times were used between all steps.

On-bead digestion. Bead-bound proteins were denatured and reduced at 37°C for 30 minutes and after bringing to room temperature, alkylated in the dark with 3 mM iodoacetamide for 45 minutes and quenched with 3 mM DTT for 10 minutes. Proteins were then incubated at 37°C, initially for 4 hours with 1.5 µl trypsin (0.5 µg/µl; Promega) and then another 1-2 hours with 0.5 µl additional trypsin. To offset evaporation, 15 µl 50 mM Tris-HCl, pH 8.0 were added before trypsin digestion. All steps were performed with constant shaking at 1,100 rpm on a ThermoMixer C incubator. Resulting peptides were combined with 50 µl 50 mM Tris-HCl, pH 8.0 used to rinse beads and acidified with trifluoroacetic acid (0.5% final, pH < 2.0). Acidified peptides were desalted for MS analysis using a BioPureSPE Mini 96-Well Plate (20mg PROTO 300 C18; The Nest Group, Inc.) according to standard protocols.

Mass spectrometry data acquisition and analysis. Samples were re-suspended in 4% formic acid, 2% acetonitrile solution, and separated by a reversed-phase gradient over a nanoflow C18 column (Dr. Maisch). Each sample was analyzed on two different mass spectrometers. First, a 75 min acquisition, in which peptides were directly injected via a Easy-nLC 1200 (Thermo) into a Q-Exactive Plus mass spectrometer (Thermo), with all MS1 and MS2 spectra collected in the orbitrap. For all acquisitions, QCloud was used to control instrument longitudinal performance during the project⁹⁴. All proteomic data was searched against the human proteome (uniprot reviewed sequences downloaded February 28th, 2020), EGFP sequence, and the SARS-CoV-2 protein

sequences using the default settings for MaxQuant^{95,96}. Detected peptides and proteins were filtered to 1% false discovery rate in MaxQuant, and identified proteins were then subjected to protein-protein interaction scoring with both SAINTexpress²⁰ and MiST^{19,97}. We applied a two step filtering strategy to determine the final list of reported interactors which relied on two different scoring stringency cutoffs. In the first step, we chose all protein interactions that possess a MiST score ≥ 0.7 , a SAINTexpress BFDR ≤ 0.05 and an average spectral count ≥ 2 . For all proteins that fulfilled these criteria we extracted information about stable protein complexes they participate in from the CORUM⁹⁸ database of known protein complexes. In the second step we then relaxed the stringency and recovered additional interactors that (1) form complexes with interactors determined in filtering step 1 and (2) fulfill the following criteria: MiST score ≥ 0.6 , SAINTexpress BFDR ≤ 0.05 and average spectral counts ≥ 2 . Proteins that fulfilled filtering criteria in either step 1 or step 2 were considered to be HC-PPIs and visualized with cytoscape⁹⁹. Using this filtering criteria, nearly all of our baits recovered a number of HC-PPIs in close alignment with previous datasets reporting an average of ~ 6 PPIs per bait¹⁰⁰. However, for a subset of baits (Orf8, Nsp8, Nsp13, and orf9c) we observed a much higher number of PPIs passing these filtering criteria. For these four baits, the MiST scoring was instead performed using an larger in-house database of 87 baits that were prepared and processed in an analogous manner to this SARS-CoV-2 dataset. This was done to provide a more comprehensive collection of baits for comparison, to minimize the classification of non-specifically binding background proteins as HC-PPIs. All mass spectrometry raw data and search results files have been deposited to the ProteomeXchange Consortium via the PRIDE partner repository with the dataset identifier PXD018117^{101,102}. PPI networks have also been uploaded to NDEx.

Gene Ontology Over-representation Analysis. The targets of each bait were tested for enrichment of Gene Ontology (GO Biological Process) terms. The over-representation analysis (ORA) was performed using the enricher function of clusterProfiler package in R with default parameters. The gene ontology terms were obtained from the c5 category of Molecular Signature Database (MSigDBv6.1). Significant GO terms (1% FDR) were identified and further refined to select non-redundant terms. In order to select non-redundant gene sets, we first constructed a GO term tree based on distances (1-Jaccard Similarity Coefficients of shared genes) between the significant terms. The GO term tree was cut at a specific level ($h=0.99$) to identify clusters of non-redundant gene sets. For a bait with multiple significant terms belonging to the same cluster, we selected the broadest term i.e. largest gene set size.

Virus Interactome Similarity Analysis. Interactome similarity was assessed by comparing the number of shared human interacting proteins between pathogen pairs, using a hypergeometric test to calculate significance. The background gene set for the test consisted of all unique proteins detected by mass spectrometry across all pathogens ($N=10,181$ genes).

Orf6 peptide modeling. The proposed interaction between Orf6 and the NUP98-RAE1 complex was modeled in PyRosetta 4¹⁰³ (release v2020.02-dev61090) using the crystal structure of Vesicular stomatitis virus matrix (M) protein bound to NUP98-RAE1 as a template⁶⁶ (PDB 4OWR downloaded from the PDB-REDO server¹⁰⁴). The M protein chain (C) was truncated after residue 54 to restrict the model to the putative interaction motif in Orf6 (M protein residues 49-54, sequence DEMDTH). These residues were mutated to the Orf6 sequence, QPMEID, using the *mutate_residue* function in the module *pyrosetta.toolbox*, without repacking at this initial step. After all six residues were mutated, the full model was relaxed to a low energy conformation using the *FastRelax* protocol in the module *pyrosetta.rosetta.protocols.relax*. *FastRelax* was run with constraints to starting coordinates and scored with the ref2015 score function. The resulting model was inspected for any large

energetic penalties associated with the modeled peptide residues or those NUP98 and RAE1 residues interacting with the peptide, and was found to have none. The model was visualized in PyMOL (The PyMOL Molecular Graphics System, Version 2.3.4 Schrödinger, LLC.).

CUL2^{ZYG11B} homology model generation. The CRL2^{ZYG11B} homology model was built with Swissmodel¹⁰⁵ and Modeller¹⁰⁶ by using the homology template of each domain from PDB database (PDB codes: 4b8o, 5jh5, 1g03, and 6r7n). The ZYG11B model has two structured domains: a leucine rich repeat (LRR) and Armadillo Repeat (ARM) at the N and C-terminus respectively. The linker between each domain was not modelled due to high flexibility between residues 32 to 49 and residues 304 to 322. Putative protein interaction surfaces on ZYG11B were modelled based on contiguous surface exposed residues that are conserved in ZYG11B orthologues from *C. elegans* to *H. sapiens* (ZY11B_HUMAN; ZY11B_MOUSE; F1M8P2_RAT; ZYG11_XENLA; ZYG11_DANRE; ZYG11_CAEEL) and located at typical substrate binding sites in the homologous structures of LRR and ARM domain co-complexes.

Alignment of Protein E and Histone H2A. In order to align protein E and histone H2A, the structure of the protein E SARS-CoV homolog (PDB ID: 2MM4) was compared to the human nucleosome structure (PDB ID: 6K1K). Protein E was structurally aligned to the histone subunits using Pymol's "align" function (<https://pymolwiki.org/index.php/Align>). *Align* performs a sequence alignment followed by a structural superposition, and then carries out zero or more cycles of refinement in order to reject structural outliers found during the fit. The best superposition was obtained for H2A residues 49-60 & 63-70 and Protein E residues 25-44 at an RMSD of 2.8Å, as reported in Figure 4d.

Chemoinformatic Analysis of SARS-CoV2 Interacting Partners. To identify drugs and reagents that modulate the 332 host factors interacting with SARS-CoV-2-HEK293T (MiST ≥ 0.70), we used two approaches: 1) a chemoinformatic analysis of open-source chemical databases and 2) a target- and pathway-specific literature search, drawing on specialist knowledge within our group. Chemoinformatically, we retrieved 2,472 molecules from the IUPHAR/BPS Guide to Pharmacology (2020-3-12) that interacted with 30 human "prey" proteins (38 approved, 71 in clinical trials), and found 10,883 molecules (95 approved, 369 in clinical trials) from the ChEMBL25 database¹⁰⁷ (Supplementary Tables 5, 6). For both approaches, molecules were prioritized on their FDA approval status, activity at the target of interest better than 1 μ M, and commercial availability, drawing on the ZINC database¹⁰⁸. FDA approved molecules were prioritized except when clinical candidates or preclinical research molecules had substantially better selectivity or potency on-target. In some cases, we considered molecules with indirect mechanisms of action on the general pathway of interest based solely on literature evidence (e.g., captopril modulates ACE2 indirectly via its direct interaction with Angiotensin Converting Enzyme, ACE). Finally, we predicted 6 additional molecules (2 approved, 1 in clinical trials) for proteins with MIST scores between 0.7-0.6 to viral baits (Supplemental Tables 3 and 4). Complete methods can be found here (www.github.com/momeara/BioChemPantry/vignette/COVID19).

SUPPLEMENTARY INFORMATION

Supplementary table 1: Scoring results for all baits and all proteins

Supplementary table 2: SARS-CoV 2 high confidence interactors

Supplementary table 3: Literature-derived drugs and reagents that modulate SARS-Cov-2 interactors. Drug-target associations drawn from chemoinformatic searches of the literature, including information about purchasability

Supplementary table 4: Expert-identified drugs and reagents that modulate SARS-CoV-2 interactors. Drug-target associations drawn from expert knowledge of human protein interactors of SARS-Co-V2 and reagents and drugs that modulate them; not readily available from the chemoinformatically-searchable literature

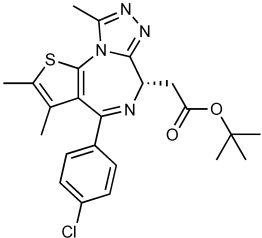
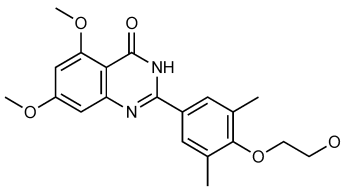
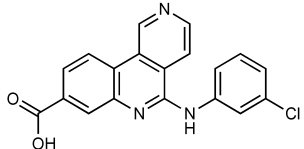
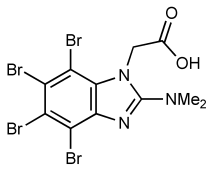
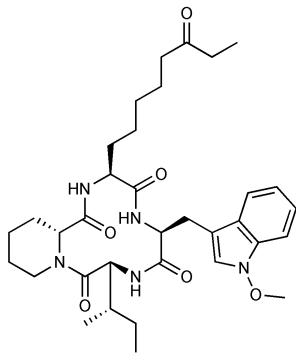
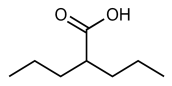
Supplementary table 5: Raw chemical associations to prey proteins IUPHAR/BPS Guide to Pharmacology (2020-3-12)

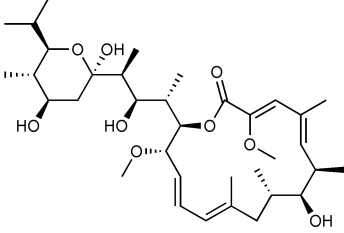
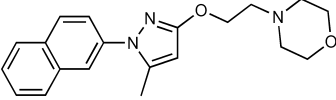
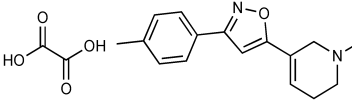
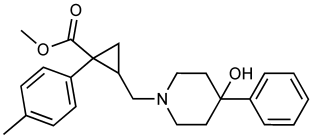
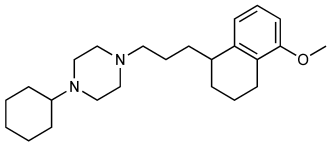
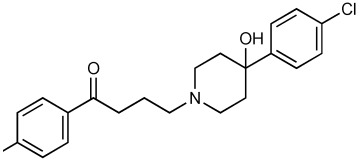
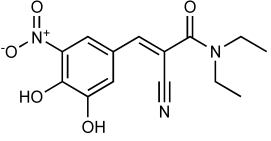
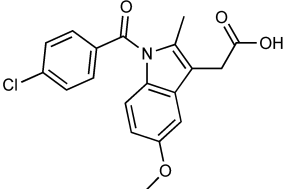
Supplementary table 6: Raw chemical associations to prey proteins ChEMBL25

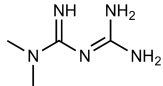
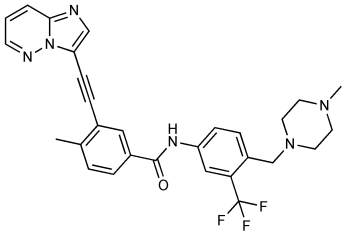
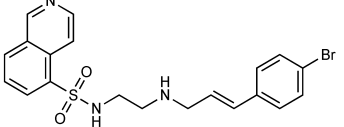
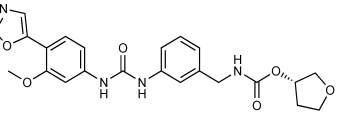
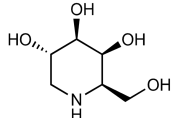
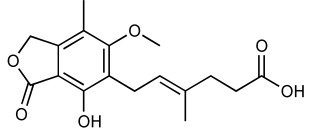
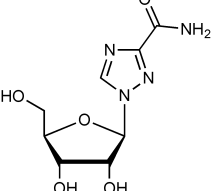
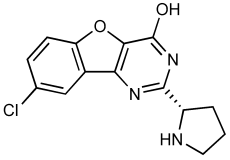
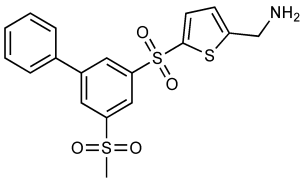
Supplementary Methods: Computational methods used to propagate tables and supplemental figures

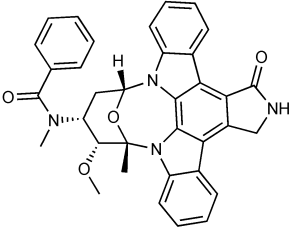
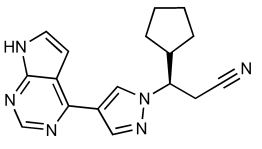
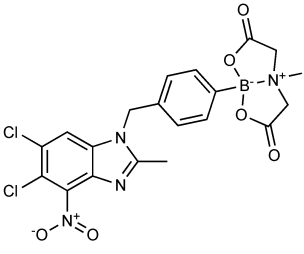
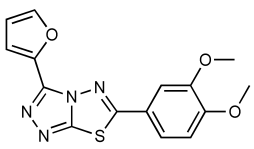
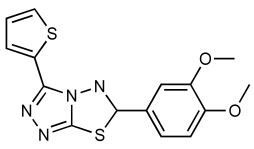
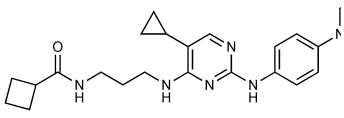
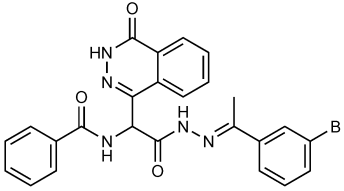
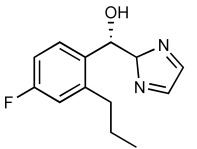
Supplementary Discussion: In depth look at the SARS-CoV-2 individual bait subnetworks

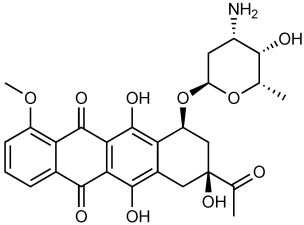
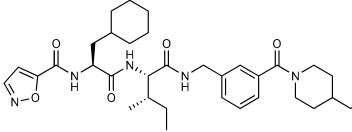
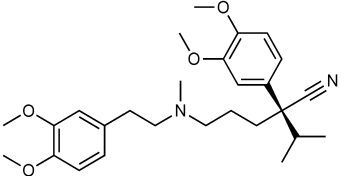
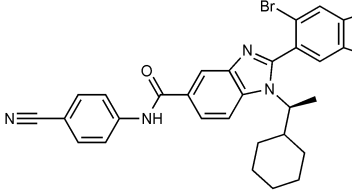
Table 1a. Literature-derived^a drugs and reagents that modulate SARS-Cov-2 interactors.

Compound Name	Compound Structure	Human Gene	Viral Bait	Drug Status	Activity (nM)
JQ1 ¹⁰⁹		BRD2/4	E	Pre-clinical	BRD inhibitor IC ₅₀ = 40-120
RVX-208 ¹⁰⁹		BRD2/4	E	Clinical Trial	BRD inhibitor IC ₅₀ = 50-1800
Silmitasertib ^{110,111}		CSNK2A2	N	Approved (Cancer)	CK2 inhibitor IC ₅₀ = 1
TMCB ¹¹²		CSNK2A2	N	Pre-clinical	Multi-targeted protein kinase inhibitor K _i = 21
Apicidin ¹¹³		HDAC2	Nsp5	Pre-clinical	HDAC inhibitor IC ₅₀ = 120
Valproic Acid ¹¹⁴⁻¹¹⁶		HDAC2	Nsp5	Approved (CNS diseases, Cancer)	HDAC2 inhibitor IC ₅₀ = 62,000

Bafilomycin A1 ¹¹⁷		ATP6AP1 ATP6V1A	Nsp6 M	Pre-clinical	ATPase inhibitor IC ₅₀ = 100
E-52862 ¹¹⁸		SIGMAR1	Nsp6	Clinical Trial	Sigma 1 antagonist IC ₅₀ = 17
PD-144418 ¹¹⁹		SIGMAR1	Nsp6	Pre-clinical	Sigma 1 antagonist K _i = 0.8
RS-PPCC ¹²⁰		SIGMAR1	Nsp6	Pre-clinical	Sigma 1 agonist K _i = 1.5
PB28 ¹²¹		SIGMAR1 TMEM97	Nsp6 Orf9c	Pre-clinical	Sigma 1/2 modulator IC ₅₀ = 15
Haloperidol ⁷²		SIGMAR1 TMEM97	Nsp6 Orf9c	Approved (CNS diseases)	Sigma 1/2 modulator K _i = 2-12
Entacapone ^{122,123}		COMT	Nsp7	Approved (Parkinson's disease)	COMT inhibitor IC ₅₀ = 151
Indomethacin ¹²⁴		PTGES2	Nsp7	Approved (Inflammation, Pain)	Prostaglandin E2 synthase inhibitor IC ₅₀ = 750

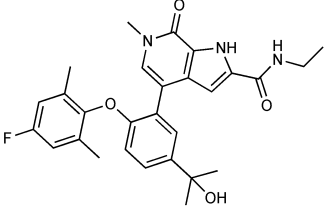
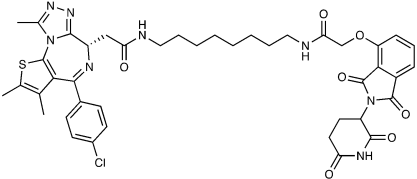
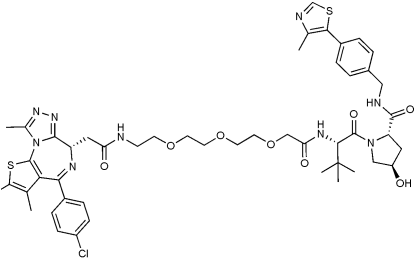
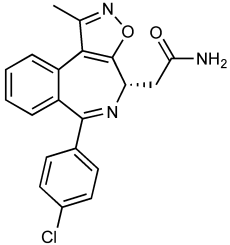
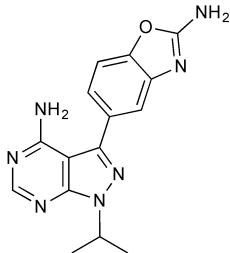
Metformin ¹²⁵		NDUFs	Nsp7 Orf9c	Approved (Diabetes)	MRC 1 inhibitor (indirect)
Ponatinib ¹²⁶		RIPK1	Nsp12	Approved (Cancer)	RIPK1 inhibitor IC ₅₀ = 12
H-89 ¹²⁷		PRKACA	Nsp13	Pre-clinical	Protein kinase A inhibitor K _D = 48
Merimepodib ¹²⁸		IMPDH2	Nsp14	Clinical Trial	IMPDH inhibitor K _i = 10
Migalastat ¹²⁹		GLA	Nsp14	Approved (Fabry disease)	α-Gal inhibitor IC ₅₀ = 40
Mycophenolic acid ¹³⁰		IMPDH2	Nsp14	Approved (Organ rejection)	IMPDH inhibitor IC ₅₀ = 20
Ribavirin ¹³¹		IMPDH2	Nsp14	Approved (Viral infection)	IMPDH inhibitor IC ₅₀ = 100-250
XL413 ¹³²		DNMT1	Orf8	Clinical Trial	CDC7 inhibitor IC ₅₀ = 3.4
CCT 365623 ¹³³		LOX	Orf8	Pre-clinical	LOXL2 inhibitor IC ₅₀ = 1500

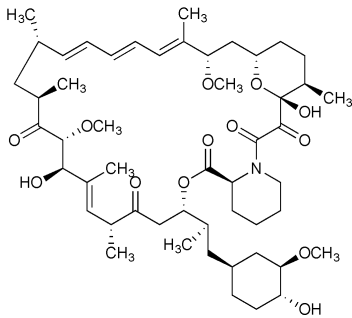
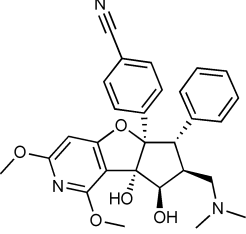
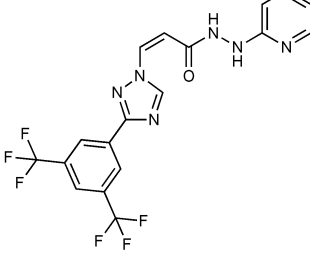
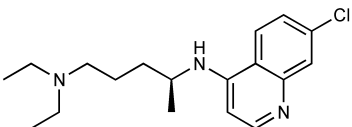
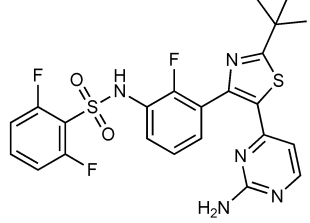
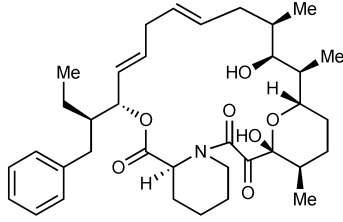
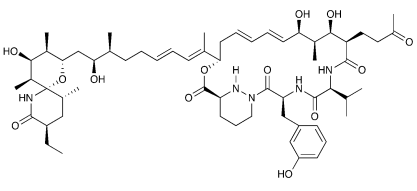
Midostaurin ¹³⁴		MARK2/3	Orf9b	Approved (Cancer)	Protein kinase inhibitor MARK1 $K_D = 100$ MARK3 $K_D = 23$
Ruxolitinib ¹³⁵		MARK2/3	Orf9b	Approved (Myelofibrosis)	Protein kinase inhibitor MARK1 $K_D = 660$ MARK3 $K_D > 10000$
ZINC1775962367 ¹³⁶		DCTPP1	Orf9b	Pre-clinical	dCTPase inhibitor $IC_{50} = 47$
ZINC4326719 ¹³⁷		DCTPP1	Orf9b	Pre-clinical	DCTPP1 inhibitor $IC_{50} = 19$
ZINC4511851 ¹³⁸		DCTPP1	Orf9b	Pre-clinical	dCTPase inhibitor $IC_{50} = 20$
ZINC95559591 ¹³⁹		MARK3 TBK1	Orf9b Nsp13	Pre-clinical	Protein kinase inhibitor MARK3 $IC_{50} = 12$ TBK1 $IC_{50} = 6$
AC-55541 ¹⁴⁰		F2RL1	Orf9c	Pre-clinical	PAR agonist $pEC_{50} = 6.7$
AZ8838 ¹⁴¹		F2RL1	Orf9c	Pre-clinical	PAR antagonist $IC_{50} = 344$

Daunorubicin ¹⁴²		ABCC1	Orf9c	Approved (Cancer)	Topoisomerase inhibitor $K_i = 70$
GB110 ¹⁴³		F2RL1	Orf9c	Pre-clinical	PAR2 agonist $EC_{50} = 280$
S-verapamil ¹⁴⁴		ABCC1	Orf9c	Approved (Hypertension)	Ca^{2+} channel inhibitor and drug efflux transporter inhibitor $K_i = 113$
AZ3451 ¹⁴¹		F2RL1	Orf9c	Pre-clinical	PAR2 negative allosteric modulator $pK_D = 15$

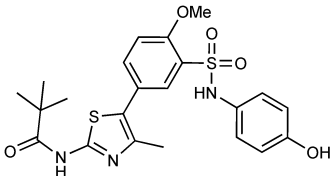
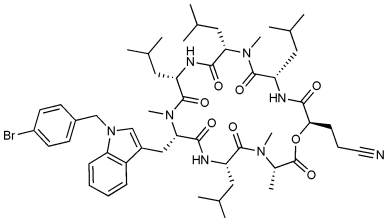
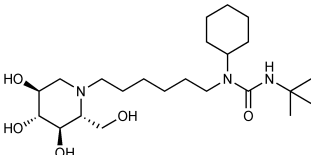
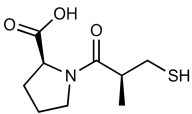
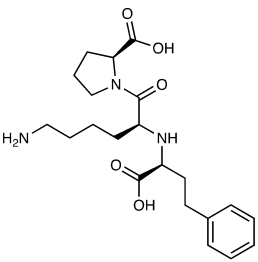
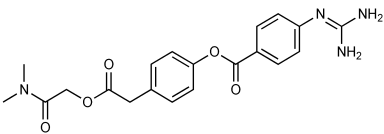
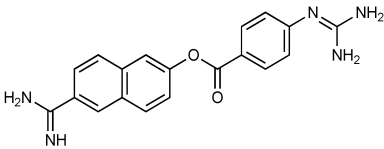
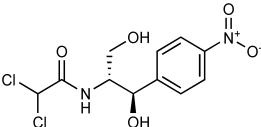
a. These drug-target associations are drawn from cheminformatic searches of the literature, drawing on databases such as ChEMBL¹⁰⁷, ZINC¹⁰⁸ and IUPHAR/BPS Guide to Pharmacology¹⁴⁵

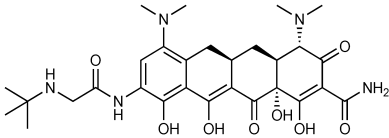
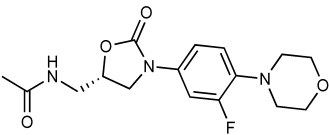
Table 1b. Expert-identified^a drugs and reagents that modulate SARS-CoV-2 interactors.

Compound Name	Compound Structure	Human Gene/ Process	Viral Bait	Drug Status	Activity (nM)
ABBV-744 ⁶⁹		BRD2/4	E	Clinical Trial	BRD inhibitor K _D = 2.1
dBET6 ¹⁴⁶		BRD2/4	E	Pre-clinical	Degrades BRD proteins IC ₅₀ < 10000
MZ1 ¹⁴⁷		BRD2/4	E	Pre-clinical	Degrades BRD proteins K _D = 120-228
CPI-0610 ¹⁴⁸		BRD2/4	E	Clinical Trial	BRD2/4 inhibitor BRD2 IC ₅₀ = 25 BRD4 IC ₅₀ = 18
Sapanisertib ^{61,149}		LARP1	N	Clinical Trial	mTOR inhibitor IC ₅₀ = 1

Rapamycin ^{61,150}		LARP1 FKBP15 FKBP7/10	N Nsp2 Orf8	Approved (Organ rejection)	mTOR inhibitor (with FKBP) IC ₅₀ = 2.0
Zotatifin ¹⁵¹		EIF4E2/H	Nsp2	Clinical Trial	EIF4a inhibitor IC ₅₀ = 1.5
Verdinexor ¹⁵²		NUPs RAE1	Nsp4 Nsp9 Orf6	Clinical Trial	XPO1 nuclear export inhibitor IC ₅₀ = 960
Chloroquine ¹⁵³		SIGMAR1	Nsp6	Approved (Malaria)	Sigma 1 binder K _i = 100
Dabrafenib ¹⁵⁴		NEK9	Nsp9	Approved (Cancer)	NEK9 inhibitor IC ₅₀ = 1
WDB002		CEP250	Nsp13	Clinical Trial	CEP250 inhibitor (with FKBP) K _d = 0.29
Sanglifehrin A ⁷³		IMPDH2	Nsp14	Pre-clinical	PPIA- IMPDH2 modulator PPIA K _D = 0.2 IDPDH2 Binding

FK-506 ¹⁵⁵		FKBP7 FKBP10	Orf8	Approved (Organ rejection)	EC ₅₀ = 11.5 (with PPIA)	FKBP binder
Pevonedistat ⁶⁸		CUL2	Orf10	Clinical Trial	NEDD8- activating enzyme inhibitor IC ₅₀ = 4.7	
Ternatin 4 ¹⁵⁶		Translation		Pre-clinical	eEF1A inhibitor IC ₅₀ = 71	
4E2RCat ¹⁵⁷		Translation		Pre-clinical	eIF4E/G PPI inhibitor IC ₅₀ = 13500	
Tomivosertib ^{158,159}		Translation		Clinical Trial	MNK1/2 inhibitor IC ₅₀ = 2.4	
Compound 2 ¹⁶⁰		Viral Transcription		Pre-clinical	Cyclophilin inhibitor K _D = 24	

Compound 10 ¹⁶¹		Viral Transcription	Pre-clinical	PI4K-III β inhibitor IC ₅₀ = 3.4
PS3061 ³⁰		ER protein processing	Pre-clinical	Sec61 inhibitor IC ₅₀ = 20-500
IHVR-19029 ^{162, 163}		ER protein processing	Clinical Trial	Antiviral activity IC ₅₀ = 1200
Captopril ¹⁶⁴		Cell Entry	Approved (Hypertension)	ACE inhibitor K _i = 3
Lisinopril ¹⁶⁵		Cell Entry	Approved (Hypertension)	ACE inhibitor K _i = 0.27
Camostat ^{166, 167}		Cell Entry	Approved (Pancreatitis)	Serine protease 1 inhibitor IC ₅₀ < 1000
Nafamostat ^{166, 168}		Cell Entry	Approved (Anticoagulant)	Serine protease 1 inhibitor IC ₅₀ = 100
Chloramphenicol ¹⁶⁹		Mitochondrial ribosome	Approved (Bacterial infection)	Mito-chondrial ribosome inhibitor IC ₅₀ = 7400

Tigecycline ¹⁷⁰		Mitochondrial ribosome	Approved (Bacterial infection)	Mitochondrial ribosome inhibitor IC ₅₀ = 3300
Linezolid ¹⁷¹		Mitochondrial ribosome	Approved (Bacterial infection)	Mitochondrial ribosome inhibitor IC ₅₀ = 16000

a. These molecules derive from expert analysis of human protein interactors of SARS-Co-V2 and reagents and drugs that modulate them; not readily available from the chemoinformatically-searchable literature.

REFERENCES

1. Wu, F. *et al.* A new coronavirus associated with human respiratory disease in China. *Nature* **579**, 265–269 (2020).
2. Novel Coronavirus (2019-nCoV) situation reports. <https://www.who.int/emergencies/diseases/novel-coronavirus-2019/situation-reports>.
3. Wang, C., Horby, P. W., Hayden, F. G. & Gao, G. F. A novel coronavirus outbreak of global health concern. *The Lancet* vol. 395 470–473 (2020).
4. Zhu, N. *et al.* China Novel Coronavirus Investigating and Research Team. A novel coronavirus from patients with pneumonia in China, 2019. *N. Engl. J. Med.* **382**, 727–733 (2020).
5. Su, S. *et al.* Epidemiology, Genetic Recombination, and Pathogenesis of Coronaviruses. *Trends Microbiol.* **24**, 490–502 (2016).
6. Wit, E. de, de Wit, E., van Doremalen, N., Falzarano, D. & Munster, V. J. SARS and MERS: recent insights into emerging coronaviruses. *Nature Reviews Microbiology* vol. 14 523–534 (2016).
7. Anderson, R. M., Heesterbeek, H., Klinkenberg, D. & Déirdre Hollingsworth, T. How will country-based mitigation measures influence the course of the COVID-19 epidemic? *The Lancet* (2020) doi:10.1016/s0140-6736(20)30567-5.
8. Gates, B. Responding to Covid-19 — A Once-in-a-Century Pandemic? *New England Journal of Medicine* (2020) doi:10.1056/nejmp2003762.
9. Zarin, D. A., Tse, T., Williams, R. J., Califf, R. M. & Ide, N. C. The ClinicalTrials.gov results database—update and key issues. *N. Engl. J. Med.* **364**, 852–860 (2011).
10. Sheahan, T. P. *et al.* Comparative therapeutic efficacy of remdesivir and combination lopinavir, ritonavir, and interferon beta against MERS-CoV. *Nat. Commun.* **11**, 222 (2020).
11. Harrison, C. Coronavirus puts drug repurposing on the fast track. *Nature Biotechnology* (2020) doi:10.1038/d41587-020-00003-1.
12. Sheahan, T. P. *et al.* An orally bioavailable broad-spectrum antiviral inhibits SARS-CoV-2 and multiple endemic, epidemic and bat coronavirus. *bioRxiv* 2020.03.19.997890 (2020) doi:10.1101/2020.03.19.997890.

13. Paton, J. Moderna's Coronavirus Vaccine Trial Set to Begin This Month. *Bloomberg News* (2020).
14. Hoffmann, M. *et al.* SARS-CoV-2 Cell Entry Depends on ACE2 and TMPRSS2 and Is Blocked by a Clinically Proven Protease Inhibitor. *Cell* (2020) doi:10.1016/j.cell.2020.02.052.
15. Prussia, A., Thepchatri, P., Snyder, J. P. & Plemper, R. K. Systematic approaches towards the development of host-directed antiviral therapeutics. *Int. J. Mol. Sci.* **12**, 4027–4052 (2011).
16. Chan, J. F.-W. *et al.* Genomic characterization of the 2019 novel human-pathogenic coronavirus isolated from a patient with atypical pneumonia after visiting Wuhan. *Emerg. Microbes Infect.* **9**, 221–236 (2020).
17. Fehr, A. R. & Perlman, S. Coronaviruses: an overview of their replication and pathogenesis. *Methods Mol. Biol.* **1282**, 1–23 (2015).
18. Chinese SARS Molecular Epidemiology Consortium. Molecular evolution of the SARS coronavirus during the course of the SARS epidemic in China. *Science* **303**, 1666–1669 (2004).
19. Jäger, S. *et al.* Global landscape of HIV-human protein complexes. *Nature* **481**, 365–370 (2012).
20. Teo, G. *et al.* SAINTexpress: improvements and additional features in Significance Analysis of INTERactome software. *J. Proteomics* **100**, 37–43 (2014).
21. SARS-CoV-2 infected host cell proteomics reveal potential therapy targets. *In Review* (2020).
22. Batra, J. *et al.* Protein Interaction Mapping Identifies RBBP6 as a Negative Regulator of Ebola Virus Replication. *Cell* **175**, 1917–1930.e13 (2018).
23. Li, M. *et al.* Identification of antiviral roles for the exon-junction complex and nonsense-mediated decay in flaviviral infection. *Nat Microbiol* (2019) doi:10.1038/s41564-019-0375-z.
24. Eckhardt, M. *et al.* Multiple Routes to Oncogenesis Are Promoted by the Human Papillomavirus-Host Protein Network. *Cancer Discov.* **8**, 1474–1489 (2018).
25. Diep, J. *et al.* Enterovirus pathogenesis requires the host methyltransferase SETD3. *Nat Microbiol* **4**, 2523–2537 (2019).
26. Mirrashidi, K. M. *et al.* Global Mapping of the Inc-Human Interactome Reveals that Retromer Restricts Chlamydia Infection. *Cell Host Microbe* **18**, 109–121 (2015).
27. Penn, B. H. *et al.* An Mtb-Human Protein-Protein Interaction Map Identifies a Switch between Host Antiviral and Antibacterial Responses. *Mol. Cell* **71**, 637–648.e5 (2018).

28. Ramage, H. R. *et al.* A combined proteomics/genomics approach links hepatitis C virus infection with nonsense-mediated mRNA decay. *Mol. Cell* **57**, 329–340 (2015).
29. Davis, Z. H. *et al.* Global mapping of herpesvirus-host protein complexes reveals a transcription strategy for late genes. *Mol. Cell* **57**, 349–360 (2015).
30. Shah, P. S. *et al.* Comparative Flavivirus-Host Protein Interaction Mapping Reveals Mechanisms of Dengue and Zika Virus Pathogenesis. *Cell* **175**, 1931–1945.e18 (2018).
31. Harcourt, J. *et al.* Severe Acute Respiratory Syndrome Coronavirus 2 from Patient with 2019 Novel Coronavirus Disease, United States. *Emerg. Infect. Dis.* **26**, (2020).
32. Wang, D. *et al.* A deep proteome and transcriptome abundance atlas of 29 healthy human tissues. *Mol. Syst. Biol.* **15**, e8503 (2019).
33. SARS-CoV-2 infected host cell proteomics reveal potential therapy targets. *In Review* (2020)
doi:10.21203/rs.3.rs-17218/v1.
34. Karczewski, K. J. *et al.* Variation across 141,456 human exomes and genomes reveals the spectrum of loss-of-function intolerance across human protein-coding genes. *bioRxiv* 531210 (2019)
doi:10.1101/531210.
35. Chamberlain, L. H. & Shipston, M. J. The physiology of protein S-acylation. *Physiol. Rev.* **95**, 341–376 (2015).
36. Petit, C. M. *et al.* Palmitoylation of the cysteine-rich endodomain of the SARS-coronavirus spike glycoprotein is important for spike-mediated cell fusion. *Virology* **360**, 264–274 (2007).
37. Sergeeva, O. A. & van der Goot, F. G. Anthrax toxin requires ZDHHC5-mediated palmitoylation of its surface-processing host enzymes. *Proc. Natl. Acad. Sci. U. S. A.* **116**, 1279–1288 (2019).
38. Barnes, P. J. Role of HDAC2 in the pathophysiology of COPD. *Annu. Rev. Physiol.* **71**, 451–464 (2009).
39. Xu, P. *et al.* NOS1 inhibits the interferon response of cancer cells by S-nitrosylation of HDAC2. *J. Exp. Clin. Cancer Res.* **38**, 483 (2019).
40. Dewe, J. M., Fuller, B. L., Lentini, J. M., Kellner, S. M. & Fu, D. TRMT1-Catalyzed tRNA Modifications Are Required for Redox Homeostasis To Ensure Proper Cellular Proliferation and Oxidative Stress Survival. *Mol. Cell. Biol.* **37**, (2017).

41. Ryzhakov, G. & Randow, F. SINTBAD, a novel component of innate antiviral immunity, shares a TBK1-binding domain with NAP1 and TANK. *EMBO J.* **26**, 3180–3190 (2007).
42. Ramasamy, S. *et al.* Tle1 tumor suppressor negatively regulates inflammation in vivo and modulates NF- κ B inflammatory pathway. *Proc. Natl. Acad. Sci. U. S. A.* **113**, 1871–1876 (2016).
43. Zhang, X., Li, X., Ning, F., Shang, Y. & Hu, X. TLE4 acts as a corepressor of Hes1 to inhibit inflammatory responses in macrophages. *Protein Cell* **10**, 300–305 (2019).
44. Tetsuka, T. *et al.* Inhibition of nuclear factor-kappaB-mediated transcription by association with the amino-terminal enhancer of split, a Groucho-related protein lacking WD40 repeats. *J. Biol. Chem.* **275**, 4383–4390 (2000).
45. Wang, C. *et al.* The E3 ubiquitin ligase Nrdp1 'preferentially' promotes TLR-mediated production of type I interferon. *Nat. Immunol.* **10**, 744–752 (2009).
46. Kondo, T., Watanabe, M. & Hatakeyama, S. TRIM59 interacts with ECSIT and negatively regulates NF- κ B and IRF-3/7-mediated signal pathways. *Biochem. Biophys. Res. Commun.* **422**, 501–507 (2012).
47. Li, S., Wang, L., Berman, M., Kong, Y.-Y. & Dorf, M. E. Mapping a dynamic innate immunity protein interaction network regulating type I interferon production. *Immunity* **35**, 426–440 (2011).
48. Xia, X. *et al.* NLRX1 negatively regulates TLR-induced NF- κ B signaling by targeting TRAF6 and IKK. *Immunity* **34**, 843–853 (2011).
49. Kanke, T. *et al.* Proteinase-activated receptor-2-mediated activation of stress-activated protein kinases and inhibitory kappa B kinases in NCTC 2544 keratinocytes. *J. Biol. Chem.* **276**, 31657–31666 (2001).
50. Matsuda, A. *et al.* Large-scale identification and characterization of human genes that activate NF-kappaB and MAPK signaling pathways. *Oncogene* **22**, 3307–3318 (2003).
51. Liu, X.-Y., Wei, B., Shi, H.-X., Shan, Y.-F. & Wang, C. Tom70 mediates activation of interferon regulatory factor 3 on mitochondria. *Cell Res.* **20**, 994–1011 (2010).
52. Reineke, L. C. & Lloyd, R. E. The stress granule protein G3BP1 recruits protein kinase R to promote multiple innate immune antiviral responses. *J. Virol.* **89**, 2575–2589 (2015).
53. Yang, W. *et al.* G3BP1 inhibits RNA virus replication by positively regulating RIG-I-mediated cellular antiviral response. *Cell Death Dis.* **10**, 946 (2019).

54. Kim, S. S.-Y., Sze, L., Liu, C. & Lam, K.-P. The stress granule protein G3BP1 binds viral dsRNA and RIG-I to enhance interferon- β response. *J. Biol. Chem.* **294**, 6430–6438 (2019).
55. Raaben, M., Groot Koerkamp, M. J. A., Rottier, P. J. M. & de Haan, C. A. M. Mouse hepatitis coronavirus replication induces host translational shutoff and mRNA decay, with concomitant formation of stress granules and processing bodies. *Cell. Microbiol.* **9**, 2218–2229 (2007).
56. Nakagawa, K., Narayanan, K., Wada, M. & Makino, S. Inhibition of Stress Granule Formation by Middle East Respiratory Syndrome Coronavirus 4a Accessory Protein Facilitates Viral Translation, Leading to Efficient Virus Replication. *J. Virol.* **92**, (2018).
57. Ivanov, P., Kedersha, N. & Anderson, P. Stress Granules and Processing Bodies in Translational Control. *Cold Spring Harb. Perspect. Biol.* **11**, (2019).
58. Slaine, P. D., Kleer, M., Smith, N. K., Khapersky, D. A. & McCormick, C. Stress Granule-Inducing Eukaryotic Translation Initiation Factor 4A Inhibitors Block Influenza A Virus Replication. *Viruses* **9**, (2017).
59. Thompson, P. A. *et al.* Abstract 2698: eFT226, a potent and selective inhibitor of eIF4A, is efficacious in preclinical models of lymphoma. *Experimental and Molecular Therapeutics* (2019) doi:10.1158/1538-7445.am2019-2698.
60. Reineke, L. C. *et al.* Casein Kinase 2 Is Linked to Stress Granule Dynamics through Phosphorylation of the Stress Granule Nucleating Protein G3BP1. *Mol. Cell. Biol.* **37**, (2017).
61. Fonseca, B. D., Jia, J. J., Hollensen, A. K. & Pointet, R. LARP1 is a major phosphorylation substrate of mTORC1. *bioRxiv* (2018).
62. Kindrachuk, J. *et al.* Antiviral potential of ERK/MAPK and PI3K/AKT/mTOR signaling modulation for Middle East respiratory syndrome coronavirus infection as identified by temporal kinome analysis. *Antimicrob. Agents Chemother.* **59**, 1088–1099 (2015).
63. Frieman, M. *et al.* Severe acute respiratory syndrome coronavirus ORF6 antagonizes STAT1 function by sequestering nuclear import factors on the rough endoplasmic reticulum/Golgi membrane. *J. Virol.* **81**, 9812–9824 (2007).
64. Faria, P. A. *et al.* VSV disrupts the Rae1/mrnp41 mRNA nuclear export pathway. *Mol. Cell* **17**, 93–102 (2005).

65. Timms, R. T. *et al.* A glycine-specific N-degron pathway mediates the quality control of protein N-myristoylation. *Science* **365**, (2019).
66. Quan, B., Seo, H.-S., Blobel, G. & Ren, Y. Vesiculoviral matrix (M) protein occupies nucleic acid binding site at nucleoporin pair (Rae1 • Nup98). *Proc. Natl. Acad. Sci. U. S. A.* **111**, 9127–9132 (2014).
67. Mahon, C., Krogan, N. J., Craik, C. S. & Pick, E. Cullin E3 ligases and their rewiring by viral factors. *Biomolecules* **4**, 897–930 (2014).
68. Soucy, T. A. *et al.* An inhibitor of NEDD8-activating enzyme as a new approach to treat cancer. *Nature* **458**, 732–736 (2009).
69. Faivre, E. J. *et al.* Selective inhibition of the BD2 bromodomain of BET proteins in prostate cancer. *Nature* **578**, 306–310 (2020).
70. Filippakopoulos, P. *et al.* Histone recognition and large-scale structural analysis of the human bromodomain family. *Cell* **149**, 214–231 (2012).
71. Mitsuda, T. *et al.* Sigma-1Rs are upregulated via PERK/eIF2 α /ATF4 pathway and execute protective function in ER stress. *Biochem. Biophys. Res. Commun.* **415**, 519–525 (2011).
72. Hellewell, S. B. *et al.* Rat liver and kidney contain high densities of sigma 1 and sigma 2 receptors: characterization by ligand binding and photoaffinity labeling. *Eur. J. Pharmacol.* **268**, 9–18 (1994).
73. Pua, K. H., Stiles, D. T., Sowa, M. E. & Verdine, G. L. IMPDH2 Is an Intracellular Target of the Cyclophilin A and Sanglifehrin A Complex. *Cell Rep.* **18**, 432–442 (2017).
74. Hanada, H., Moriyama, Y., Maeda, M. & Futai, M. Kinetic studies of chromaffin granule H⁺-ATPase and effects of bafilomycin A1. *Biochem. Biophys. Res. Commun.* **170**, 873–878 (1990).
75. Wang, M. *et al.* Remdesivir and chloroquine effectively inhibit the recently emerged novel coronavirus (2019-nCoV) in vitro. *Cell Res.* **30**, 269–271 (2020).
76. Gao, J., Tian, Z. & Yang, X. Breakthrough: Chloroquine phosphate has shown apparent efficacy in treatment of COVID-19 associated pneumonia in clinical studies. *Biosci. Trends* **14**, 72–73 (2020).
77. McKee, E. E., Ferguson, M., Bentley, A. T. & Marks, T. A. Inhibition of mammalian mitochondrial protein synthesis by oxazolidinones. *Antimicrob. Agents Chemother.* **50**, 2042–2049 (2006).
78. Skrtić, M. *et al.* Inhibition of mitochondrial translation as a therapeutic strategy for human acute myeloid

- leukemia. *Cancer Cell* **20**, 674–688 (2011).
79. Hultquist, J. F. *et al.* A Cas9 Ribonucleoprotein Platform for Functional Genetic Studies of HIV-Host Interactions in Primary Human T Cells. *Cell Rep.* **17**, 1438–1452 (2016).
80. Gordon, D. E. *et al.* A Quantitative Genetic Interaction Map of HIV Infection. *Mol. Cell* (2020) doi:10.1016/j.molcel.2020.02.004.
81. Naffouje, R. *et al.* Anti-Tumor Potential of IMP Dehydrogenase Inhibitors: A Century-Long Story. *Cancers* **11**, (2019).
82. Franklin, T. J. & Cook, J. M. The inhibition of nucleic acid synthesis by mycophenolic acid. *Biochem. J* **113**, 515–524 (1969).
83. Organization, W. H. & Others. *World Health Organization model list of essential medicines: 21st list 2019*. <https://apps.who.int/iris/handle/10665/325771> (2019).
84. Tan, E. L. C. *et al.* Inhibition of SARS coronavirus infection in vitro with clinically approved antiviral drugs. *Emerg. Infect. Dis.* **10**, 581–586 (2004).
85. Markland, W., McQuaid, T. J., Jain, J. & Kwong, A. D. Broad-spectrum antiviral activity of the IMP dehydrogenase inhibitor VX-497: a comparison with ribavirin and demonstration of antiviral additivity with alpha interferon. *Antimicrob. Agents Chemother.* **44**, 859–866 (2000).
86. Le Sage, V., Cinti, A., Amorim, R. & Mouland, A. J. Adapting the Stress Response: Viral Subversion of the mTOR Signaling Pathway. *Viruses* **8**, (2016).
87. Ranadheera, C., Coombs, K. M. & Kobasa, D. Comprehending a Killer: The Akt/mTOR Signaling Pathways Are Temporally High-Jacked by the Highly Pathogenic 1918 Influenza Virus. *EBioMedicine* **32**, 142–163 (2018).
88. Cota, D. *et al.* Hypothalamic mTOR signaling regulates food intake. *Science* **312**, 927–930 (2006).
89. Hägglund, M. G. A. *et al.* B(0)AT2 (SLC6A15) is localized to neurons and astrocytes, and is involved in mediating the effect of leucine in the brain. *PLoS One* **8**, e58651 (2013).
90. Yang, D. & Leibowitz, J. L. The structure and functions of coronavirus genomic 3' and 5' ends. *Virus Res.* **206**, 120–133 (2015).
91. Barretto, N. *et al.* The papain-like protease of severe acute respiratory syndrome coronavirus has

- deubiquitinating activity. *J. Virol.* **79**, 15189–15198 (2005).
92. Yang, H. *et al.* The crystal structures of severe acute respiratory syndrome virus main protease and its complex with an inhibitor. *Proc. Natl. Acad. Sci. U. S. A.* **100**, 13190–13195 (2003).
93. Thiel, V. *et al.* Mechanisms and enzymes involved in SARS coronavirus genome expression. *J. Gen. Virol.* **84**, 2305–2315 (2003).
94. Chiva, C. *et al.* QCloud: A cloud-based quality control system for mass spectrometry-based proteomics laboratories. *PLoS One* **13**, e0189209 (2018).
95. Cox, J. & Mann, M. MaxQuant enables high peptide identification rates, individualized p.p.b.-range mass accuracies and proteome-wide protein quantification. *Nat. Biotechnol.* **26**, 1367–1372 (2008).
96. Cox, J. *et al.* Accurate Proteome-wide Label-free Quantification by Delayed Normalization and Maximal Peptide Ratio Extraction, Termed MaxLFQ. *Mol. Cell. Proteomics* **13**, 2513–2526 (2014).
97. Verschueren, E. *et al.* Scoring Large-Scale Affinity Purification Mass Spectrometry Datasets with MiST. *Curr. Protoc. Bioinformatics* **49**, 8.19.1–16 (2015).
98. Giurgiu, M. *et al.* CORUM: the comprehensive resource of mammalian protein complexes-2019. *Nucleic Acids Res.* **47**, D559–D563 (2019).
99. Shannon, P. *et al.* Cytoscape: a software environment for integrated models of biomolecular interaction networks. *Genome Res.* **13**, 2498–2504 (2003).
100. Huttlin, E. L. *et al.* The BioPlex Network: A Systematic Exploration of the Human Interactome. *Cell* **162**, 425–440 (2015).
101. Vizcaíno, J. A. *et al.* ProteomeXchange provides globally coordinated proteomics data submission and dissemination. *Nat. Biotechnol.* **32**, 223–226 (2014).
102. Deutsch, E. W. *et al.* The ProteomeXchange consortium in 2017: supporting the cultural change in proteomics public data deposition. *Nucleic Acids Res.* **45**, D1100–D1106 (2017).
103. Chaudhury, S., Lyskov, S. & Gray, J. J. PyRosetta: a script-based interface for implementing molecular modeling algorithms using Rosetta. *Bioinformatics* **26**, 689–691 (2010).
104. Joosten, R. P., Long, F., Murshudov, G. N. & Perrakis, A. The PDB_REDO server for macromolecular structure model optimization. *IUCrJ* **1**, 213–220 (2014).

105. Waterhouse, A. *et al.* SWISS-MODEL: homology modelling of protein structures and complexes. *Nucleic Acids Res.* **46**, W296–W303 (2018).
106. Webb, B. & Sali, A. Comparative Protein Structure Modeling Using MODELLER. *Curr. Protoc. Bioinformatics* **54**, 5.6.1–5.6.37 (2016).
107. Gaulton, A. *et al.* The ChEMBL database in 2017. *Nucleic Acids Res.* **45**, D945–D954 (2017).
108. Sterling, T. & Irwin, J. J. ZINC 15--Ligand Discovery for Everyone. *J. Chem. Inf. Model.* **55**, 2324–2337 (2015).
109. McLure, K. G. *et al.* RVX-208, an inducer of ApoA-I in humans, is a BET bromodomain antagonist. *PLoS One* **8**, e83190 (2013).
110. Pierre, F. *et al.* Discovery and SAR of 5-(3-chlorophenylamino)benzo[c][2,6]naphthyridine-8-carboxylic acid (CX-4945), the first clinical stage inhibitor of protein kinase CK2 for the treatment of cancer. *J. Med. Chem.* **54**, 635–654 (2011).
111. Siddiqui-Jain, A. *et al.* CX-4945, an orally bioavailable selective inhibitor of protein kinase CK2, inhibits prosurvival and angiogenic signaling and exhibits antitumor efficacy. *Cancer Res.* **70**, 10288–10298 (2010).
112. Janeczko, M., Orzeszko, A., Kazimierczuk, Z., Szyszka, R. & Baier, A. CK2 α and CK2 α' subunits differ in their sensitivity to 4,5,6,7-tetrabromo- and 4,5,6,7-tetraiodo-1H-benzimidazole derivatives. *Eur. J. Med. Chem.* **47**, 345–350 (2012).
113. Khan, N. *et al.* Determination of the class and isoform selectivity of small-molecule histone deacetylase inhibitors. *Biochem. J* **409**, 581–589 (2008).
114. Göttlicher, M. *et al.* Valproic acid defines a novel class of HDAC inhibitors inducing differentiation of transformed cells. *EMBO J.* **20**, 6969–6978 (2001).
115. Krämer, O. H. *et al.* The histone deacetylase inhibitor valproic acid selectively induces proteasomal degradation of HDAC2. *EMBO J.* **22**, 3411–3420 (2003).
116. Fass, D. M. *et al.* Effect of Inhibiting Histone Deacetylase with Short-Chain Carboxylic Acids and Their Hydroxamic Acid Analogs on Vertebrate Development and Neuronal Chromatin. *ACS Med. Chem. Lett.* **2**, 39–42 (2010).

117. Gagliardi, S. *et al.* 5-(5,6-Dichloro-2-indolyl)-2-methoxy-2,4-pentadienamides: novel and selective inhibitors of the vacuolar H⁺-ATPase of osteoclasts with bone antiresorptive activity. *J. Med. Chem.* **41**, 1568–1573 (1998).
118. Díaz, J. L. *et al.* Synthesis and biological evaluation of the 1-arylpyrazole class of $\sigma(1)$ receptor antagonists: identification of 4-{2-[5-methyl-1-(naphthalen-2-yl)-1H-pyrazol-3-yloxy]ethyl}morpholine (S1RA, E-52862). *J. Med. Chem.* **55**, 8211–8224 (2012).
119. Akunne, H. C. *et al.* The pharmacology of the novel and selective sigma ligand, PD 144418. *Neuropharmacology* **36**, 51–62 (1997).
120. Prezzavento, O. *et al.* Novel sigma receptor ligands: synthesis and biological profile. *J. Med. Chem.* **50**, 951–961 (2007).
121. Azzariti, A. *et al.* Cyclohexylpiperazine derivative PB28, a sigma2 agonist and sigma1 antagonist receptor, inhibits cell growth, modulates P-glycoprotein, and synergizes with anthracyclines in breast cancer. *Mol. Cancer Ther.* **5**, 1807–1816 (2006).
122. Nissinen, E., Lindén, I. B., Schultz, E. & Pohto, P. Biochemical and pharmacological properties of a peripherally acting catechol-O-methyltransferase inhibitor entacapone. *Naunyn. Schmiedebergs. Arch. Pharmacol.* **346**, 262–266 (1992).
123. De Santi, C., Giulianotti, P. C., Pietrabissa, A., Mosca, F. & Pacifici, G. M. Catechol-O-methyltransferase: variation in enzyme activity and inhibition by entacapone and tolcapone. *Eur. J. Clin. Pharmacol.* **54**, 215–219 (1998).
124. Vane, J. R. Inhibition of prostaglandin synthesis as a mechanism of action for aspirin-like drugs. *Nat. New Biol.* **231**, 232–235 (1971).
125. Wheaton, W. W. *et al.* Metformin inhibits mitochondrial complex I of cancer cells to reduce tumorigenesis. *Elife* **3**, e02242 (2014).
126. Najjar, M. *et al.* Structure guided design of potent and selective ponatinib-based hybrid inhibitors for RIPK1. *Cell Rep.* **10**, 1850–1860 (2015).
127. Chijiwa, T. *et al.* Inhibition of forskolin-induced neurite outgrowth and protein phosphorylation by a newly synthesized selective inhibitor of cyclic AMP-dependent protein kinase, N-[2-(p-

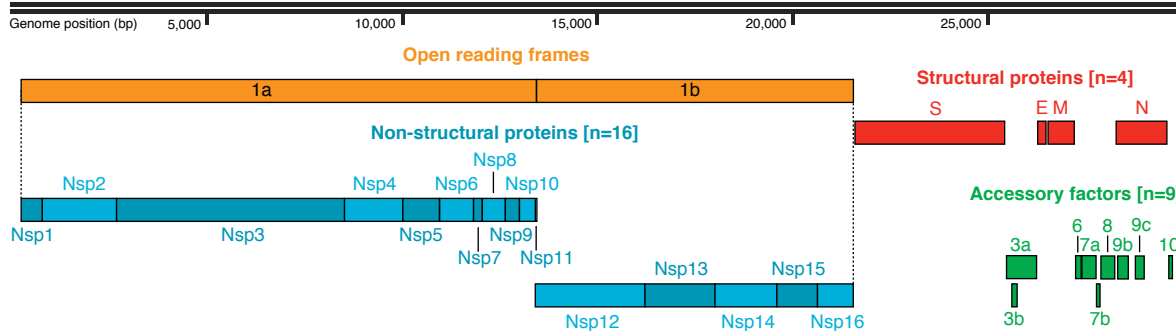
- bromocinnamylamino)ethyl]-5-isoquinolinesulfonamide (H-89), of PC12D pheochromocytoma cells. *J. Biol. Chem.* **265**, 5267–5272 (1990).
128. Sintchak, M. D. & Nimmesgern, E. The structure of inosine 5'-monophosphate dehydrogenase and the design of novel inhibitors. *Immunopharmacology* **47**, 163–184 (2000).
129. Asano, N. *et al.* In vitro inhibition and intracellular enhancement of lysosomal alpha-galactosidase A activity in Fabry lymphoblasts by 1-deoxygalactonojirimycin and its derivatives. *Eur. J. Biochem.* **267**, 4179–4186 (2000).
130. Carter, S. B. *et al.* Mycophenolic acid: an anti-cancer compound with unusual properties. *Nature* **223**, 848–850 (1969).
131. Wittine, K. *et al.* Novel 1,2,4-triazole and imidazole derivatives of L-ascorbic and imino-ascorbic acid: synthesis, anti-HCV and antitumor activity evaluations. *Bioorg. Med. Chem.* **20**, 3675–3685 (2012).
132. Koltun, E. S. *et al.* Discovery of XL413, a potent and selective CDC7 inhibitor. *Bioorg. Med. Chem. Lett.* **22**, 3727–3731 (2012).
133. Leung, L. *et al.* Anti-metastatic Inhibitors of Lysyl Oxidase (LOX): Design and Structure-Activity Relationships. *J. Med. Chem.* **62**, 5863–5884 (2019).
134. Karaman, M. W. *et al.* A quantitative analysis of kinase inhibitor selectivity. *Nat. Biotechnol.* **26**, 127–132 (2008).
135. Davis, M. I. *et al.* Comprehensive analysis of kinase inhibitor selectivity. *Nat. Biotechnol.* **29**, 1046–1051 (2011).
136. Llona-Minguez, S. *et al.* Discovery of the First Potent and Selective Inhibitors of Human dCTP Pyrophosphatase 1. *J. Med. Chem.* **59**, 1140–1148 (2016).
137. Llona-Minguez, S. *et al.* Identification of Triazolothiadiazoles as Potent Inhibitors of the dCTP Pyrophosphatase 1. *J. Med. Chem.* **60**, 2148–2154 (2017).
138. Llona-Minguez, S. *et al.* Diverse heterocyclic scaffolds as dCTP pyrophosphatase 1 inhibitors. Part 2: Pyridone- and pyrimidinone-derived systems. *Bioorg. Med. Chem. Lett.* **27**, 3219–3225 (2017).
139. McIver, E. G. *et al.* Synthesis and structure-activity relationships of a novel series of pyrimidines as potent inhibitors of TBK1/IKK ϵ kinases. *Bioorg. Med. Chem. Lett.* **22**, 7169–7173 (2012).

140. Seitzberg, J. G. *et al.* Discovery of potent and selective small-molecule PAR-2 agonists. *J. Med. Chem.* **51**, 5490–5493 (2008).
141. Cheng, R. K. Y. *et al.* Structural insight into allosteric modulation of protease-activated receptor 2. *Nature* **545**, 112–115 (2017).
142. Priebe, W. *et al.* Doxorubicin- and Daunorubicin-Glutathione Conjugates, but Not Unconjugated Drugs, Competitively Inhibit Leukotriene C₄ Transport Mediated by MRP/GS-X Pump. *Biochemical and Biophysical Research Communications* vol. 247 859–863 (1998).
143. Barry, G. D. *et al.* Novel agonists and antagonists for human protease activated receptor 2. *J. Med. Chem.* **53**, 7428–7440 (2010).
144. Perrotton, T., Trompier, D., Chang, X.-B., Di Pietro, A. & Baubichon-Cortay, H. (R)- and (S)-verapamil differentially modulate the multidrug-resistant protein MRP1. *J. Biol. Chem.* **282**, 31542–31548 (2007).
145. Armstrong, J. F. *et al.* The IUPHAR/BPS Guide to PHARMACOLOGY in 2020: extending immunopharmacology content and introducing the IUPHAR/MMV Guide to MALARIA PHARMACOLOGY. *Nucleic Acids Res.* **48**, D1006–D1021 (2020).
146. Xu, L. *et al.* Targetable BET proteins- and E2F1-dependent transcriptional program maintains the malignancy of glioblastoma. *Proc. Natl. Acad. Sci. U. S. A.* **115**, E5086–E5095 (2018).
147. Zengerle, M., Chan, K.-H. & Ciulli, A. Selective Small Molecule Induced Degradation of the BET Bromodomain Protein BRD4. *ACS Chem. Biol.* **10**, 1770–1777 (2015).
148. Albrecht, B. K. *et al.* Identification of a Benzoisoxazoloazepine Inhibitor (CPI-0610) of the Bromodomain and Extra-Terminal (BET) Family as a Candidate for Human Clinical Trials. *J. Med. Chem.* **59**, 1330–1339 (2016).
149. Schenone, S., Brullo, C., Musumeci, F., Radi, M. & Botta, M. ATP-competitive inhibitors of mTOR: an update. *Curr. Med. Chem.* **18**, 2995–3014 (2011).
150. Toral-Barza, L. *et al.* Characterization of the cloned full-length and a truncated human target of rapamycin: activity, specificity, and enzyme inhibition as studied by a high capacity assay. *Biochem. Biophys. Res. Commun.* **332**, 304–310 (2005).
151. Thompson, P. A. *et al.* Abstract 2698: eFT226, a potent and selective inhibitor of eIF4A, is efficacious in

- preclinical models of lymphoma. in *Experimental and Molecular Therapeutics* 2698–2698 (American Association for Cancer Research, 2019).
152. Jorquera, P. A. *et al.* Verdinexor (KPT-335), a Selective Inhibitor of Nuclear Export, Reduces Respiratory Syncytial Virus Replication In Vitro. *J. Virol.* **93**, (2019).
153. Tesei, A. *et al.* Sigma Receptors as Endoplasmic Reticulum Stress ‘Gatekeepers’ and their Modulators as Emerging New Weapons in the Fight Against Cancer. *Front. Pharmacol.* **9**, 711 (2018).
154. Phadke, M. *et al.* Dabrafenib inhibits the growth of BRAF-WT cancers through CDK16 and NEK9 inhibition. *Mol. Oncol.* **12**, 74–88 (2018).
155. Nakamura, T. *et al.* Molecular cloning, characterization, and chromosomal localization of FKBP23, a novel FK506-binding protein with Ca²⁺-binding ability. *Genomics* **54**, 89–98 (1998).
156. Carelli, J. D. *et al.* Ternatin and improved synthetic variants kill cancer cells by targeting the elongation factor-1A ternary complex. *Elife* **4**, (2015).
157. Cencic, R. *et al.* Blocking eIF4E-eIF4G interaction as a strategy to impair coronavirus replication. *J. Virol.* **85**, 6381–6389 (2011).
158. Reich, S. H. *et al.* Structure-based Design of Pyridone-Aminal eFT508 Targeting Dysregulated Translation by Selective Mitogen-activated Protein Kinase Interacting Kinases 1 and 2 (MNK1/2) Inhibition. *J. Med. Chem.* **61**, 3516–3540 (2018).
159. Xu, Y. *et al.* Translation control of the immune checkpoint in cancer and its therapeutic targeting. *Nat. Med.* **25**, 301–311 (2019).
160. Mackman, R. L. *et al.* Discovery of a Potent and Orally Bioavailable Cyclophilin Inhibitor Derived from the Sanglifehrin Macrocycle. *J. Med. Chem.* **61**, 9473–9499 (2018).
161. Rutaganira, F. U. *et al.* Design and Structural Characterization of Potent and Selective Inhibitors of Phosphatidylinositol 4 Kinase III β . *J. Med. Chem.* **59**, 1830–1839 (2016).
162. Ma, J. *et al.* Ester Prodrugs of IHVR-19029 with Enhanced Oral Exposure and Prevention of Gastrointestinal Glucosidase Interaction. *ACS Med. Chem. Lett.* **8**, 157–162 (2017).
163. Ma, J. *et al.* Enhancing the antiviral potency of ER α -glucosidase inhibitor IHVR-19029 against hemorrhagic fever viruses in vitro and in vivo. *Antiviral Res.* **150**, 112–122 (2018).

164. Michaud, A., Williams, T. A., Chauvet, M. T. & Corvol, P. Substrate dependence of angiotensin I-converting enzyme inhibition: captopril displays a partial selectivity for inhibition of N-acetyl-seryl-aspartyl-lysyl-proline hydrolysis compared with that of angiotensin I. *Mol. Pharmacol.* **51**, 1070–1076 (1997).
165. Natesh, R., Schwager, S. L. U., Sturrock, E. D. & Acharya, K. R. Crystal structure of the human angiotensin-converting enzyme-lisinopril complex. *Nature* **421**, 551–554 (2003).
166. Hoffmann, M. *et al.* The novel coronavirus 2019 (2019-nCoV) uses the SARS-coronavirus receptor ACE2 and the cellular protease TMPRSS2 for entry into target cells. *bioRxiv* 2020.01.31.929042 (2020) doi:10.1101/2020.01.31.929042.
167. Kawase, M., Shirato, K., van der Hoek, L., Taguchi, F. & Matsuyama, S. Simultaneous treatment of human bronchial epithelial cells with serine and cysteine protease inhibitors prevents severe acute respiratory syndrome coronavirus entry. *J. Virol.* **86**, 6537–6545 (2012).
168. Yamamoto, M. *et al.* Identification of Nafamostat as a Potent Inhibitor of Middle East Respiratory Syndrome Coronavirus S Protein-Mediated Membrane Fusion Using the Split-Protein-Based Cell-Cell Fusion Assay. *Antimicrob. Agents Chemother.* **60**, 6532–6539 (2016).
169. Kandasamy, J. *et al.* Increased selectivity toward cytoplasmic versus mitochondrial ribosome confers improved efficiency of synthetic aminoglycosides in fixing damaged genes: a strategy for treatment of genetic diseases caused by nonsense mutations. *J. Med. Chem.* **55**, 10630–10643 (2012).
170. Martin, T. D. *et al.* A Role for Mitochondrial Translation in Promotion of Viability in K-Ras Mutant Cells. *Cell Rep.* **20**, 427–438 (2017).
171. Nagiec, E. E. *et al.* Oxazolidinones inhibit cellular proliferation via inhibition of mitochondrial protein synthesis. *Antimicrob. Agents Chemother.* **49**, 3896–3902 (2005).

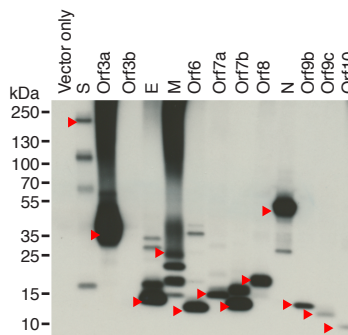
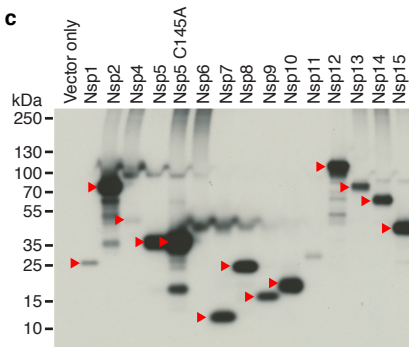
SARS-CoV-2 Genome



b

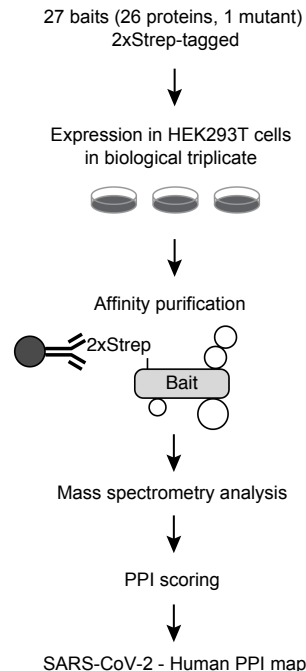
Protein	Mol. weight (kDa)	Seq. similarity with SARS-CoV	Description
Nsp1	19.8	91.1%	Suppresses host antiviral response
Nsp2	70.5	82.9%	
Nsp3	217.3	86.5%	Nsp3-Nsp4-Nsp6 complex involved in viral replication
Nsp4	56.2	90.8%	Nsp3-Nsp4-Nsp6 complex involved in viral replication
Nsp5	33.8	98.7%	Main protease (3C-like)
Nsp6	33.0	94.8%	Nsp3-Nsp4-Nsp6 complex involved in viral replication
Nsp7	9.2	100.0%	Nsp7-Nsp8 complex is part of RNA polymerase
Nsp8	21.9	99.0%	Nsp7-Nsp8 complex is part of RNA polymerase
Nsp9	12.4	98.2%	ssRNA binding
Nsp10	14.8	99.3%	Essential for Nsp16 methyltransferase activity
Nsp11	1.3	92.3%	Short peptide
Nsp12	106.7	98.3%	RNA polymerase
Nsp13	66.9	100.0%	Helicase/triphosphatase
Nsp14	59.8	98.7%	3'-5' exonuclease
Nsp15	38.8	95.7%	Uridine-specific endoribonuclease
Nsp16	33.3	98.0%	RNA-cap methyltransferase
S	141.2	87.0%	Spike protein, mediates binding to ACE2
Orf3a	31.1	85.1%	Activates the NLRP3 inflammasome
Orf3b	6.5	9.5%	
E	8.4	96.1%	Envelope protein, involved in virus morphogenesis and assembly
M	25.1	96.4%	Membrane glycoprotein, predominant component of the envelope
Orf6	7.3	85.7%	Type I IFN antagonist
Orf7a	13.7	90.2%	Virus-induced apoptosis
Orf7b	5.2	84.1%	
Orf8	13.8	45.3%	
N	45.6	94.3%	Nucleocapsid phosphoprotein, binds to RNA genome
Orf9b	10.8	84.7%	Type I IFN antagonist
Orf9c	8.0	78.1%	
Orf10	4.4	-	

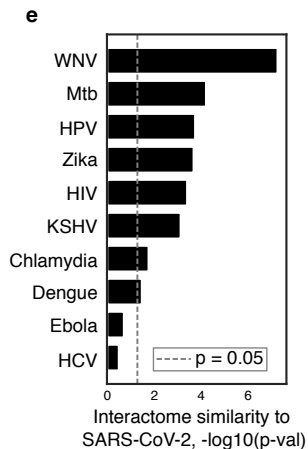
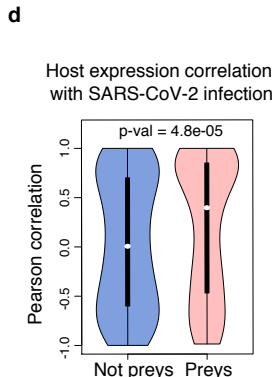
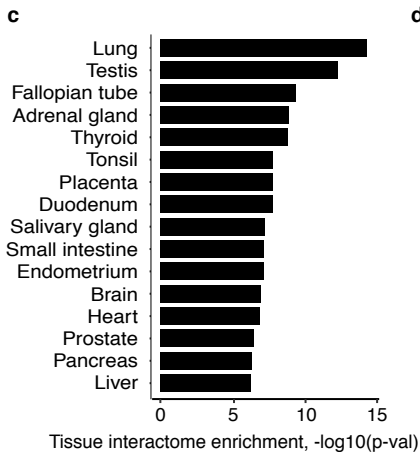
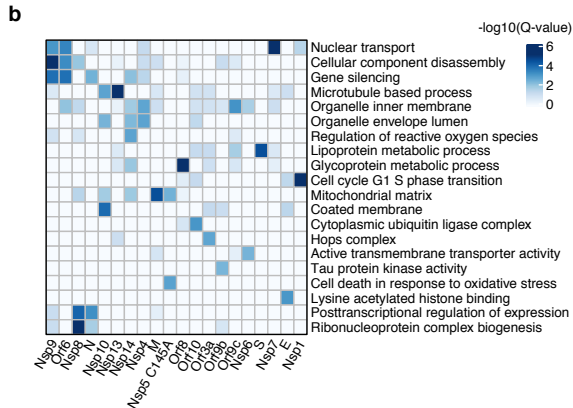
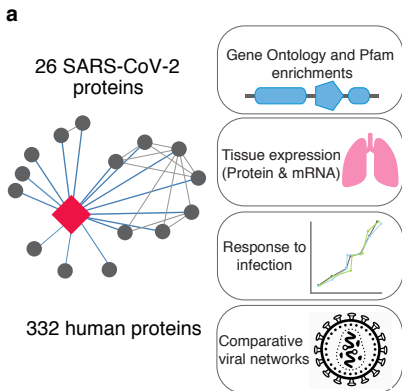
c

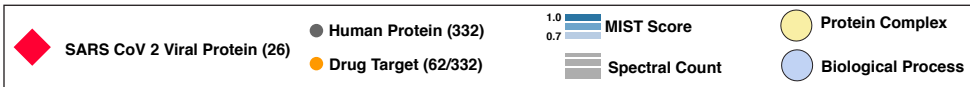
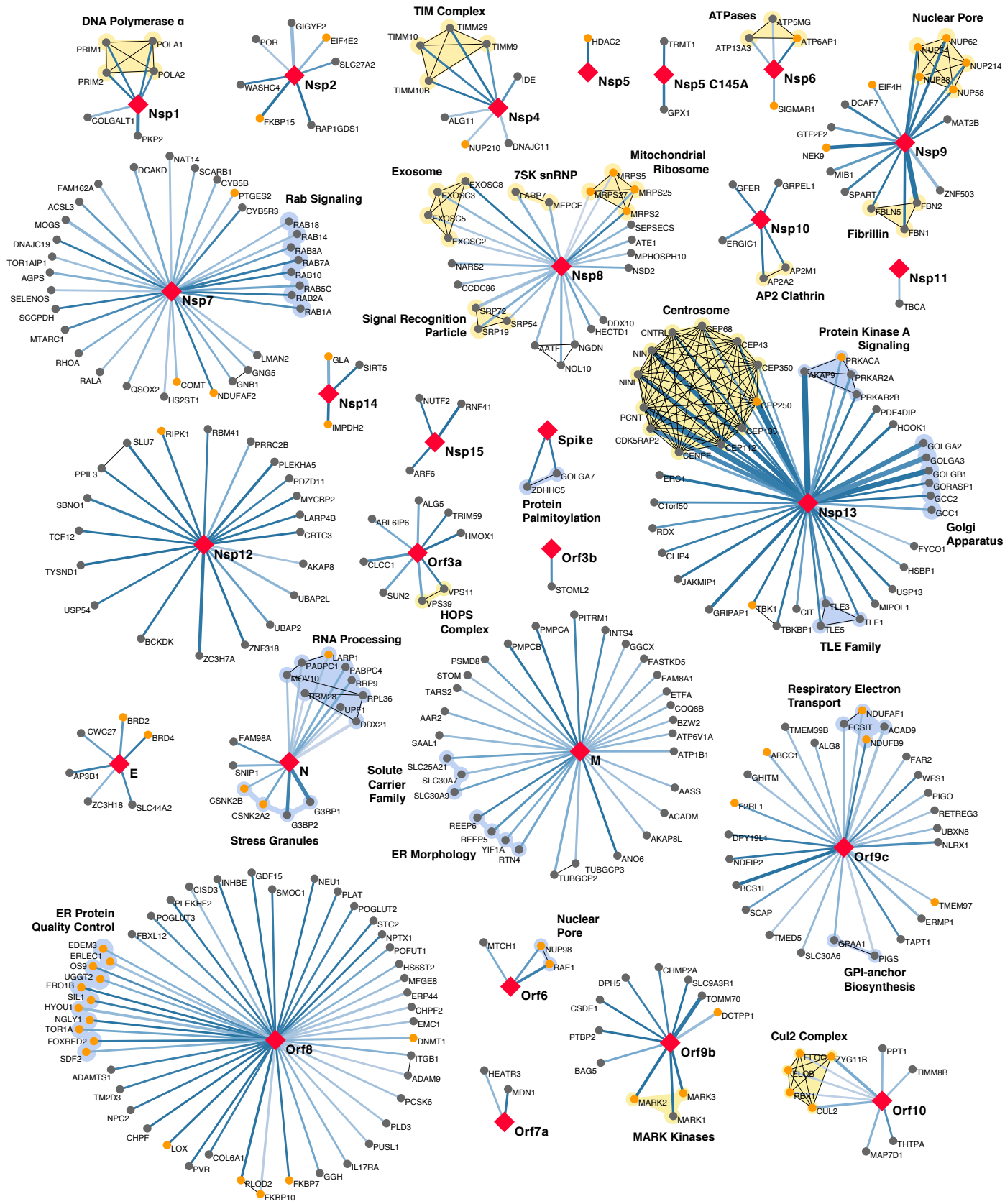


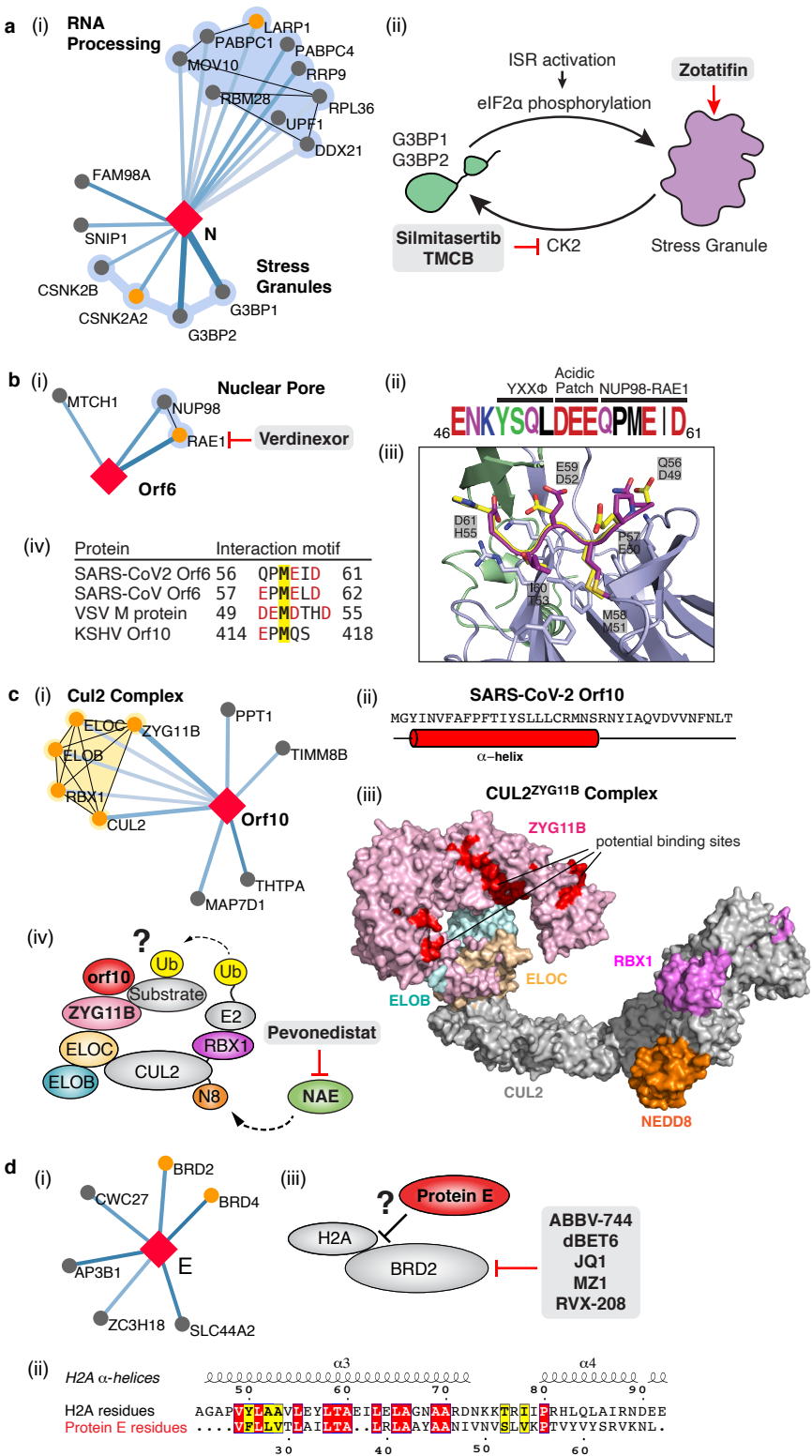
▶ Predominant band near expected molecular weight

d

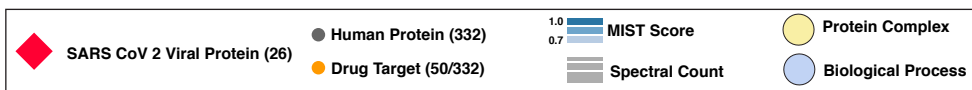
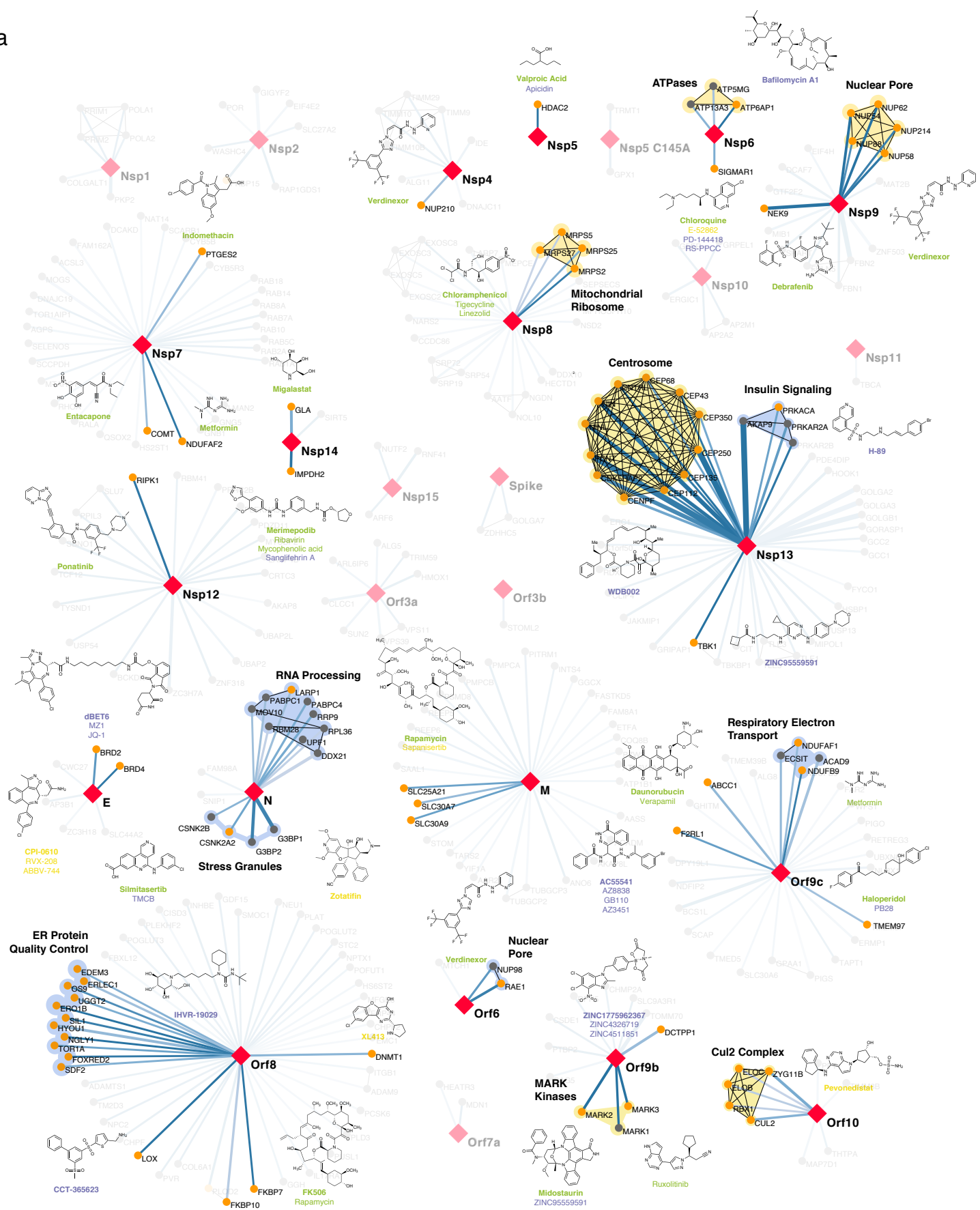




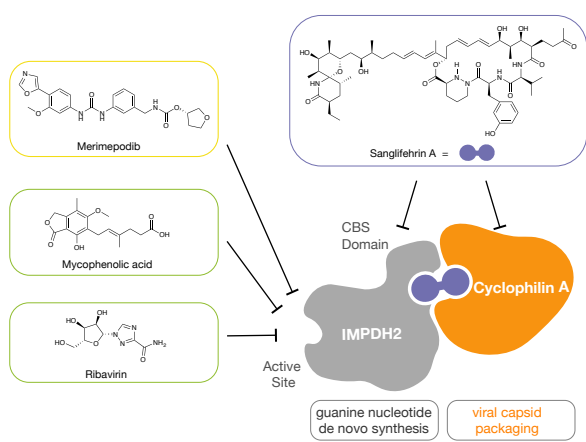




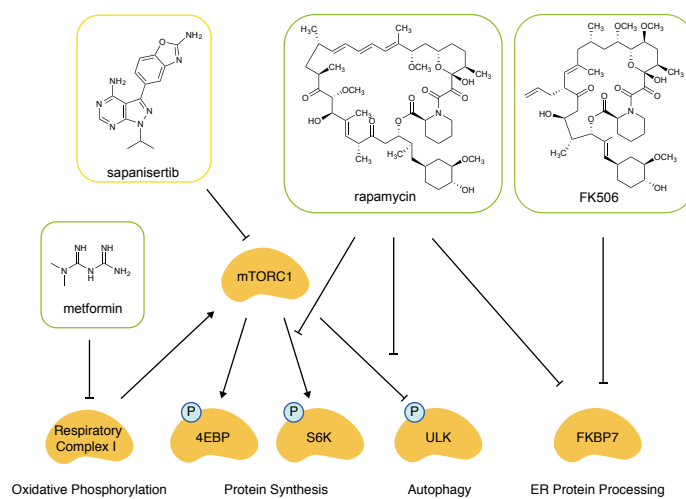
a



b

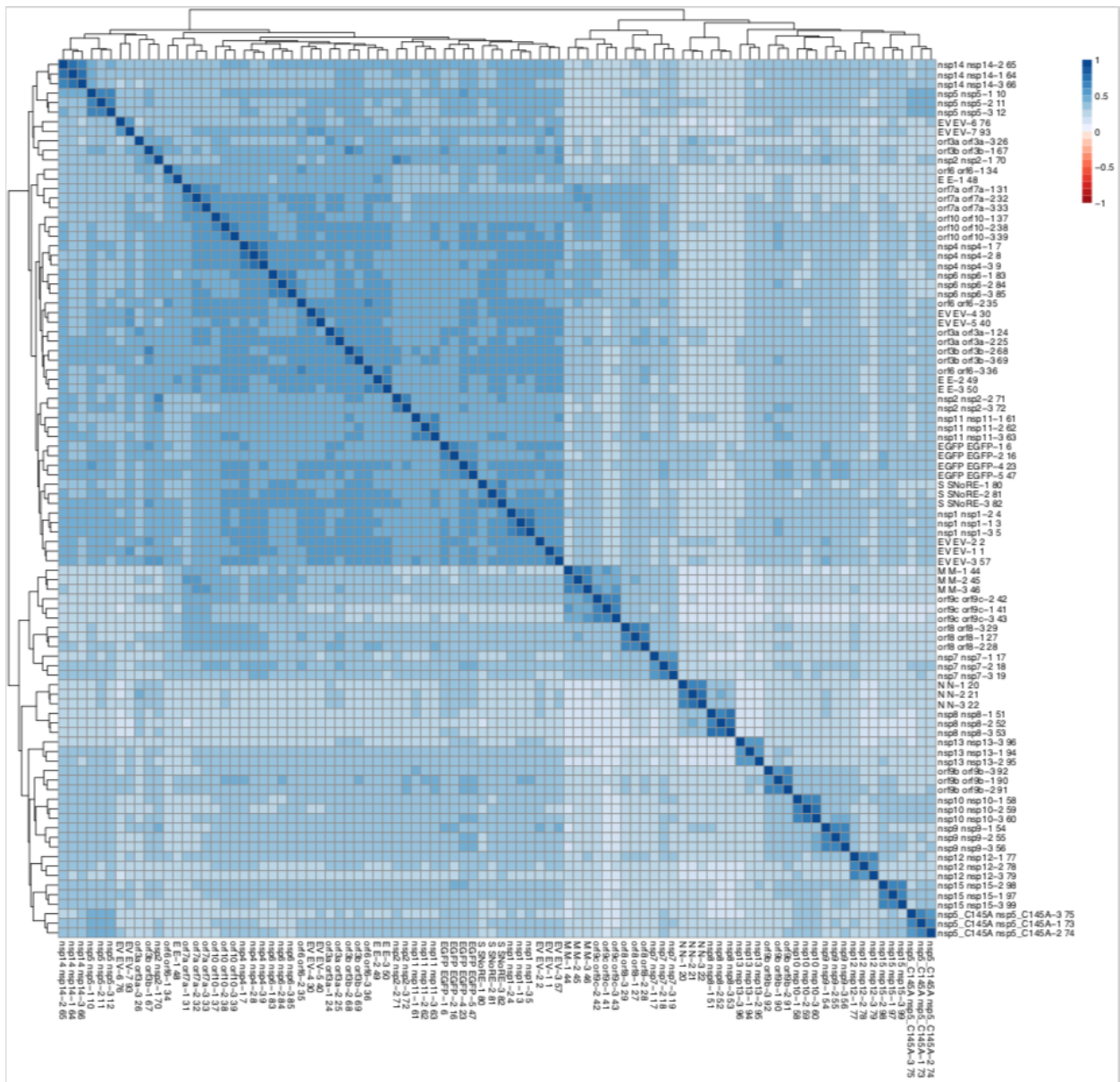


c

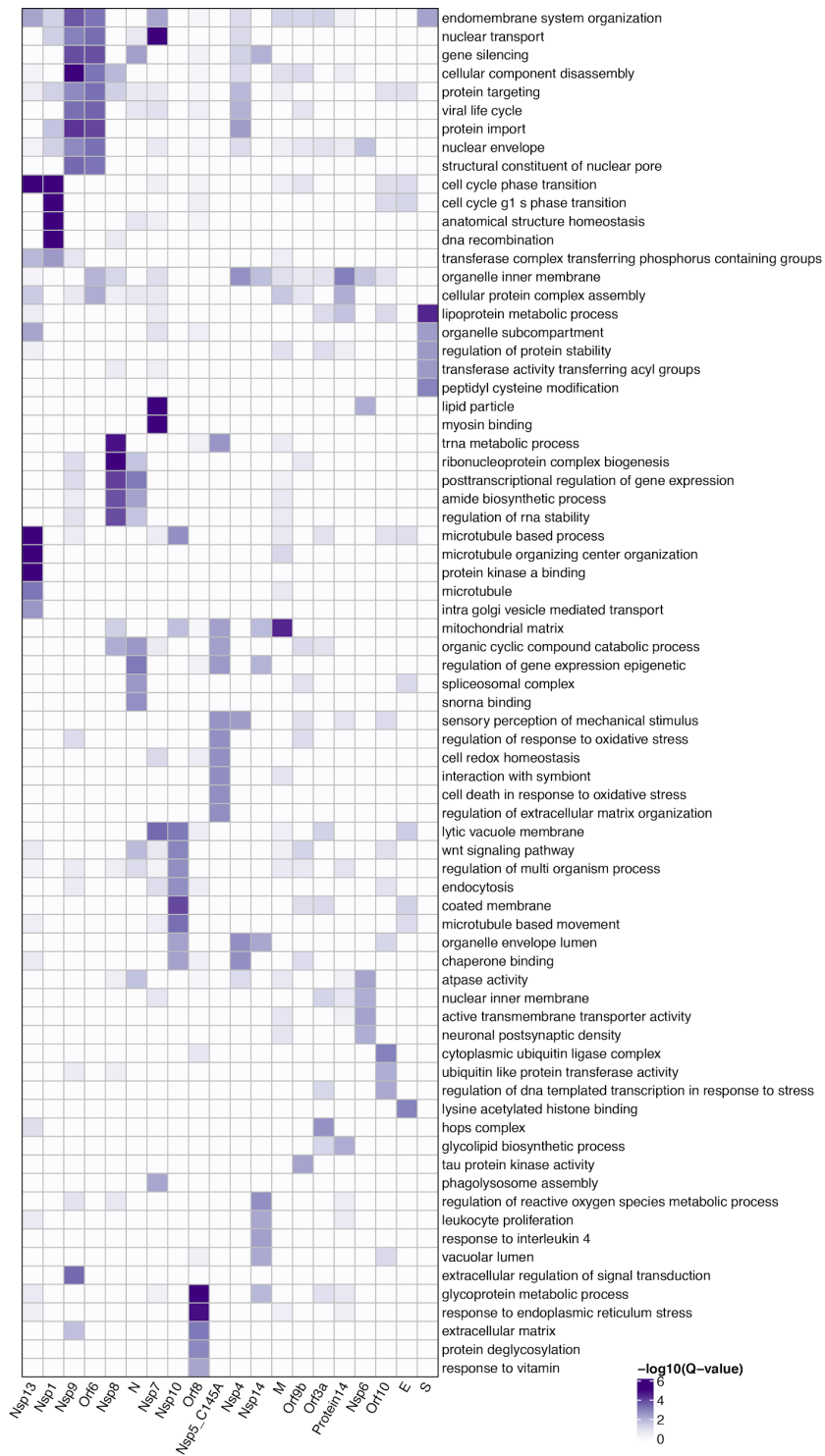


A SARS-CoV-2-Human Protein-Protein Interaction Map Reveals Drug Targets and Potential Drug-Repurposing

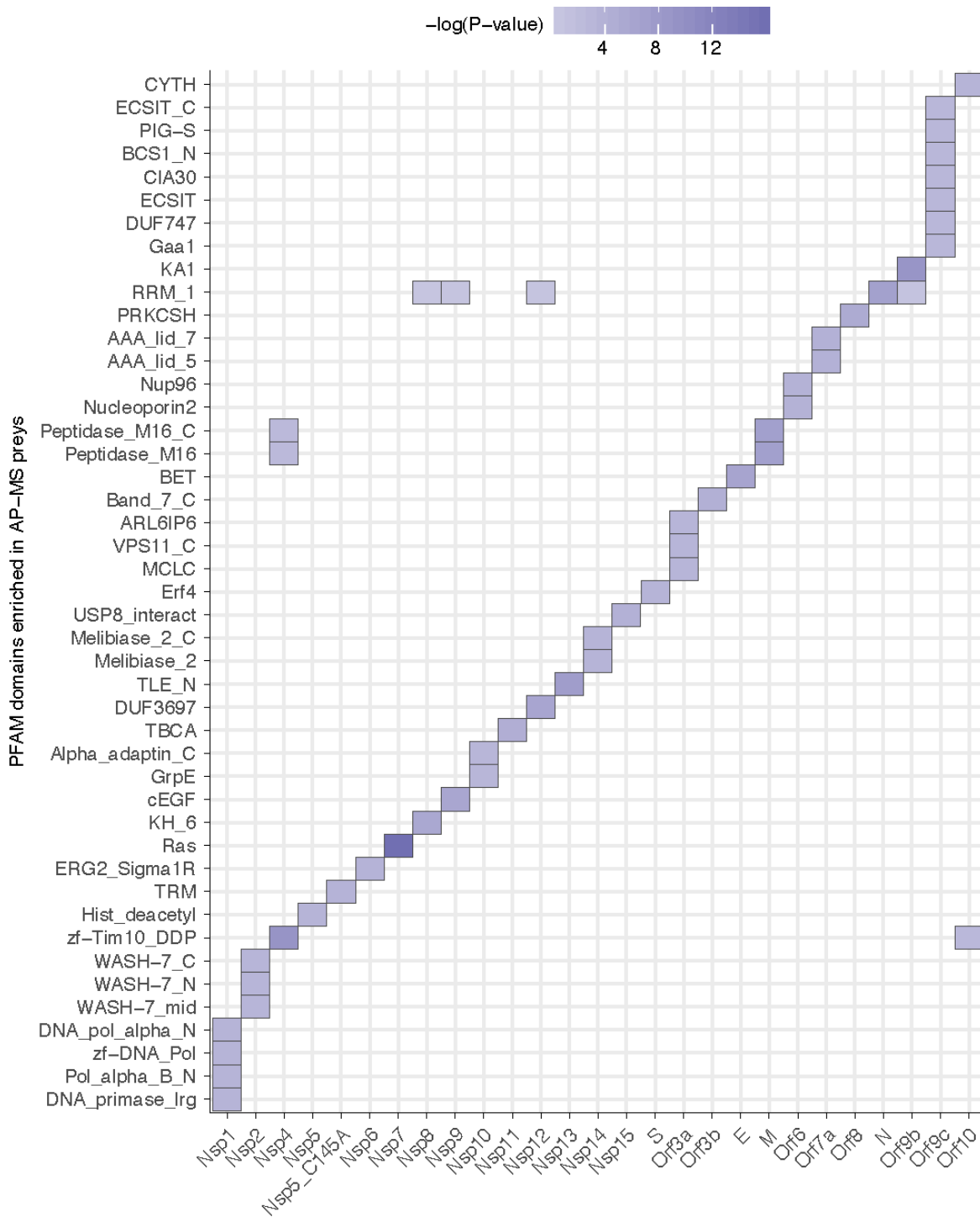
Extended Data



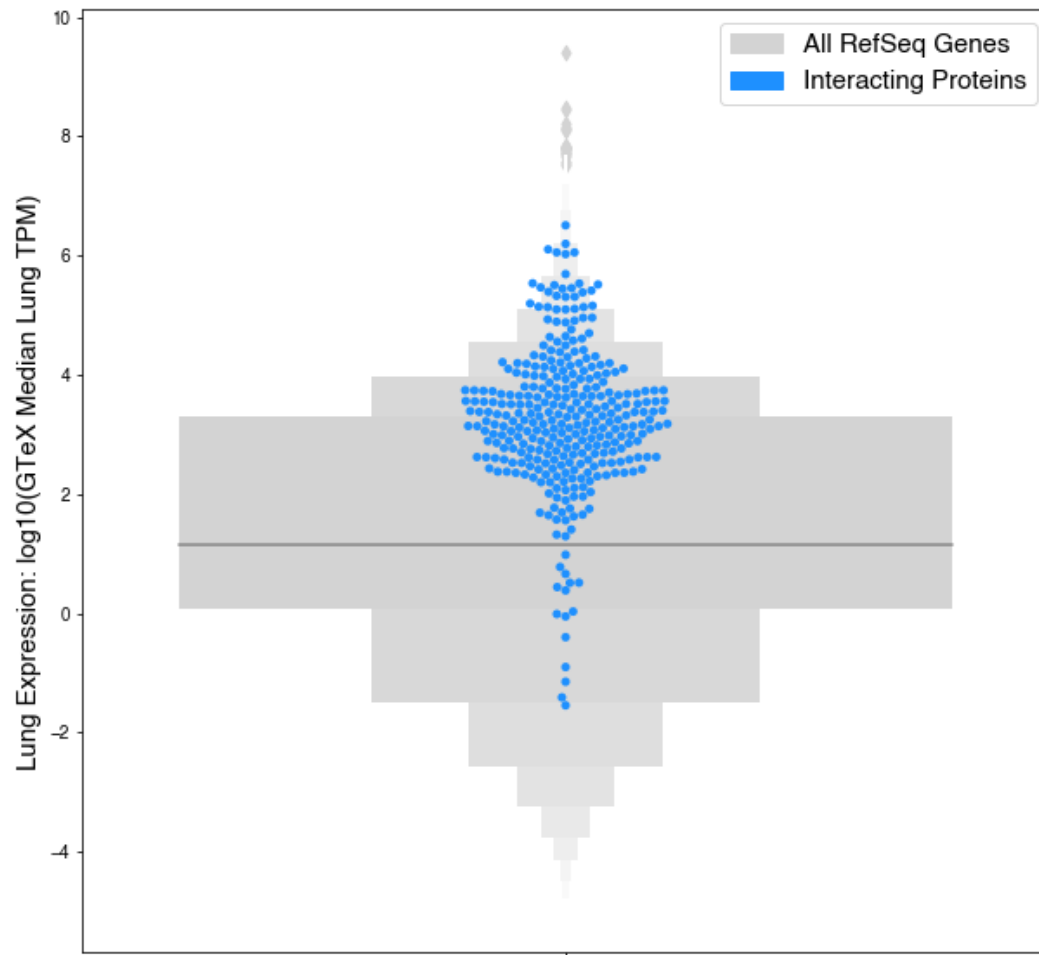
Extended Data Figure 1. Clustering analysis of AP-MS dataset reveals biological replicates of individual baits are well correlated. All MS runs were compared and clustered using artMS (David Jimenez-Morales, Alexandre Rosa Campos and John Von Dollen. (2019). artMS: Analytical R tools for Mass Spectrometry. R package version 1.3.9. <https://github.com/biodavidjm/artMS>). This figure depicts all Pearson’s pairwise correlations between MS runs, and is clustered according to similar correlation patterns.



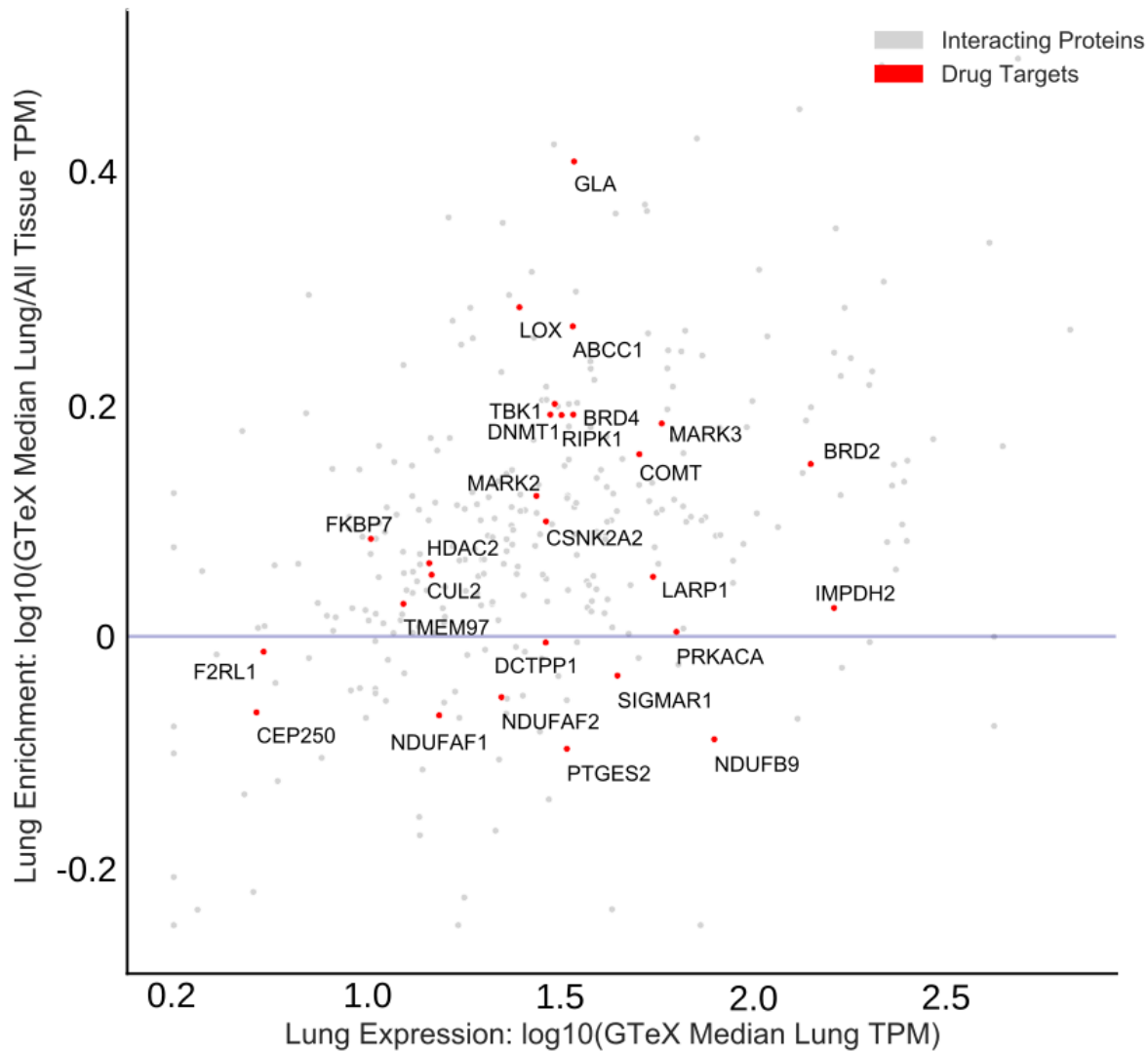
Extended Data Figure 2. Gene Ontology Biological Process Enrichments for SARS-CoV-2 Host Factors. We performed GO biological process enrichments (Methods) for the host factors identified as binding to each SARS-CoV-2 viral protein and represent here the top 5 most significant terms for each viral protein.



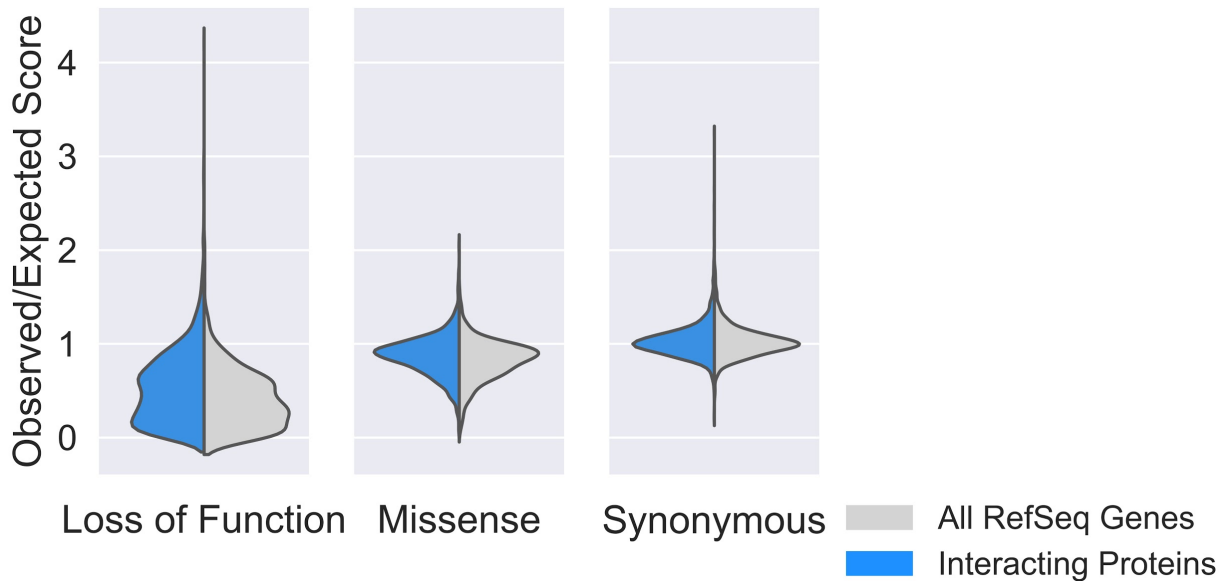
Extended Data Figure 3. Pfam Protein Families Enrichments for SARS-CoV-2 Host Factors. The enrichment of individual PFAM domains was calculated using a hypergeometric test where success is defined as the number of domains, and the number of trials is the number of individual preys pulled-down with each viral bait. The population values were the numbers of individual PFAM domains in the human proteome. To make sure that the p-values that signify enrichment were meaningful, we only considered PFAM domains that have been pulled-down at least three times with any SARS-CoV-2 protein, and which occur in the human proteome at least five times. Here, we show PFAM domains with the lowest p-value for a given viral bait protein.



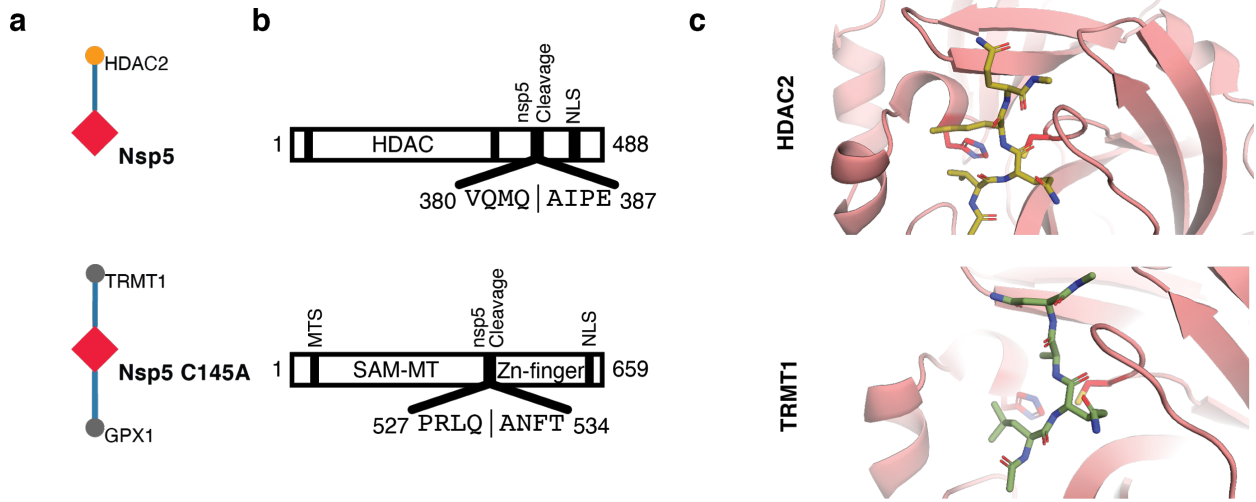
Extended Data Figure 4. Lung mRNA expression of the interacting human proteins relative to other proteins. The gene expression in the lung of the interacting proteins was observed to be higher than all other proteins (blue interacting proteins; median=25.52 TPM, grey all other proteins; median=3.198 TPM), $p=0.0007$.



Extended Data Figure 5. Gene level expression values and specificity for the lung. Scatterplot of the lung mRNA expression (TPM) versus enrichment of lung mRNA expression (lung TPM/median all tissue TPM) for human interacting proteins. Red points denote drug targets that are labelled with their gene names. Points above the horizontal blue line represent interacting proteins that are enriched in lung expression and show how most human interacting proteins tend to be enriched in the lung.



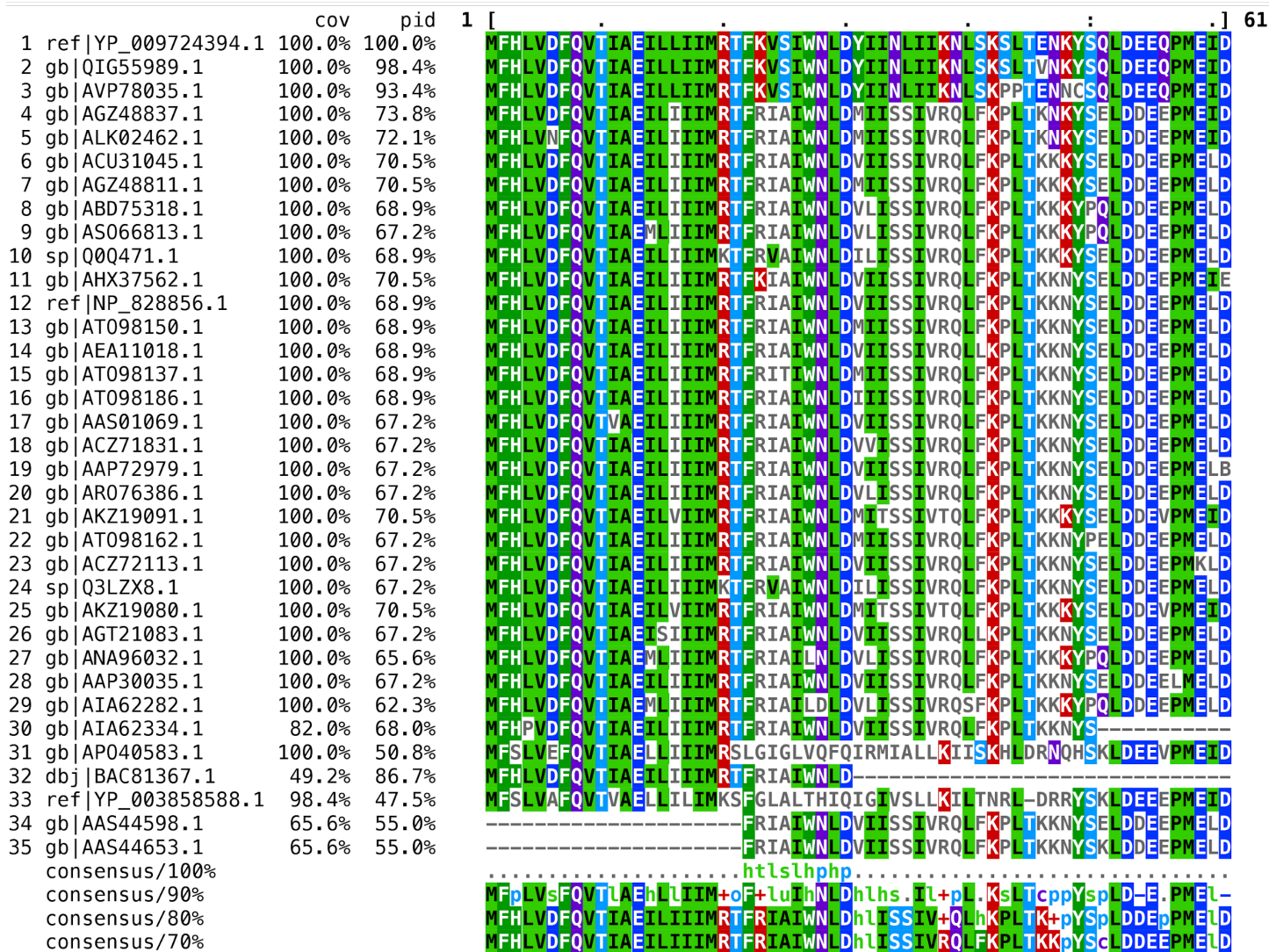
Extended Data Figure 6. Evolutionary Conservation of SARS-CoV-2 Interacting Proteins. We calculated the observed/expected ratio from gnomAD¹ for loss of function, missense, and synonymous mutations across all RefSeq genes. Compared to other genes (RefSeq Genes, grey), interacting proteins (blue) had lower ratios (indicating stronger intolerance of mutations) of observed/expected missense (median refseq score: 0.49, median interacting score: 0.36, $p=2.46 \times 10^{-11}$; t-test), and loss of function (median refseq score: 0.89, median interacting score: 0.85 $p=9.12 \times 10^{-7}$; t-test) but no difference in observed/expected synonymous mutations (median refseq score: 1.009 median interacting score: 1.004, $p=0.48$; t-test). Collectively, these results indicate that the interacting proteins have reduced genetic variation in human populations.



Extended Data Figure 7. Candidate targets for the viral Nsp5 protease. (a) nsp5 WT and nsp5 C145A (catalytic dead mutant) interactome. (b) Domain maps of HDAC2 and TRMT1 illustrating predicted cleavage sites (using Coronanet 1.0). HDAC: Histone Deacetylase Domain, NLS: Nuclear Localization Sequence, MTS: Mitochondrial Targeting Sequence, SAM-MT: S-adenosylmethionine-Dependent Methyltransferase Domain. (c) Peptide docking of predicted cleavage peptides into the crystal structure of SARS-CoV nsp5.

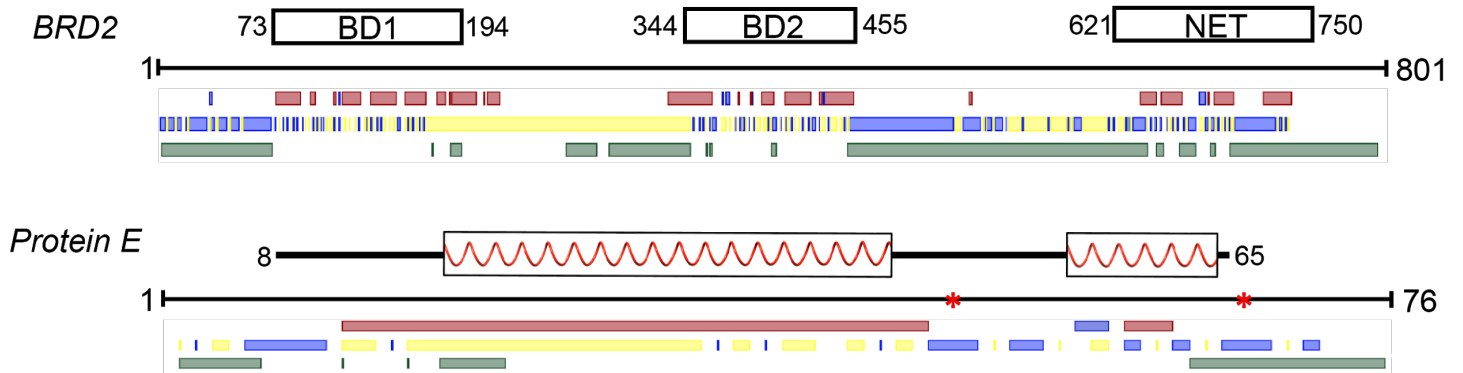
Consensus analysis of SARS-CoV-2 Orf6 homologs

Reference sequence (1): ref|YP_009724394.1
 Identities normalised by aligned length.
 Colored by: identity



Extended Data Figure 8. Consensus analysis of SARS-CoV-2 Orf6 homologs. Multiple sequence alignment of 34 homologs of SARS-CoV-2 Orf6. Sequence coverage (*cov*) and percent identity (*pid*) shown for each homologous sequence. Amino acids are colored according to identity with SARS-CoV-2 Orf6 (sequence 1 ref|YP_009724394.1). Colors indicate chemical properties of amino acids: small and/or hydrophobic (bright green, A, V, L, I, M, P, G), bulky (dark green, F, Y, W, H), basic (red, R, K), acidic (blue, D, E), neutral (purple, Q, N), polar (light blue, S, T), cysteine (C, yellow). The key methionine M58, and the acidic residues E55, D59, D61 of the putative NUP98-RAE1 binding motif are shown to be highly conserved. Multiple sequence alignment was visualized using the MView web server²: <https://www.ebi.ac.uk/Tools/msa/mview/>.

Experimental and predicted structural features of BRD2 and Protein E



Extended Data Figure 9. Experimental and predicted structural features of BRD2 and Protein E. Domain names are indicated for BRD2 along with residue numbers. Areas of protein E where its SARS-CoV homolog has been described by high-resolution structural models (PDB ID: 2MM4) are shown in white blocks and thick black lines above the sequence line. The ribbons indicate alpha helical sections. Protein E is predicted to have two N-linked glycosylation sites³ (red stars on sequence line). Structural predictions, as generated using PredictProtein⁴ are found below the sequence line. The first row indicates secondary structure predictions for alpha helices (red) and beta sheets (blue). The second row beneath the sequence line indicates areas expected to be buried (yellow) and exposed (blue). At the bottom, green bars indicate areas predicted to be disordered.

Extended Data References

1. Karczewski, K. J. *et al.* Variation across 141,456 human exomes and genomes reveals the spectrum of loss-of-function intolerance across human protein-coding genes. *bioRxiv* 531210 (2019)
doi:10.1101/531210.
2. Brown, N. P., Leroy, C. & Sander, C. MView: a web-compatible database search or multiple alignment viewer. *Bioinformatics* **14**, 380–381 (1998).
3. Fung, T. S. & Liu, D. X. Post-translational modifications of coronavirus proteins: roles and function. *Future Virol.* **13**, 405–430 (2018).
4. Yachdav, G. *et al.* PredictProtein--an open resource for online prediction of protein structural and functional features. *Nucleic Acids Res.* **42**, W337–43 (2014).

A SARS-CoV-2-Human Protein-Protein Interaction Map Reveals Drug Targets and Potential Drug-Repurposing

Supplementary Information

Supplementary Discussion

All SARS-CoV-2 protein and gene functions described in the subnetwork appendices, including the text below and the text found in the individual bait subnetworks, are based on the functions of homologous genes from other coronavirus species. These are mainly from SARS-CoV and MERS-CoV, but when available and applicable other related viruses were used to provide insight into function. The SARS-CoV-2 proteins and genes listed here were designed and researched based on the gene alignments provided by Chan et. al. 2020¹. Though we are reasonably sure the genes here are well annotated, we want to note that not every protein has been verified to be expressed or functional during SARS-CoV-2 infections, either *in vitro* or *in vivo*. In an effort to be as comprehensive and transparent as possible, we are reporting the sub-networks of these functionally unverified proteins along with the other SARS-CoV-2 proteins. In such cases, we have made notes within the text below, and on the corresponding subnetwork figures, and would advise that more caution be taken when examining these proteins and their molecular interactions. Due to practical limits in our sample preparation and data collection process, we were unable to generate data for proteins corresponding to Nsp3, Orf7b, and Nsp16. Therefore these three genes have been left out of the following literature review of the SARS-CoV-2 proteins and the protein-protein interactions (PPIs) identified in this study. Below we provide what we hope is a thorough, well sourced, review of the principal interactions for each bait. Given the urgent and unprecedented nature of the current crisis and global pandemic, we hope that this will be of significant use to both the scientific and global communities.

STRUCTURAL PROTEINS (S, E, M, N)

S

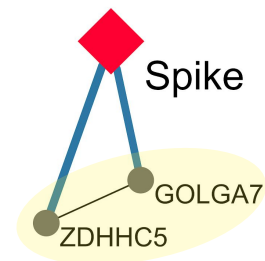
Function*: Spike (S) surface glycoprotein is responsible for binding and fusion with the host membrane.

- Classified as a class I fusion protein.

- Has 2 subunits that need to be processed by cellular protease TMPRSS2. S1 mediates receptor (ACE2) binding whereas S2 mediates fusion.

Similarity to SARS

Identity: 76.3% **Similarity:** 87.0%



Protein Palmitoylation:

GOLGA7-ZDHHC5 is a protein acyl-transferase (PAT) complex that may play a role in Spike palmitoylation.

E

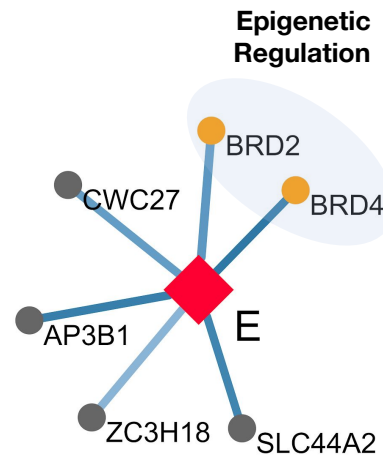
Function*: Envelope (E) protein plays a central role in virus morphogenesis and assembly.

- Acts as a viroporin, assembling in host membranes and forming pentameric protein-lipid pores that allow ion transport.

- Binds to protein M. Co-expression of M and E is sufficient for VLP formation and release. Lack of E reduces viral titers about 20-fold.

Similarity to SARS

Identity: 94.7% **Similarity:** 96.1%



Epigenetic Regulation

BRD2/BRD4:

Bromodomain extra terminal (BET) proteins are implicated as epigenetic factors that regulate genes crucial for cell cycle progression, inflammation and immune response.

M

Function*: Membrane (M) protein is the major driver for virus assembly and budding.

- Exists as a dimer in two major conformations, long and compact, which together determine the membrane curvature and spike density.

- M-M, M-S and M-N protein interactions contribute to virus assembly.

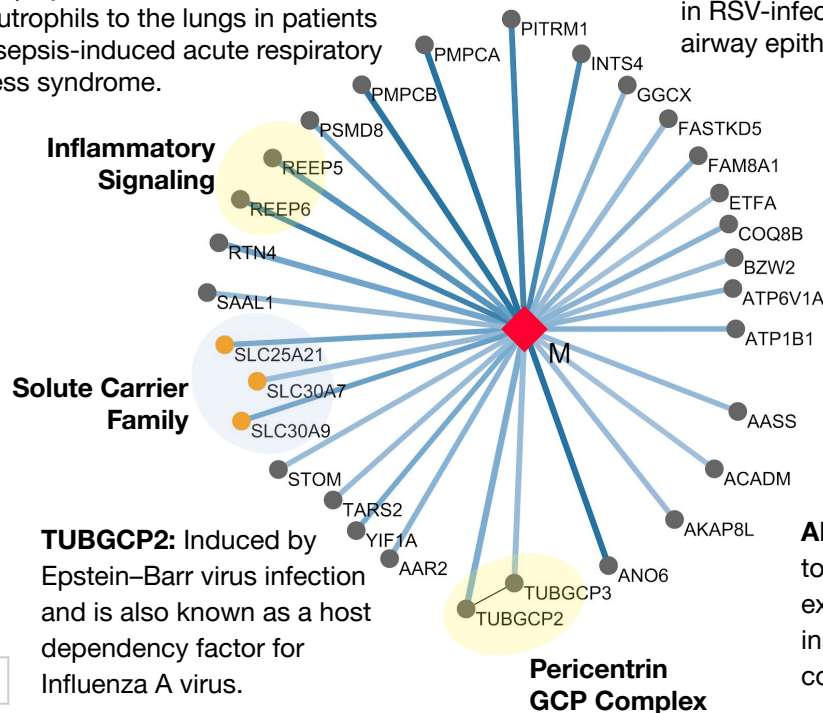
REEP6: Involved in IL-8 secretion, which plays a role in the recruitment of neutrophils to the lungs in patients with sepsis-induced acute respiratory distress syndrome.

PITRM1: Differentially expressed in RSV-infected human small airway epithelial cells.

BZW2: A known host restriction factor for Dengue virus infection.

ATP6V1A: Affects Dengue, West Nile and Influenza A H1N1 virus infections.

ANO6: Deficiency leads to severe T cell exhaustion and the inability of the host to control viral burden.



Inflammatory Signaling

Solute Carrier Family

TUBGCP2: Induced by Epstein-Barr virus infection and is also known as a host dependency factor for Influenza A virus.

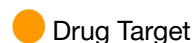
Pericentriolar GCP Complex

Similarity to SARS

Identity: 90.5% **Similarity:** 96.4%

1.0
0.7 MIST Score

Spectral Counts



*Function based on SARS

N

Function*: Nucleocapsid (N) protein binds to the RNA genome.

G3BP1 and G3BP2: G3BP1 and G3BP2 are core structural components of stress granules (SGs) which are broadly refractory to replication of viruses. Viruses have evolved diverse mechanisms such as direct cleavage of G3BPs (poliovirus, FMDV) or sequestration away from other granule components (SmFV, VV, TMCV, SAFV-2, Mengovirus, DENV, JEV, Ebola virus) to prevent granule formation. Coronaviridae like MERS and IBV also possess specific mechanisms to abrogate SG assembly. Certain viruses utilize G3BPs to promote their replication cycle, a function that is almost exclusively extra-granular.

CK2 (CSNK2A2 and CSNK2B): CSNK2A2 and CSNK2B are subunits of the tetrameric Casein Kinase 2. CK2 phosphorylates G3BPs and disassembles and/or inhibits the formation of stress granules. The activity of CK2 is thus presumptively proviral. CK2 is inhibited at sub-nanomolar concentrations by an orally bioavailable molecule, Silmitasertib.

LARP1: LARP1 is a major effector of the mTOR pathway, suppressing translation of terminal oligopyrimidine mRNAs. LARP1 binds the N protein in a variety of viruses (e.g. IBV, IAV). LARP1 knockdown decreases DENV viral titers, while inhibition of mTOR (e.g. with rapamycin) impairs MERS-CoV replication and exerts immunosuppressant functions.

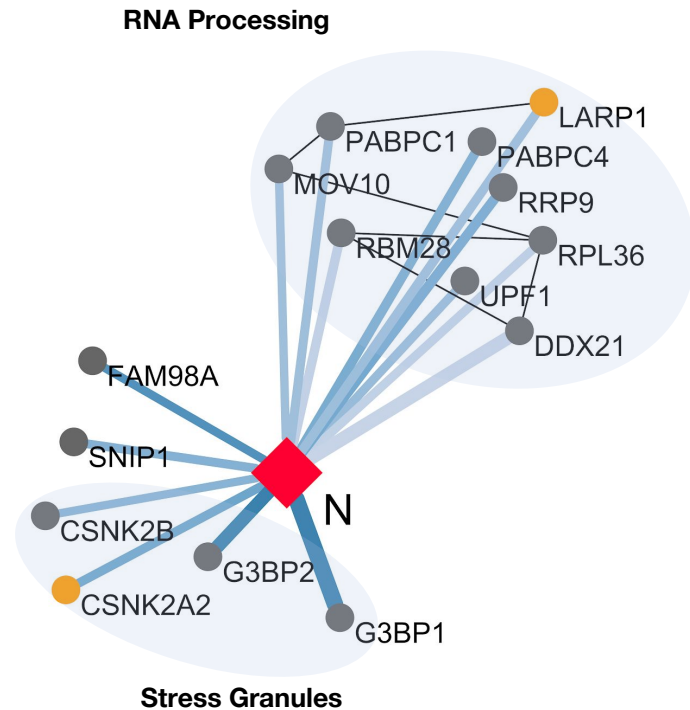
MOV10: MOV10 is a 5' to 3' RNA helicase that interacts with UPF1 and binds 3'UTRs. Its antiviral functions are independent of the helicase activity, and often through IFN stimulation. MOV10 exhibits P-body dependent antiviral activity by binding the N protein and preventing its nuclear localization.

PABPC1/4: Poly-A binding proteins are involved in many steps of mRNA processing. Viral factors cause PABPC1/4 to shuttle into the nucleus, causing mRNA hyperadenylation and nuclear retention. In a complex with LARP1 and RyDEN, PABPC1/4 can promote virulence.

UPF1: UPF1 is a RNA helicase that functions in the nonsense-mediated mRNA decay (NMD) pathway. Murine Hepatitis Virus (MHV) mRNAs are subjected to NMD, while the MHV N protein has been shown to have NMD inhibitory functions.

Similarity to SARS

Identity: 90.5%	Similarity: 94.3%
------------------------	--------------------------



NON-STRUCTURAL PROTEINS

Nsp1

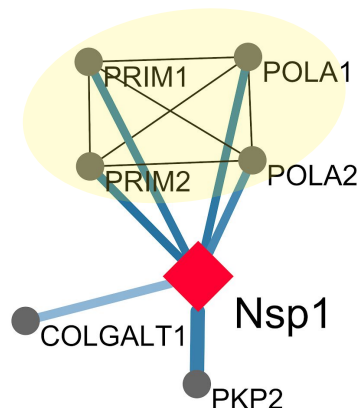
Function*: Nsp1 antagonizes interferon induction to suppress host antiviral response.

- Overexpression of Nsp1 in A549 cells increases production of pro-inflammatory chemokines CCL5, CXCL10, and CCL3.

- Can also inhibit host gene expression by binding to ribosomes and modifying host mRNAs.

Similarity to SARS

Identity: 84.4%	Similarity: 91.1%
------------------------	--------------------------



DNA Polymerase Alpha Complex: Regulates the activation of type I interferons through cytosolic RNA-DNA synthesis and primes DNA replication in the nucleus.

PKP2 (Plakophilin): Binds cadherins and intermediate fibers, crucial for desmosome formation.

COLGALT1 (Collagen Beta (1-O) Galactosyltransferase 1): Required for galactosylation of collagen IV and VI to form the collagen triple helix.

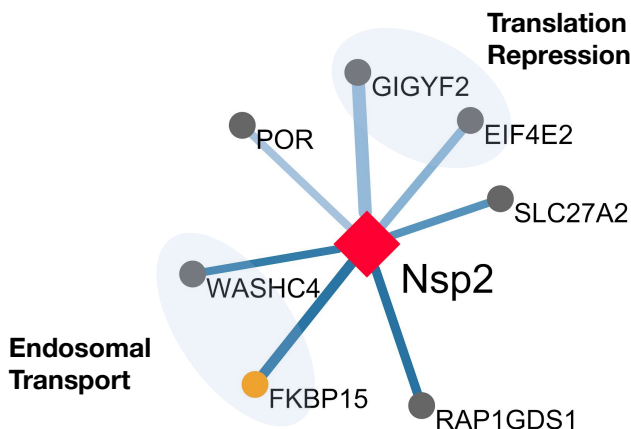
Nsp2

Function*: Nsp2 is translated as part of a single protein along with Nsp3 and may serve as an adaptor for Nsp3.

-While not essential for viral replication, deletion of Nsp2 diminishes viral growth and RNA synthesis

Similarity to SARS

Identity: 68.3%	Similarity: 82.9%
------------------------	--------------------------



SLC27A2: Previously described as a Dengue virus restriction factor.

Nsp4

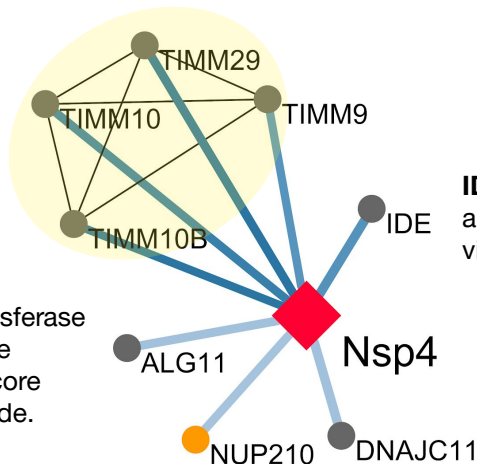
Function*: Nsp4 forms a complex with Nsp3 and Nsp6.

- Together, these proteins are predicted to nucleate and anchor viral replication complexes on double-membrane vesicles in the cytoplasm.

Similarity to SARS

Identity: 80.0%	Similarity: 90.8%
------------------------	--------------------------

TIM Complex: Involved in the import and insertion of hydrophobic membrane proteins into the mitochondrial inner membrane. Regulates import of transmembrane proteins into the inner mitochondrial membrane.



IDE: Involved in antigen presentation via MHC class I.

ALG11: Mannosyltransferase involved in the synthesis of core oligosaccharide.

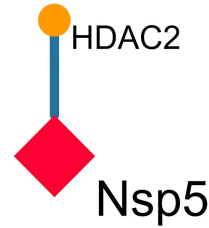
Nsp5

Function*: Nsp5 is the 3C-like protease.

- Cleaves the viral polyprotein.

HDAC2: Deacetylates lysines at the N-terminus of histones. Reduced levels of HDAC2 leads to increased transcription of inflammatory genes. Low HDAC2 expression contributes to disease severity in COPD patients.

Epigenetic Regulation



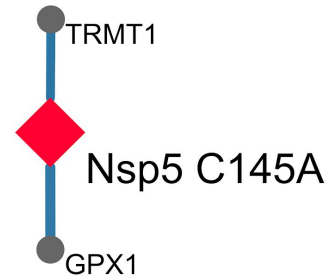
Similarity to SARS

Identity: 96.1% **Similarity:** 98.7%

Nsp5_C145A

Function*: Nsp5_C145A is a catalytically dead mutant of the Nsp5 3C-like protease.

- The catalytic residues of SARS-CoV Nsp5 align to H41 and C145 of SARS-CoV-2 Nsp5.



Similarity to SARS

Identity: 96.1% **Similarity:** 98.7%

Nsp6

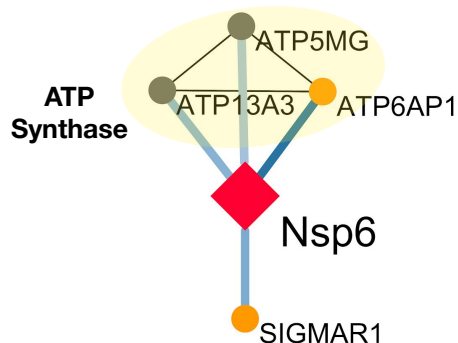
Function*: Nsp6 limits autophagosome expansion.

- Nsp6 may favor SARS-CoV infection by compromising the ability of autophagosomes to deliver viral components to lysosomes for degradation.

- Complexes with Nsp3 and Nsp4 to form double-membrane vesicles that anchor viral replication complexes.

ATP Synthase in the Mitochondria:

Components of the Mitochondrial Complex V co-purify with Nsp6. This complex regenerates ATP from ADP.



ATP6AP1: Subunit of the vacuolar ATP synthase protein pump. Dysregulation of ATP6AP1 results in impaired vesicle acidification and intracytoplasmic granules, resulting in a range of pathologies including an immunodeficiency syndrome and granular cell tumors. Identified as a potential host factor for IAV, WNV, and DENV. Is similar to the known IAV host factor ATP6V1A.

Similarity to SARS

Identity: 87.2% **Similarity:** 94.8%

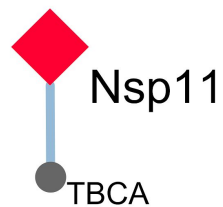
Nsp11

Function*: It is unclear if Nsp11 encodes a functional viral protein.

- Short peptide (13 amino acids) at the end of Orf1a.

Similarity to SARS

Identity: 84.6%	Similarity: 92.3%
------------------------	--------------------------



TBCA: Involved in the early step of the tubulin folding pathway.

REPLICATION COMPLEX (Nsp7, Nsp8 and Nsp12)

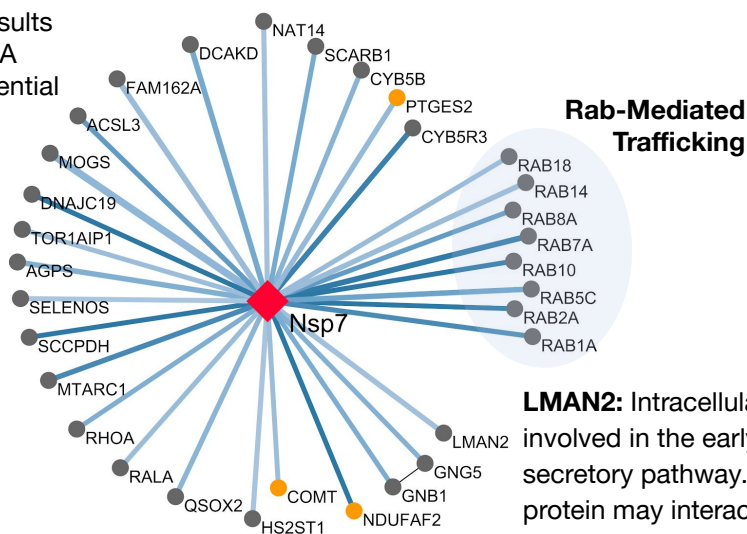
Nsp7

Function*: The Nsp7-Nsp8 complex is part of a unique multimeric RNA-dependent RNA replicase capable of both *de novo* initiation and primer extension.

- Forms the primase in complex with Nsp8.

ACSL3: Induction results in increased acyl-CoA synthesis that is essential for providing prostaglandin.

MOGS: Cleaves the distal alpha 1,2-linked glucose residue from the N-linked oligosaccharide precursor in a highly specific manner.



LMN2: Intracellular lectin involved in the early secretory pathway. The protein may interact with O-linked glycans and N-acetyl-D-galactosamine.

Similarity to SARS

Identity: 98.8% **Similarity:** 100.0%

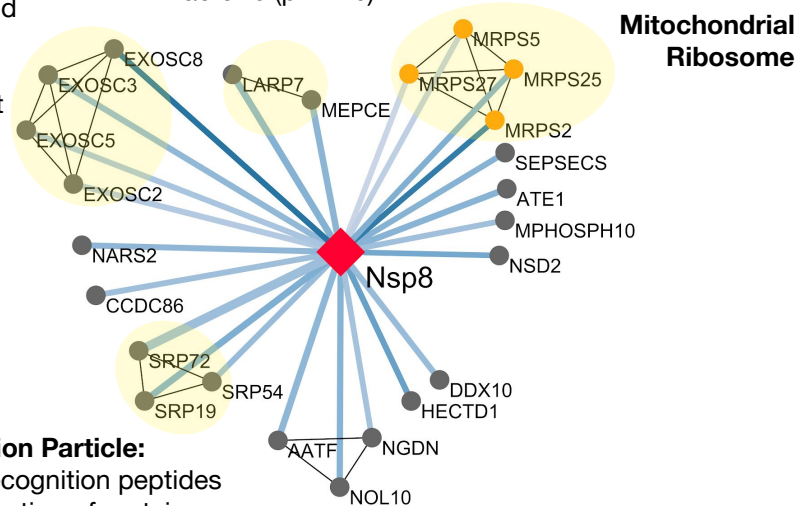
Nsp8

Function*: Nsp8 forms a primase in complex with Nsp7.

-Eight Nsp8 proteins complex with eight Nsp7 proteins to form a hexadecameric structure surrounding dsRNA.

Exosome Complex: Degrades ssRNA in a 3' to 5' direction and is involved in homeostatic degradation of host RNA as well as antiviral immunity.

7SK snRNP: Regulates activity of the positive Transcription Elongation Factor b (p-TEFb).



Signal Recognition Particle: Binds to signal recognition peptides and mediates insertion of proteins into the endoplasmic reticulum.

Similarity to SARS

Identity: 97.5% **Similarity:** 99.0%

Nsp12

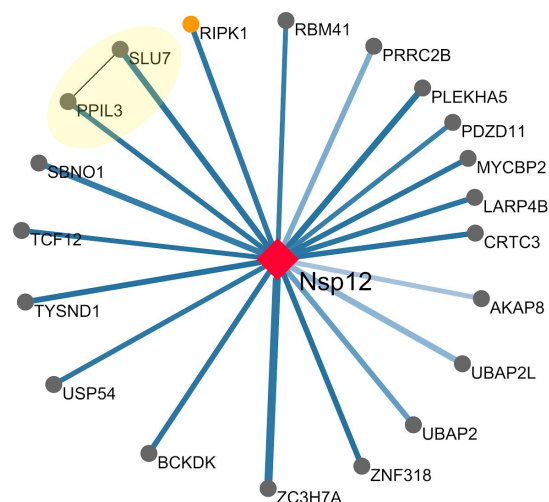
Function*: Nsp12 is the RNA-dependent RNA polymerase (RdRp).

- Nsp12 contains a large two-domain N-terminus of little known function and a canonical RdRp domain in the C-terminus.

- Nsp7-Nsp8 heterodimer binds the RdRp domain of Nsp12.

Spliceosome: Removes introns from pre-mRNA. SLU7 is essential for the second catalytic step of pre-mRNA splicing.

RIPK1: Triggers cell death by apoptosis or necrosis as an active regulatory kinase. Regulates inflammatory signaling and inhibits cell death as a scaffold protein.



Similarity to SARS

Identity: 96.4% **Similarity:** 98.3%

1.0
0.7 MIST Score

Spectral Counts

◆ Bait

● Prey

● Drug Target

*Function based on SARS

Nsp15

Function*: Nsp15 has uridine-specific endoribonuclease (endoU) activity and is essential for viral RNA synthesis.

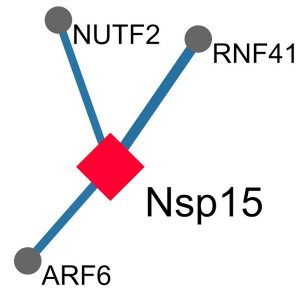
- The endoUs were shown to: (i) have endonucleolytic activity; (ii) cleave 3' of pyrimidines, preferring uridine over cytidine; and (iii) release reaction products with 2'-3'-cyclic phosphate and 5'-OH ends.

- Shown to form homohexamers composed of a dimer of trimers.

Similarity to SARS

Identity: 88.7% **Similarity:** 95.7%

NUTF2: Mediates the import of GDP-bound RAN from the cytoplasm into the nucleus, thus indirectly plays a more general role in cargo receptor-mediated nucleocytoplasmic transport.



RNF41: Acts as a E3 ubiquitin-protein ligase. Promotes TRIF-dependent production of type I interferon and inhibits infection with vesicular stomatitis virus.

ARF6: GTP-binding protein involved in protein trafficking that regulates endocytic recycling and cytoskeleton remodeling as well as the activation of cholera toxin.

Nsp9

Function*: Nsp9 is an essential single-stranded RNA binding protein.

- Shown to interact with the replication complex (Nsp7, Nsp8, and Nsp12).

- Binds to both DNA and RNA but preferentially binds single-stranded RNA.

Similarity to SARS

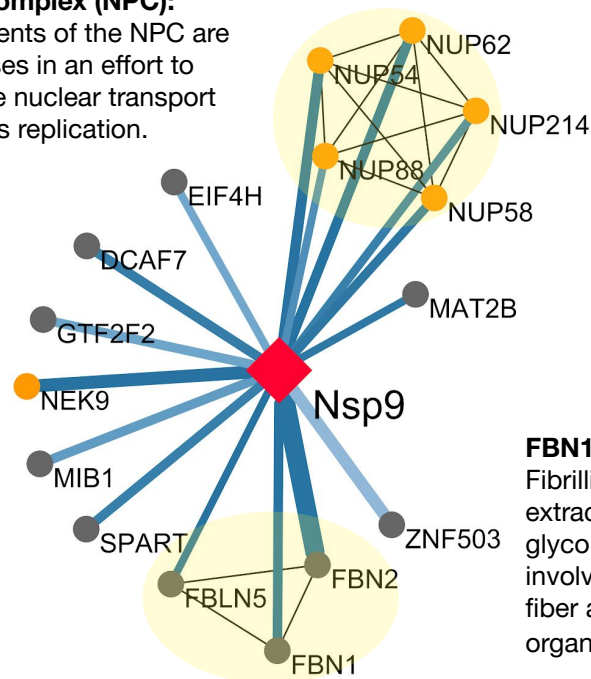
Identity: 97.3% **Similarity:** 98.2%

Nuclear Pore Complex (NPC):

Several components of the NPC are targeted by viruses in an effort to block or promote nuclear transport beneficial to virus replication.

NEK9:

Serine/threonine kinase that regulates mitotic progression and has been shown as an adenovirus dependency factor.



FBN1/FBN2:

Fibrillin-1 and -2 are extracellular matrix glycoproteins involved in elastin fiber and respiratory organ development.

Nsp10

Function*: Nsp10 is a zinc-finger protein essential for replication.

- Has been implicated in negative-strand RNA synthesis.

- Acts as a stimulatory factor for Nsp16 to execute its methyltransferase activity.

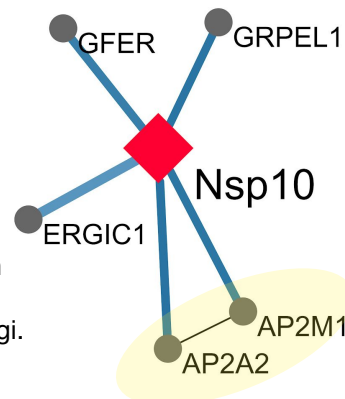
Similarity to SARS

Identity: 97.1% **Similarity:** 99.3%

GFER: FAD-dependent sulfhydryl oxidase that regenerates the redox-active disulfide bonds in CHCHD4/MIA40.

GRPEL1: Essential component of the PAM complex, required for the translocation of transit peptide-containing proteins from the inner membrane into the mitochondrial matrix in an ATP-dependent manner.

ERGIC1: Plays a possible role in transport between the endoplasmic reticulum and Golgi.



AP2 Clathrin: Nsp10 may utilize this interaction to hijack the clathrin machinery and endocytose host proteins.

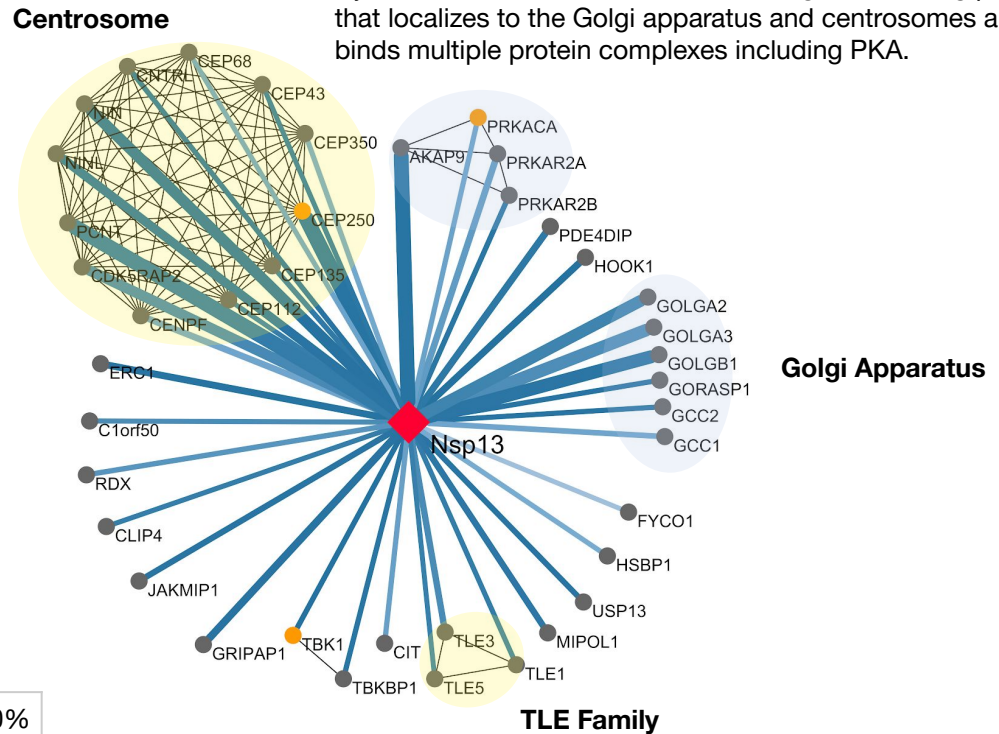
CAPPING ENZYMES (Nsp13, Nsp14)

Nsp13

Function*: Nsp13 is a helicase and triphosphatase that initiates the first step in viral mRNA capping.

- Nsp13, along with Nsp14 and Nsp16, installs the cap structure onto viral mRNA in the cytoplasm instead of the nucleus where host mRNA is capped.

Protein Kinase A Signaling Pathway: PKA signalling coordinates multiple steps of membrane transport and may be hijacked for viral benefit. AKAP9 is a large scaffolding protein that localizes to the Golgi apparatus and centrosomes and binds multiple protein complexes including PKA.



Similarity to SARS

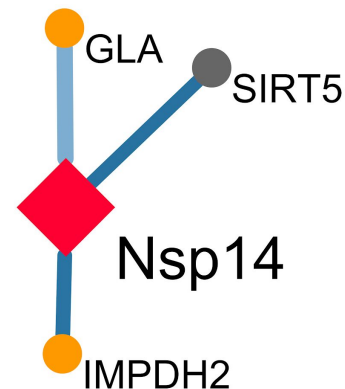
Identity: 99.8%	Similarity: 100.0%
------------------------	---------------------------

Nsp14

Function*: Nsp14 is a bifunctional enzyme encoding both an exonuclease domain and a separate domain that acts as a SAM dependent methyltransferase.

- The exonuclease domain corrects mutations that arise during genome replication.

- The SAM dependent methyltransferase domain facilitates capping of viral mRNA.



IMPDH2: Catalyzes the conversion of isosine 5' phosphate (IMP) ultimately to guanine 5' monophosphate for *de novo* synthesis of guanine nucleotides. Nsp14's interaction with IMPDH2 may reflect an interplay with purine nucleotide metabolism.

Similarity to SARS

Identity: 95.1%	Similarity: 98.7%
------------------------	--------------------------

OPEN READING FRAMES

Orf3a

Function*: Orf3a is not essential for replication but contributes to pathogenesis. It is packaged into virions.

- Mediates trafficking of Spike (S protein) by providing an ER/Golgi retention signal.

- Induces elevation of IL-1 β secretion and activates NF- κ B and the NLRP3 inflammasome by promoting TRAF3-dependent ubiquitination of p105 and ASC.

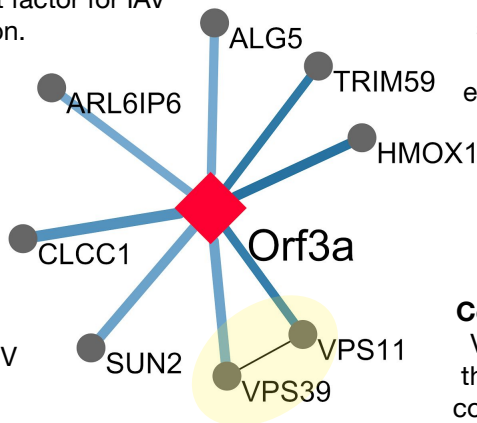
- Expression of Orf3a induces apoptosis in viral infection and cell line models.

Similarity to SARS

Identity: 72.4%	Similarity: 85.1%
------------------------	--------------------------

ALG5: Involved in N-linked protein glycosylation. Identified as a host factor for IAV replication.

CLCC1: An intracellular chloride channel implicated in ER stress. Interacts physically with RSV and druggable protein SLC5A13.

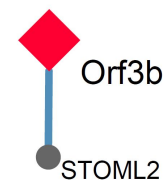


HMOX1: Key enzyme in heme catabolism. Has shown a cytoprotective and anti-inflammatory effect both in pulmonary pathologies and viral pathogenesis.

Lysosomal Fusion Complexes: VPS11 and VPS39 are members of the HOPS and CORVET complexes, respectively, which coordinate fusion of the lysosome with the endosome and autophagosome.

Orf3b

Function*: Orf3b is shown to be an interferon antagonist and is involved in pathogenesis.



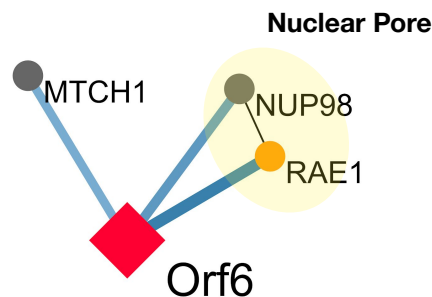
Similarity to SARS

Identity: 7.1%	Similarity: 9.5%
-----------------------	-------------------------

Orf6

Function*: Orf6 is a type 1 interferon antagonist. Expression of Orf6 suppresses the induction of interferon and interferon signaling pathways.

- C-terminal region of SARS-CoV Orf6 interacts with the nuclear import protein, karyopherin alpha-2, sequestering it in the cytoplasm. This prevents import of STAT1, activator of interferon response genes, into the nucleus.



Similarity to SARS

Identity: 66.7%	Similarity: 85.7%
------------------------	--------------------------

Orf7a

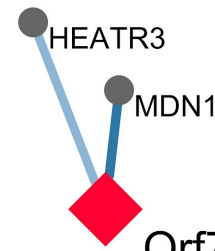
Function*: Orf7a may play a role in pathogenesis via its role in virus-induced apoptosis.

- ΔOrf7a SARS-CoV is still able to release virions at similar levels as wild-type virus.

Similarity to SARS

Identity: 85.2%	Similarity: 90.2%
------------------------	--------------------------

HEATR3: Involved in ribosomal protein transport. Implicated in mediating NF-κB signaling.



MDN1: Nuclear chaperone that is critical for the export of pre-60s ribosome subunits.

Orf8

Function*: Orf8 is an accessory protein not essential for virus replication *in vitro* and *in vivo*.

- Previously shown to be a recombination hotspot, one of the most rapidly evolving regions among SARS-CoV genomes.

- SARS-CoV Orf8b was shown to induce ER stress and activate NLRP3 inflammasomes.

Similarity to SARS

Identity: 28.5%	Similarity: 45.3%
------------------------	--------------------------

ER Protein Processing



Orf9b

Function*: Orf9b is an accessory protein synthesized from an alternative complete reading frame within the viral N gene.

- Targets the mitochondrial-associated adaptor molecule MAVS signalosome by utilizing PCBP2 and E3 ligase AIP4, resulting in the degradation of MAVS and therefore limiting host cell interferon responses.

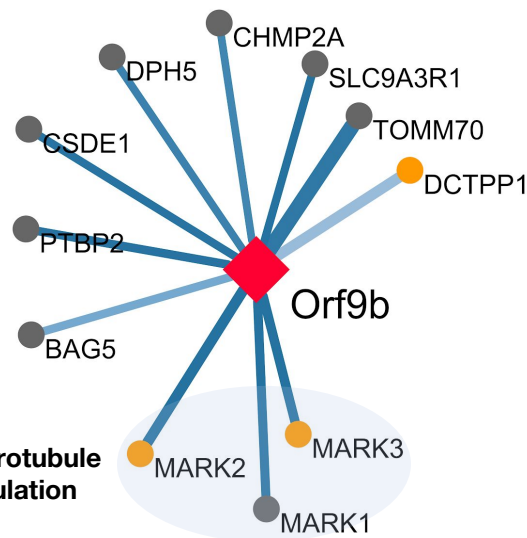
Similarity to SARS

Identity: 72.4%	Similarity: 84.7%
------------------------	--------------------------

TOMM70 (Translocase Of Outer Mitochondrial Membrane 70):

Receptor that accelerates the import of all mitochondrial precursor proteins. TOMM70 interacts with MAVS protein upon virus infection.

Microtubule regulation



Orf9c

Function*: Orf9c is a short polypeptide (70 amino acids) dispensable for viral replication. There is no data yet providing evidence that the protein is expressed during SARS-CoV-2 infection.

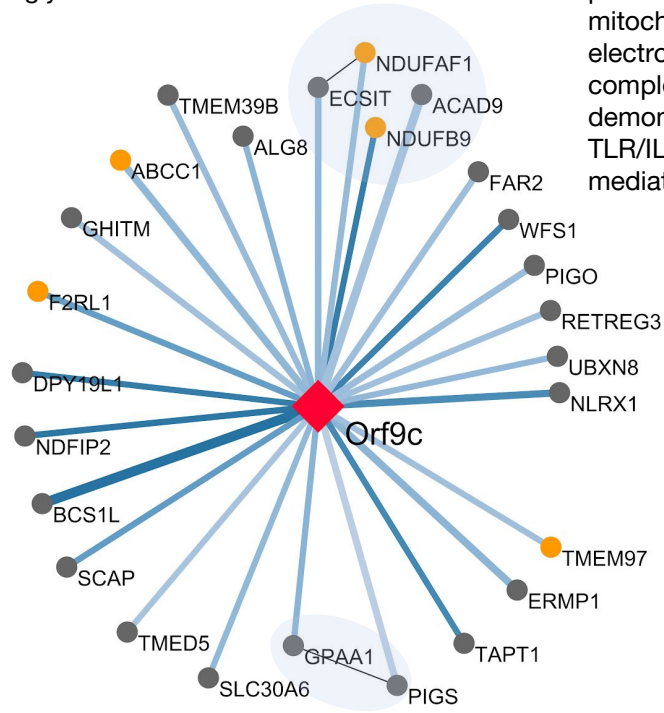
ABCC1: ABCC1 (also MRP1) is a multifunctional ATP-binding cassette protein involved in controlling the efflux of drugs in cells. MRP1 is a well-known viral host factor and physical interactor of both IAV and WNV proteins. Further, it has been implicated in disease progression of pneumonia and COPD, as well as drug resistance in the lung.

F2LR1: The protein product of F2LR1, PAR2, is a protease-activated receptor that has a cytoprotective and inflammatory role in the pathogenesis of viral infection and progression of pulmonary disease.

BCS1L: BCS1L is a mitochondrial chaperone located in the inner mitochondrial membrane. Loss of BCS1L is associated with severe clinical disorders such as GRACILE and Bjornstad Syndrome.

ALG8: This enzyme adds the second glucose residue to the lipid-linked N-linked glycan.

Respiratory Electron Transport: Orf9c interacts with four proteins in the mitochondrial respiratory electron transport chain complex I, which has demonstrated roles in TLR/IL-1 signaling and mediating inflammation.



Similarity to SARS

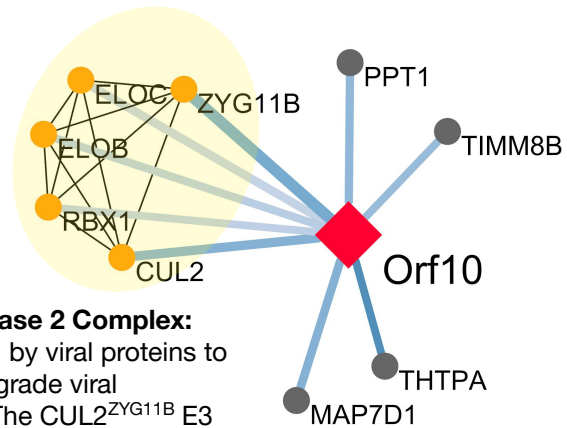
Identity: 74.0%	Similarity: 78.1%
------------------------	--------------------------

GPI-Anchor Biosynthesis: GPA1 is essential for GPI-anchoring of precursor proteins, while PIGS and PIGO are involved in GPI-synthesis.

Orf10

Function*: Orf10 codes for a peptide only 38 amino acids long. There is no data yet providing evidence that the protein is expressed during SARS-CoV-2 infection.

- Does not have a homolog in SARS-CoV.



Cullin RING E3 Ligase 2 Complex: Commonly hijacked by viral proteins to ubiquitinate and degrade viral restriction factors. The CUL2^{ZYG11B} E3 ligase targets substrates with exposed N-terminal glycines for degradation.

SARS-CoV Structural Proteins

SARS-CoV-2 Spike/S Protein

Spike (S protein) is the viral surface protein that mediates viral entry through its interaction with cellular host factor angiotensin-converting enzyme 2 (ACE2)². The full-length S protein is 141 kDa (1273 amino acids (aa)) and encodes a N-terminal signal peptide, a transmembrane region (aa 1214-1237), and a patch of cysteine residues (aa 1235-1254) which are predicted to be palmitoylated (protein S-acylation of cysteine residues)^{3,4}. In previous studies, mutation of these cytosolic cysteine residues inhibited fusogenicity of S, and suggest that targeting the s-acylation modifications via acyl-transferase inhibitors could potentially be a therapeutic strategy for inhibiting coronavirus infection⁵.

In our interactome, we demonstrate high-confidence binding of SARS-CoV-2 Spike to the GOLGA7-ZDHHC5 complex, a protein acyl-transferase (PAT) complex. GOLGA7 characteristically localizes to the Golgi apparatus⁶ but the GOLGA7-ZDHHC5 complex has been found at the plasma membrane⁷. While this interaction is exciting and could potentially point to a targetable enzymatic activity responsible for Spike palmitoylation, further experiments need to be done to fully clarify the functional role of this complex and the consequence of its inhibition. ZDHHC5 is highly expressed in neuronal tissue and is reported to have a role in hippocampal function⁸. In addition, ZDHHC5 is shown to palmitoylate G protein-coupled receptors⁹ and activate nucleotide oligomerization domain (NOD)-like receptors 1 and 2 (NOD1/2)¹⁰ which recognize pathogenic peptidoglycans and activate immune signaling¹⁰. GOLGA7 is also a general adaptor for ZDHHC proteins and, in complex with these acyl-transferase proteins, can regulate additional processes including the palmitoylation of Ras¹¹. It should also be noted that the ZDHHC5-GOLGA7 complex is required for the non-apoptotic cell death phenotype attributed to the synthetic oxime CIL56, indicating a role for this complex in the cell death pathway⁷. Thus, we would caution against long-term inhibition of this enzyme as a general treatment strategy.

Though identified just below our cutoffs, one of the lower confidence hits for Spike was ATP1A1, a protein at the plasma membrane that promotes viral entry and replication of related coronaviruses (M-CoV, FCoV, MERS-CoV), and a number of other viruses including Ebola, Lassa, live-attenuated Junin virus, and respiratory syncytial virus (RSV)¹²⁻¹⁵. Interestingly, this protein is from the same ATPase family as ATP1B1, a high-confidence interactor of M protein.

SARS-CoV-2 E Protein

The SARS-CoV Envelope (E) protein, a small integral membrane protein, is important for virus production, assembly, intracellular trafficking, morphogenesis and virulence^{16,17}. The transmembrane domain of E has amphipathic properties and can oligomerize to form cation-permeant ion channels¹⁸. The C-terminal cytoplasmic domain contains a targeting signal for protein localization to the Golgi complex^{19,20} and a PDZ binding motif important for virulence²¹. Interestingly, E protein is expressed at very high levels inside the infected cells, but only a small portion is incorporated in virions and the rest is largely distributed in intracellular membranes between ER and Golgi compartments indicating an important role of E protein in manipulating the cellular environment²². Increased cellular stress, unfolded protein response, apoptosis, and heightened host immune response were all observed in infected cells lacking E protein¹⁷. In addition, E has also been implicated in inflammasome activation and consequential inflammation in the lung parenchyma¹⁷.

In our study, we identify six high-confidence host protein interactions with E protein: AP31B, BRD2, BRD4, CWC27, SLC44A2, and ZC3H18. BRD2 and BRD4 are bromodomain extra terminal (BET) family proteins that bind acetylated chromatin and activate transcription²³. BRD4 is a co-activator of NF- κ B and facilitates the transcription of NF- κ B-dependent inflammatory response²⁴. Sequestration of BRD4 by E protein may represent a means for SARS-CoV-2 to protect against the host immune response. Previously it's been shown that inhibition of BRD4 activity in primary lung epithelial cells results in diminished innate immune response after challenge with poly(I:C), a viral pattern that simulates acute RNA virus infections²⁵. In addition, the interaction of BRD4 with Bovine Papillomavirus E2 Protein tethers viral DNA to host mitotic chromosomes ensuring viral persistence in infected cells²⁶. BRD2 is a transcriptional regulator that binds hyperacetylated histones and is implicated in a variety of cellular processes^{27,28}. Though functionally similar, BRD2 and BRD4

are shown to regulate different transcriptional programs²⁹. Interestingly, the $\alpha 3$ helix at the N-terminus of histone 2A shares local sequence similarity (~15 non-contiguous aa residues) with an α -helix of E protein (see main text **Fig. 4d**). This aligned sequence spans many acetylated lysine residues shown to bind BRD2³⁰. This information suggests a potential role for E protein to act as a sort of molecular mimic, disrupting the H2A-BRD2 interaction in order to disrupt BRD2 regulated transcription programs in a manner beneficial to the virus. Given that bromodomain proteins and their ability to regulate transcription are implicated in the life cycle of several viruses^{26,27,31,32}, the observed interactions of E protein with BRD2 and BRD4 present exciting avenues to pursue. However, future research is still needed to fully establish the structural basis of these interactions and the resulting functional implication for SARS-CoV-2 infection.

E protein also interacts with host factors involved in protein and mRNA trafficking, important for potentially carrying out many of E's functions. AP3B1 encodes the beta-1 subunit of adaptor protein complex 3 (AP-3), that is involved in signal-mediated protein sorting from Golgi membranes to endosomal-lysosomal organelles^{33,34}. Mutations in AP3B1 affect protease activity in endosomes and produce pathology-associated defects with aberrant transmembrane lysosomal protein trafficking³⁵. AP-3 depletion resulted in decreased localization of the HIV-1 major structural protein Gag from plasma membrane and late endosome, suggesting that intact AP-3 is required for HIV-1 particle production and release³⁴. Also, we have previously shown that AP-3 is targeted by the NS5 protein of West Nile virus³⁶. SARS-CoV-2 may also utilize AP-3 for particle assembly, transport, and release.

Other notable high-confidence host protein interactions with E protein include CWC27 and SLC44A2. Both SLC44A2 and CWC27 are proteins implicated in other diseases, but have yet to be characterized in relation to viral infections.

SARS-CoV-2 M Protein

Membrane (M) protein, the most abundant protein in coronavirus particles, is a type III transmembrane glycoprotein located in the virus envelope. M protein manipulates cellular membranes to bring viral and host factors together and therefore is the main driver for virus assembly and budding processes. M-M, M-S and M-N protein interactions all contribute to this assembly process³⁷. In the virion, M exists as a dimer in two major conformations (long and compact), which together determine the membrane curvature and spike density^{38,39}. SARS-CoV M protein is known to affect various host processes in a manner beneficial to viral replication and infectivity⁴⁰. M suppresses key inflammatory molecules (e.g. NF- κ B and Cox-2)⁴¹ and counteracts host viral defenses by inhibiting type I interferon production⁴². SARS-CoV M protein modulates apoptosis by interfering with PDK1-PKB/Akt signaling. This interaction between M protein and PDK1 could be targeted as a plausible therapeutic approach to modulate the pro-apoptotic properties attributed to coronavirus infection⁴³⁻⁴⁵.

In this study, we identified 30 high-confidence physical interactors of SARS-CoV-2 M protein. Transmembrane domain-mediated oligomerization of M protein at ERGIC membranes drives the assembly of coronavirus which buds into the lumen of the ERGIC⁴⁶. Therefore, it was not surprising to find many SARS-CoV-2 M protein interactors were transmembrane proteins including mitochondrial proteases (PITRM1, PMPCA, PMPCB), ATPases (ATP6V1A, ATP1B1) and kinases (AKAP8L, COQ8B, FASTKD5). In addition, we identify known host dependency (ATP6V1A, ATP1B1, TUBGCP2, RTN4) and restriction (BZW2) factors of other viruses that bind to SARS-CoV M protein. ATP6V1A is a dependency factor for Dengue virus⁴⁷, West Nile virus⁴⁷ and Influenza A H1N1 virus⁴⁸, ATP1B1 is involved in viral autophagy⁴⁹ and has a role in Sindbis virus (SINV) infection⁵⁰, and TUBGCP2 is a host dependency factor for Influenza A virus^{51,52}. RTN4 is a reticulon protein involved in the formation and stabilization of endoplasmic reticulum (ER) tubules^{53,54}. Reticulon proteins play crucial roles in viral RNA replication, compartment formation, and function⁵⁵ and are known to protect ER membrane integrity during polyomavirus SV40 infection⁵⁶. RTN4 also is involved in the formation of the *Legionella pneumophila* containing vacuoles⁵⁷. In a functional RNAi screen, BZW2 was identified as a host restriction factor for DENV infection⁵⁸. BZW2 is a translation repressor known to regulate the PI3K/AKT/mTOR signaling pathway⁵⁹⁻⁶¹. Recently, BZW2 was identified as an oncogene implicated in a number of cancers including lung adenocarcinoma, where overexpression was negatively correlated with

overall disease free survival⁶⁰⁻⁶⁴. Studies suggest that BWZ2 overexpression could also contribute to drug resistance in cancer cells, including resistance to rapamycin⁶¹.

The mechanism behind acute respiratory distress in severe SARS-CoV-2 infections is not understood but the host immune response is likely to determine the pathogenesis to some extent. We found that two related host factors REEP5 and REEP6 copurify with SARS-CoV-2 M protein. REEP5 and REEP6 can refine CXCR1-mediated cellular responses and lung cancer progression⁶⁵. REEP6 is also involved in IL-8 secretion⁶⁶. IL-8 is the major chemoattractant for neutrophils and is implicated to have a major role in the recruitment of neutrophils to the lungs in patients with sepsis-induced acute respiratory distress syndrome⁶⁷. Another high-confidence M protein interactor ANO6 is also very exciting from the perspective of viral pathogenesis. ANO6 is required to curb excessive T cell responses in chronic viral infections. ANO6-deficient T cells are hyperactivated during the early phase of infection, exhibiting increased proliferation and cytokine production. This overactivation ultimately leads to severe T cell exhaustion and the inability of the host to control viral burden⁶⁸. Interestingly, ANO6 is localized in late endosomes and SARS-CoV is also targeted to endosomes⁶⁹. Mice deficient for a related protein ANO1 suffer from tracheomalacia and die shortly after birth because of respiratory failure; ANO6 is highly expressed in the respiratory system and its involvement in respiratory functions is likely⁷⁰ which makes it an interesting candidate for future mechanistic studies in the context of SARS-CoV-2 infection.

SARS-CoV-2 N Protein

SARS-CoV nucleocapsid (N) protein is an essential structural protein that binds to viral genomic RNA (gRNA) in virions. N protein dimerization and its association with viral gRNA are crucial for viral assembly^{71,72}. It has been shown that the N protein binds to both intracellular gRNA and subgenomic RNA (sgRNA), suggesting functions in viral transcription and translation⁷³. N protein also has implications in a variety of cellular responses, including stress granule formation and host translation shutoff⁷⁴, inhibition of the nonsense mediated mRNA decay (NMD) pathway⁷⁵ and cell cycle regulation⁷⁶.

The SARS-CoV-2 N interactome includes 15 high-confidence host protein interactions, many of which are host mRNA binding proteins, including stress granule (SG)-related factors (G3BP1/2, MOV10, CK2 subunits, PABP), mRNA decay factors (MOV10 and UPF1), mTOR translational repressors (LARP1), and protein kinases (CK2). Several N protein interactors including G3BP1, G3BP2, LARP1, MOV10, PABPC1 and PABPC4 have also been detected in a mouse hepatitis virus interactome⁷⁷ and in two previous nucleocapsid protein interactomes, namely infectious bronchitis virus⁷⁸ and Influenza A virus⁷⁹. Numerous viruses have evolved diverse mechanisms to abrogate SG assembly. Poliovirus specifically cleaves G3BP to facilitate translation of viral mRNAs⁸⁰. Foot and Mouth Disease virus cleaves G3BP and inhibits SG formation⁸¹. Several other viruses including Semliki Forest virus, vaccinia virus, cardioviruses, dengue virus, Japanese encephalitis virus, Ebola virus sequester G3BP to inhibit SG formation and to promote virus replication^{82,83,84,85,86,87,88}. Amongst *Coronaviridae*, MERS virus employs its dsRNA-binding 4a protein to inhibit SG formation and promote viral replication⁸⁹ whereas IBV infection prevents the formation of SGs via yet-unknown mechanisms⁹⁰.

N protein also interacts with subunits of the broad-spectrum Casein Kinase 2 (CK2) complex (CSNK2A2 and CSNK2B). The N protein of other *Coronaviridae* has been shown to be phosphorylated at sites predicted to be substrates for CK2⁹¹, and there is a NetPhos predicted CK2 phosphorylation site in N. CK2 has also previously been shown to inhibit granule formation or promote granule disassembly in a G3BP phosphorylation-dependent manner⁹². CK2 inhibition sequesters N protein in the nucleus, away from the G3BP subunits of SGs⁷⁶. It is possible that the SARS-CoV-2 N protein inhibits the formation of cellular SGs, potentially by scaffolding the phosphorylation of G3BP by CK2. siRNA-mediated knockdown of either CSNK2A2 or CSNK2B reduced viral replication of SARS-CoV, indicating that CK2 may have a proviral function⁹³. These findings suggest that the CK2 inhibitor Silmitasertib (also known as CX-4945) could be effective in slowing SARS-CoV-2 replication. Silmitasertib is a sub-nanomolar inhibitor of CK2 currently in phase II trials for indications such as multiple myeloma or metastatic basal cell carcinoma⁹⁴. Potential antiviral effects of Silmitasertib via inhibition of CK2 and subsequent increase in the formation of antiviral SGs merits further investigation.

UPF1 is an RNA helicase functioning in the nonsense-mediated mRNA decay (NMD) pathway. In common with other virus species in the order *Nidovirales*, SARS-CoV-2 produces a nested set of sgRNAs sharing the same 3'UTR but are different in number of ORFs contained⁹⁵. In principle, only the first ORF in the 5' end is translated. Thus, many of the subgenomic mRNAs have long 3' UTRs and are potentially targeted for NMD. A previous study showed that Murine Hepatitis Virus (MHV) mRNAs were subjected to NMD⁷⁵. Transfection of plasmids containing MHV N protein had an NMD inhibitory function and prevented MHV mRNA from rapid decay. Based on the observation that SARS-CoV-2 shares a similar feature of nested sgRNA with MHV, we expect it is also subjected to NMD, and its N protein may have similar NMD inhibitory function. It is also possible that UPF1 is involved in the programmed ribosomal frameshifting during SARS-CoV-2 translation given its discovered function in suppressing nonsense mutations⁹⁶.

LARP1 is an RNA binding protein, which is known to regulate protein synthesis as well as modulate mTOR pathway⁹⁷. LARP interacts with actively translating ribosomes via another hit from our list, PABPC1, also a regulator of mTOR pathway⁹⁸. Activation of the mTOR pathway is advantageous for a broad spectrum of virus species, as it counteracts the host cell response, by inhibiting autophagy and apoptosis⁹⁹, therefore inhibition of mTOR activity has been proven useful to counteract viral infection and replication. For instance, Sirolimus (rapamycin) has been used to reduce MERS-CoV infection^{100,101} and alleviate H1N1 pneumonia and acute respiratory failure¹⁰², therefore mTOR pathway is a potential therapeutic target for SARS-CoV-2 as well. Another interesting aspect about PABPC1/4 is that they are known to shuttle into the nucleus on interaction with Nsp1 proteins from different viruses (including SARS-CoV), down-regulating gene expression via hyperadenylation and nuclear retention of mRNAs¹⁰³. Also, in a complex with LARP1 and RyDEN, PABPC1/4 can promote DENV replication¹⁰⁴. PABPC4 has been described as a potential biomarker for primary lung adenocarcinoma¹⁰⁵.

Moloney Leukemia Virus 10 Protein (MOV10) is a host cytoplasmic 5' to 3' RNA helicase that interacts with UPF1 and binds 3'UTRs¹⁰⁶. It exhibits antiviral functions independent of its helicase activity towards PRRSV, DENV and Influenza A viruses, through IFN stimulation^{107,108}. Additionally, MOV10 exhibits P-body dependent antiviral activity by binding the N protein and preventing its nuclear localization^{109,110}.

SARS-CoV Non-Structural Proteins

SARS-CoV-2 Nsp1

In SARS-CoV, Nsp1 is likely dispensable for CoV RNA synthesis¹¹¹, but may play specific roles in the interaction of the virus with the innate immune response via directly antagonizing IFN induction¹¹². In addition, overexpression of Nsp1 in the lung epithelial cell line A549 increases the production of the chemokines CCL5, CXCL10 and CCL3 30-200-fold compared with mock-transfected cells or cells expressing Nsp5, suggesting that Nsp1 may contribute to the inflammatory phenotype of SARS-CoV and SARS-CoV-2 pathology¹¹³.

In our interactome, SARS-CoV-2 Nsp1 interacts with six host proteins. Four of these host proteins form the DNA polymerase alpha complex (POLA1, POLA2, PRIM1, and PRIM2). The DNA polymerase alpha complex was recently shown to modulate the type I interferons through cytosolic RNA:DNA synthesis¹¹⁴, raising a possibility that SARS-CoV-2 Nsp1 may bind to the DNA polymerase alpha complex in the cytosol and modulate its activity to antagonize the innate immune response. Alternatively but not exclusively, Nsp1 may also interfere with the canonical DNA replication function of the complex, causing DNA replication stress and ATR activation¹¹⁵. Along this line, treatment with ATR inhibitors significantly reduced viral RNA replication, but it remains elusive how ATR activation promotes viral replication. Other proteins interacting with Nsp1 are PKP2, which interacts with Influenza A virus PB1 protein and restricts Influenza A virus replication¹¹⁶; and therefore may act as a restriction factor for SARS-CoV-2.

SARS-CoV-2 Nsp2

Nsp2 is highly variable among *Coronaviridae*, and while not essential for viral replication, deletion of Nsp2 in SARS-CoV diminishes viral growth and RNA synthesis^{117,118}. Nsp2 is translated as part of a single protein along with Nsp3 and may serve as an adaptor for Nsp3¹¹⁸.

In this study, we identified seven high-confidence host protein interactions of Nsp2. Among these are endosomal proteins FKBP15 and WASHC4 that regulate endosome transport¹¹⁹⁻¹²¹. Because the related virus SARS-CoV is translocated to endosomes after cell entry², interaction with endosomal transport proteins may reflect a mechanism by which SARS-CoV-2 gains cell entry. Nsp2 also interacts with translational repressors EIF4E2 and GIGYF2, and disruption of the EIF4E2-GIGYF2 complex leads to increased translation¹²². Nsp2 may bind to EIF4E2 and GIGYF2 to modulate translation of host and viral mRNAs. Nsp2 was also shown to interact with the acyl-CoA synthetase SLC27A2, a previously described Dengue virus restriction factor¹²³.
SARS-CoV-2 Nsp4

Nsp4 is likely essential, as loss of the Nsp3-Nsp4 interaction eliminated viral replication using an infectious cDNA clone and replicon system of SARS-CoV¹²⁴. Nsp4 is a non-structural, transmembrane protein that complexes with Nsp3 and Nsp6, and is involved in double membrane vesicle (DMV) formation¹²⁵. Together, Nsp3, Nsp4, and Nsp6 are predicted to function to nucleate and anchor viral replication complexes on DMVs in the cytoplasm¹²⁶.

We identified eight high-confidence host protein interactions with Nsp4. Nsp4 interacts with IDE, which is involved in intercellular signaling through the cellular breakdown of diverse signaling peptides^{127,128}. IDE is also involved in antigen processing through the production of an antigenic peptide that is presented to cytotoxic T lymphocytes by MHC class I¹²⁹. IDE acts as an entry receptor for varicella-zoster virus (VZV), where VZV glycoprotein E interacts with IDE through its extracellular domain^{130,131}. Nsp4 interacts with various mitochondrial proteins linked to transport, including TIMM10, TIMM10B, TIMM9 and TIMM29, members of the TIM22 complex. TIMM22 facilitates the import and insertion of multi-pass transmembrane proteins into the mitochondrial inner membrane, with TIMM9 additionally involved in protein homodimerization and chaperone binding¹³². Nsp4 also interacts with DNAJC11, which is required for mitochondrial inner membrane assembly and functions through involvement with the MICOS complex and the MOM sorting assembly machinery complex¹³³. Other interactions include ALG11, a mannosyltransferase catalyzing oligosaccharide linkage^{134,135} and NUP210, a nuclear pore membrane glycoprotein involved in nuclear pore assembly and fusion, nuclear pore spacing, and structural integrity^{136,137}.

SARS-CoV-2 Nsp5/Nsp5_C145

Nsp5 encodes the coronavirus main protease (M^{pro}) responsible for cleaving itself and the other subunits from the polyproteins Orf1/1ab¹³⁸. As these proteins include the replicase machinery, Nsp5 M^{pro} is essential for all coronaviruses, and indeed is functionally and structurally conserved throughout order *Nidovirales*¹³⁹. The catalytic residues of SARS-CoV align to H41 and C145 in our SARS-CoV-2 construct. We have used as baits both catalytically active Nsp5 as well as a catalytically dead C145A mutant.

Notably, we see the catalytically active Nsp5, but not the C145A mutant, interact with Histone Deacetylase 2 (HDAC2). HDAC2 is known to regulate genes of the inflammatory response, especially in the pulmonary context, where low HDAC2 expression contributes to increased disease severity in chronic obstructive pulmonary disease¹⁴⁰.

SARS-CoV-2 Nsp6

Nsp6 complexes with two other transmembrane proteins, Nsp3 and Nsp4, to form double membrane vesicles (DMV), anchoring viral replication complexes inside¹⁴¹⁻¹⁴³. Chemical inhibition and targeted mutagenesis studies have shown that these DMVs are crucial to viral replication and are formed early after viral entry into the cell¹⁴⁴⁻¹⁴⁷. The most well-characterized function of the Nsp6 protein is limiting autophagosome expansion, which likely benefits the virus by preventing its components from being sent to the lysosome for degradation¹⁴⁸. Further, in the context of IBV, it was shown that the generation of autophagosomes by Nsp6 can be induced by chemical inhibition of the mTOR pathway¹⁴⁸. While this behavior has been shown for SARS-CoV Nsp6 (showing 95% similarity to SARS-CoV-2 Nsp6) and related viruses such as MSV and IBV, its exact mechanism and whether SARS-CoV-2 Nsp6 will function similarly remains uncertain.

In this study, we identified four high confidence interactors of SARS-CoV-2 Nsp6 (ATP5MG, ATP6AP1, ATP13A3, and SIGMAR1). Notably, three out of four of these prey proteins are subunits of different ATP

synthases, suggesting that Nsp6 may be manipulating the metabolic program of the cell through ATP synthases of different organelles. As viral infection requires a new surplus of energy, it is unsurprising that viruses hijack host metabolic machinery to carry out a wide variety of cellular functions^{149–152}. Specifically, ATPases are crucial for budding by multiple viruses, including HIV-1, IAV, and Ebola^{153–155}. One such target is vacuolar ATPases (vATPases), which are responsible for modulating endo-lysosomal acidification and thus a number of processes like membrane trafficking and protein degradation¹⁵⁶. In the context of IAV infection, vATPase ATP6V1A was identified as a key host dependency factor for viral replication across multiple RNAi knockdown screens^{48,157}. Influenza A virus is believed to leverage this interaction to lower the pH of the lysosomal environment to accelerate the process of viral uncoating in the early stages of viral infection^{158,159}. ATP6AP1, a subunit of the vATPase protein pump and high-confidence physical interactor of Nsp6 in this study, has also been described as a host factor for a number of viruses, including IAV, WNV, and DENV^{47,48,157,160,161}. Further, dysregulation of ATP6AP1 leads to impaired vesicle acidification and intracytoplasmic granules, resulting in multiple clinical pathologies including an immunodeficiency syndrome and granular cell tumors^{162,163}. Given the known role of ATP6V1A as an IAV host factor, the mechanism of SARS-CoV-2 Nsp6 could leverage its interaction with ATP6AP1 similarly to speed replication in DMV complexes.

ATP13A3 is a poorly understood cation-transporting P-type subunit of the mitochondrial ATPase that has recently been implicated in both host innate immunity to pathogens and pulmonary pathologies. In the case of HSV-1, ATP13A3 was shown to be less abundant in the plasma membrane of infected cells, but its expression could be rescued by the deletion of a specific HSV-1 protein pUL56, suggesting that it may be specifically targeted as a host factor in the context of some viral infections¹⁶⁴. Further, ATP13A3 was identified in the plasma membrane of primary CD4+ T cells infected with Vpu-deficient and Nef-deficient HIV-1, and was differentially expressed in CD8+ T cells during IAV infection¹⁶⁵. More broadly, ATP13A3 expression was found to be a significant variable in determining interindividual response to lipopolysaccharide sensing in human dendritic cells¹⁶⁶. While ATP13A3 is lowly expressed in the lungs (though more highly expressed in the nasopharynx and bronchus), a rare variant of ATP13A3 is known to cause pulmonary arterial hypertension. It was recently reported that loss of function of *ATP13A3* results in disruption of polyamine homeostasis in pulmonary arterial endothelial cells, leading to endothelial dysfunction and ultimately pulmonary arterial hypertension^{167,168}. Notably, ATP13A3 is also amenable to direct drug targeting.

SARS-CoV RNA polymerases: Nsp7, Nsp8 and Nsp12

SARS-CoV Nsp7, Nsp8 and Nsp12 proteins form the RNA-dependent RNA polymerase (RdRp)^{169,170}. Eight Nsp7 proteins complex stoichiometrically with eight Nsp8 proteins to form a hexadecameric barrel-shaped structure thought to surround double-stranded RNA¹⁷¹. Mutations in Nsp8 that disrupt interaction with Nsp7, RNA, or Nsp12 are lethal to SARS-CoV, demonstrating the function of Nsp8 is essential. The catalytic activity of the Nsp7-Nsp8 complex is much weaker than that of Nsp12 though it is primer-independent, and RNA products of Nsp7-Nsp8 complex are typically ≤ 6 bases. Thus it is believed that the Nsp7-Nsp8 complex functions as a primase, generating short RNA primers for Nsp12's more processive, primer-dependent RNA polymerase activity^{172,173}.

Nsp12 encodes a canonical, primer-dependent RdRp domain in its C-terminus^{172,174}, and is essential for viral RNA synthesis. A Nsp7-Nsp8 heterodimer binds to and stabilizes loops in the polymerase domain of Nsp12, and is thought to facilitate interactions between Nsp12 and RNA synthesis/processing machinery¹⁷⁰. Nsp12 contains an unusually large N-terminal extension with a conserved, essential nucleotidyltransferase domain¹⁷⁵ and protein interface domain that binds a second Nsp8¹⁷⁰. The full functions of these domains in virus replication or fitness and host biology are not known. Nsp12 may have additional roles outside of the RdRp complex mediated through interactions with the uncharacterized N-terminus^{170,172,175} and/or other virus proteins including Nsp5, Nsp8 and Nsp9¹⁷⁶.

The structure of SARS-CoV-2 Nsp7/Nsp8/Nsp12 complex closely mimics that of SARS-CoV¹⁷⁷, and the complex members bear 98.8%, 97.5%, and 96.4% genetic similarity at the codon level respectively, suggesting that function will be conserved.

SARS-CoV-2 Nsp7

We identified 32 high-confidence host protein interactions with Nsp7. Groups of Nsp7 interactors include multiple Rab GTPases with various roles in exocytic and endocytic membrane trafficking, mitochondrial proteins such as cytochromes, and several other factors that were previously identified in the host interactomes of other viruses, yet without defined roles in infection.

Rab GTPases function in networks of crosstalk¹⁷⁸. Among the identified Rab GTPases, Rab14 regulates the membrane recycling pathway from endosomes to the plasma membrane which is required for ADAM protease trafficking and regulation of cell-cell junctions¹⁷⁹. Rab14 was previously characterized to be required for HIV-1 envelope glycoprotein particle incorporation¹⁸⁰. Rab1a regulates vesicular protein transport from the ER to the Golgi and was identified to be required for production of extracellular enveloped virions of VACV¹⁸¹, as well as for CSFV particle assembly¹⁸². Rab7a and Rab5c are essential for HBV infection¹⁸³. Rab7a is implied to promote virus entry in early stages¹⁸³ and restrict exocytic virion release in late stages¹⁸⁴. Rab8a was shown to be an important regulator of HIV-1 trafficking to the virological synapses¹⁸⁵. Virological synapses enable delivery of the virus to CD4+ T-cells.

ACSL3-LPIAT1 fusion protein is a known cancer gene and ACSL3 is highly expressed in human lung cancer¹⁸⁶. ACSL3 induction results in increased acyl-CoA synthesis that is essential for providing the prostaglandin required for the maintenance of non-small cell lung cancer¹⁸⁷ and mutant KRAS lung cancer tumorigenesis in vivo¹⁸⁶. Besides the function of ACSL3 in lung cancer, it is a host factor that interacts with several viral proteins and is required for poliovirus replication¹⁸⁸⁻¹⁹⁰.

MOGS is another host factor that was identified in the interactomes of various virus proteins, including HBV, HBe, HCV core, HIV VPR and gp120 and Mtb Ppe11^{189,191,192}. This gene is well characterized in the context of a congenital disorder of glycosylation. Interestingly, patients with genetic defects in MOGS manifest decreased susceptibility to viral infections¹⁹³, providing a potential target for broad spectrum therapy of viral infections.

SARS-CoV-2 Nsp8

We find that Nsp8 interacts with 23 host proteins, a number of which are known host-dependency factors of various pathogens. For example, five of the ten members of the exosome complex are identified here as high confidence Nsp8 interactors, with the remaining five just narrowly missing our stringent threshold. LARP7, a member of the 7SK snRNP RNA complex, interacts with WNV, ZIKV capsid, and HIV-1 Tat in such a way as to compete with viral proteins for the transcriptional elongator pTEFb. The interaction of LARP7 and coronavirus primase points to a mechanism by which the virus promotes elongation of its vRNA.

Interestingly, we find that Nsp8 interacts with proteins just under our scoring threshold found to be differentially regulated or expressed during acute lung disease secondary to pathogen infection, including CEBPZ, DAP3, NKRF and ZN512. NFKR for example is upregulated in the circulating monocytes and alveolar macrophages of patients with active pulmonary TB, and NKRF serves as an endogenous repressor for IP-10 and IL-8 synthesis to hinder host from robust response to MTb infection^{194,195}.

SARS-CoV-2 Nsp12

In our study, SARS-CoV-2 Nsp12 interacts with 20 high confidence host proteins. Consistent with Nsp12 RdRp activity, eight host protein interactors are RNA binding factors involved at multiple steps of RNA processing and regulation. These host proteins could facilitate long-range RNA interactions that occur during genome replication and discontinuous transcription¹⁹⁶, or mediate viral protein translation. Five of these host interactions are identified with proteins from other RNA and DNA viruses^{36,190}. Of note, Nsp12 interacts with three proteins involved in pre-mRNA splicing: A-kinase anchor protein 8 (AKAP8)¹⁹⁷; and spliceosome components pre-mRNA-splicing factor SLU7 (SLU7)¹⁹⁸ and peptidyl-prolyl cis-trans isomerase-like 3 (PPIL3). Notably, siRNA knockdown of SLU7 inhibits early stages of HIV-1 replication¹⁹⁹. Nsp12 also interacts with La-related protein 4B (LARP4B), a cytoplasmic RNA binding protein that promotes mRNA translation and interacts with PABPC1 and RACK1 kinase, potentially connecting 3' mRNA factors with translation machinery²⁰⁰. PABP, a 3' poly(A) tail binding protein, is a cis acting element on coronavirus RNA that is essential for bovine coronavirus replication^{201,202}. Nsp12 could be targeting LARP4B as a bridge to recruit

members of the PABP family for efficient RNA replication and translation. Nsp12 interacts with two RNA binding proteins that localize to and nucleate formation of stress granules: ubiquitin-associated protein 2 (UBAP2) and ubiquitin-associated protein 2-like (UBAP2L)²⁰³. UBAP2L interaction is identified in our data with SARS-CoV-2 Nsp9, although it falls below our scoring threshold. Coronavirus species mouse hepatitis virus Nsp9 has been shown to interact with Nsp12¹⁷⁶. This may suggest a potential role for SARS-CoV-2 Nsp12 and Nsp9 in coordinating host and/or viral RNA regulation (see also Nsp9), as stress granules are sites of RNA storage and intermediate stages between translation and mRNA decay²⁰⁴. Additionally, since MERS-CoV has been shown to inhibit stress granule formation to promote viral replication⁸⁹, SARS-CoV-2 Nsp12 may interact with and sequester UBAP2L as a potential mechanism to inhibit stress granule nucleation and promote virus replication (see also N protein for role of stress granules).

Although coronavirus genome replication and transcription occurs in the cytoplasm, SARS-CoV-2 Nsp12 interacts with five nuclear, DNA-related factors: transcription factors CREB-regulated transcription coactivator 3 (CRTC3), transcription factor 12 (TCF12) and zinc finger protein 318 (ZNF318); chromatin factor SBNO1; and AKAP8 which regulates histone methylation and gene expression²⁰⁵. Nsp12 shows DNA-dependent activity and can synthesize nucleotides from a DNA template *in vitro*^{172,173}. Nsp12 may have novel roles in chromatin and transcription regulation, although the advantage to the virus is unclear.

Nsp12 also interacts with host proteins that regulate inflammatory signaling and apoptotic pathways. Nsp12 interacts with receptor-interacting serine/threonine-protein kinase 1 (RIPK1) with very high confidence. As an active regulatory kinase, RIPK1 triggers cell death by apoptosis or necroptosis; as a scaffold independent of its kinase activity, RIPK1 regulates inflammatory signaling and inhibits cell death²⁰⁶⁻²⁰⁸. Many diverse viral and bacterial proteins interact with and/or modify RIPK1 to modulate host defense pathways, cytokine signaling and/or host cell death²⁰⁹⁻²¹¹. For example, HIV-1 protease cleaves and inactivates RIPK1, which then impairs host defense pathways²¹¹. Importantly, RIPK1 is a druggable target, and many inhibitors are being tested as anti-inflammatory treatments for neurodegenerative diseases and cancer²¹². However, given the two faces of RIPK1 regulating apoptosis for pathogen clearance²¹⁰ or stimulating cytokine production as part of the inflammatory response²⁰⁸, the usefulness of drugs targeting RIPK1 as a treatment for SARS-CoV-2 will depend on future research identifying which pathway is engaged by Nsp12. In addition, Nsp12 interactor AKAP8 binds and shuttles caspase 3 to the nucleus as part of caspase-mediated proteolysis and apoptosis²¹³. These interactions suggest additional novel roles for Nsp12 outside of canonical RdRp activity in regulating host inflammation and cell death, perhaps mediated through the large uncharacterized N-terminal domain of Nsp12.

SARS-CoV-2 Nsp15

In SARS-CoV, Nsp15 has uridine-specific endoribonuclease (endoU) activity, and is essential for viral RNA synthesis²¹⁴. The Nsp15-associated endoU domain is one of the most conserved proteins among CoVs and related viruses, suggesting important functions in the viral replicative cycle. The endoUs were shown (i) to have endonucleolytic activity, (ii) to cleave 3' of pyrimidines, preferring uridine over cytidine, and (iii) to release reaction products with 2'-3'-cyclic phosphate and 5'-OH ends. Nsp15s were shown to form homohexamers composed of a dimer of trimers²¹⁵. Deletion of a conserved domain for this enzymatic activity led to loss of viral RNA generation measured by RT-PCR²¹⁴. Nsp15 is also known to be critical for evasion of host dsRNA sensors in macrophages²¹⁶. In our map, Nsp15 interacts with three host proteins. NUFT2 mediates the import of GDP-bound RAN from the cytoplasm into the nucleus, and thus indirectly plays a more general role in cargo receptor-mediated nucleocytoplasmic transport^{217,218}. ARF6 is a GTP-binding protein involved in protein trafficking that regulates endocytic recycling and cytoskeleton remodeling²¹⁹⁻²²³ as well as the activation of cholera toxin²²⁴. RNF41 acts as E3 ubiquitin-protein ligase and promotes TRIF-dependent production of type I interferon and inhibits infection with vesicular stomatitis virus²²⁵.

SARS-CoV-2 Nsp9

In SARS-CoV and related coronaviruses, Nsp9 is an essential non-structural protein that binds to RNA and DNA, with a preference for single-stranded RNA²²⁶⁻²²⁹. The function of Nsp9 is not well annotated, though in SARS-CoV it is believed to interact with Nsp8 and the viral replication complex (Nsp7, Nsp8, and

Nsp12)^{229,230}. In our hands, SARS-CoV-2 Nsp9 interacts with 16 high confidence host proteins, with many having been shown in previous studies to regulate nuclear transport, transcription, and mRNA degradation in response to various viral infections. Unexpectedly, Nsp9 also demonstrates some strong interactions with extracellular matrix proteins involved in elastin formation, lung development, and lung injury and repair.

Nsp9 interacts with Nup62, Nup58, and Nup54, the three components of the Nup62 subcomplex which forms the channel of the nuclear pore complex (NPC)²³¹⁻²³⁵. In addition, Nsp9 interacts with nucleoporins on the cytoplasmic side of the nuclear pore complex (i.e. NUP214 and NUP88) but none from the nucleoplasmic side²³⁶ indicating a cytoplasmic role of Nsp9 at the NPC. Many viruses have been shown to exploit cellular nuclear transport machinery to block host-related transport or promote viral transport in a manner beneficial to the virus²³⁷⁻²⁵⁰. Nup62 in particular interacts with a number of viral proteins including EBV BGLF4 protein kinase²⁵¹, HPV16 and HPV8 E7 proteins^{252,253}, and HIV-1 IN²⁵⁴. Several positive-sense single strand RNA viruses (e.g. poliovirus, EV71, rhinovirus, and coronaviruses) target Nup62 either through viral protease-directed cleavage²⁴⁰⁻²⁴⁶ or induced hyperphosphorylation²⁴⁷⁻²⁴⁹ in order to limit nuclear transport. Vaccinia virus, a DNA poxvirus, replicates in cytoplasmic virus factories that recruit G3BP1 and Nup62²⁵⁰. Nup54 interacts with Influenza A virus polymerase and was shown to be important for virus replication and transcriptional activity²⁵⁵. In addition to the nucleoporins, Nsp9 interacts with MIB1, a RING-type E3 ubiquitin ligase shown to act as a dependency factor during adenovirus infection²⁵⁶. Adenoviruses are non-enveloped DNA viruses that utilize the NPC to dock and deliver genomic cargo into the nucleus, and in this study, the authors demonstrate that MIB1 mediates the delivery of viral DNA through the NPC²⁵⁶.

In addition to nuclear transport machinery, Nsp9 interacts with three transcription regulators, Nek9, DCAF7 and eIF4H. Nek9 is a serine/threonine kinase that regulates mitotic progression²⁵⁷. It has been shown as an adenovirus dependency factor promoting viral growth, interacting with E1A protein to silence the expression of certain host genes, and was demonstrated to colocalize at adenovirus replication centers²⁵⁸. DCAF7 is a potential substrate adaptor for CUL4-DDB1 E3 ligase²⁵⁹ that has also been shown to interact with adenovirus E1A protein to suppress innate immune response and depresses IFN stimulated genes (ISGs)²⁶⁰. In combination with eIF4A, eIF4H was shown to interact with HSV virus host shut off proteins, with eIF4A shown to help degrade mRNA and switch from host to viral gene expression²⁶¹⁻²⁶⁴. Taken together, these interactors suggest a potential function of Nsp9 in the inhibition of host mRNA expression potentially to limit the express of ISGs.

Somewhat unexpectedly, Nsp9 interacts with several proteins involved in lung development, lung injury and repair, and lung cancers. The most abundant interactor in the Nsp9 interactome is Fibrillin-2 (FBN2), an extracellular matrix glycoprotein protein involved in elastin fiber and respiratory organ development²⁶⁵. Additional related interactors were identified, albeit with lower abundance. Fibrillin-1 (FBN1) and Fibulin-5 (FBLN5) are both extracellular matrix proteins, also involved in elastin fibre development. Mutations in FBN1 cause Marfan syndrome (MFS), a connective tissue disease that can result in early morbidity and mortality mainly caused by aortic aneurysm and rupture, though additional clinical manifestations include lung complications²⁶⁶. FBLN5 is indicated to serve a role during lung injury and repair, is frequently silenced in lung cancer, and has been shown to suppress cell invasion²⁶⁷⁻²⁷².

The Nsp9 interactome reveals a potential function for the protein not only in viral replication, but potentially in regulating nuclear transport, though it is unclear if this regulation would block host cell transport or promote viral transport. In addition, the interaction with transcription regulators indicates a potential role in inhibition of host cell transcription and potentially host shut off. And finally, the unexpected interaction with fibrillins-1 and -2, and fibulin-5 could implicate Nsp9 as a potential complicating factor during disease pathogenesis, and may point to additional molecular reasons underlying SARS-CoV-2 complications in the lungs.

SARS-CoV-2 Nsp10

Nsp10 contains two Zn-finger motifs, binds nucleic acids non-specifically, and has been implicated in minus-strand RNA synthesis, thus performing an essential role in viral replication^{273,274}. A unique feature for SARS-CoV is that Nsp16 requires Nsp10 as a stimulatory factor to execute its methyltransferase activity²⁷⁵.

Nsp10 on its own forms a dodecameric homomeric complex²⁷⁶ which excludes its interfaces with Nsp14 and Nsp16, meaning that Nsp10 could have at least two different functional quaternary structures. In our map, we identify five high-confidence host protein interactions with Nsp10. Nsp10 interacts with two subunits of the clathrin adaptor protein complex 2 (AP-2), AP2A2 and AP2M1. This interaction is reminiscent of the Nef protein from Human and Simian Immunodeficiency Viruses which are shown to bind the AP-2 complex through a canonical AP-2 recognition acidic dileucine motif ([RQED]XXXL[LIV])²⁷⁷. HIV and SIV are thought to use the interaction between Nef and AP-2 to hijack the clathrin machinery and endocytose host proteins such as CD4 and MHC-I²⁷⁸. Interestingly, coronavirus Nsp10 proteins do not appear to contain the canonical AP-2 binding motifs (the acidic dileucine motif [RQED]XXXL[LIV] for binding AP2A2 nor YXXΦ for binding AP2M1).

Nsp10 also interacts with GFER which was identified as a host dependency factor for West Nile and Dengue virus infections⁴⁷. Two other Nsp10 interactors ERGIC1 and GRPEL do not have a known role in viral pathogenesis. ERGIC1 plays a possible role in transport between endoplasmic reticulum and Golgi²⁷⁹; and GRPEL1 participates in the translocation of transit peptide-containing proteins from the inner membrane into the mitochondrial matrix²⁸⁰.

SARS-CoV-2 Nsp11

SARS-CoV-2 Nsp11 is a short peptide (13 aa) at the end of Orf1a, and it is not clear if Nsp11 encodes a functional protein. Nsp11 was only found to interact with two proteins, ERP29 and TBCA. ERP29, a PDI like protein localized to the ER which plays a role in processing of secretory proteins within the endoplasmic reticulum (ER). It has been shown ERP29 triggers a conformational change and exposes the C-terminal arm of polyomavirus VP1 protein, leading to formation of a hydrophobic particle that binds to a lipid bilayer. Therefore, this ER protein mediates the penetration of polyomavirus across the ER membrane²⁸¹.

SARS-CoV Capping Enzymes: Nsp13, Nsp14 and Nsp16

The m7GpppN (N any nucleotide) cap of mRNA promotes translation. SARS-CoV Nsp13, Nsp14, and Nsp16 encode enzymes that install cap structure onto mRNA^{282,283}. The pathway of cap synthesis on nascent viral mRNA is thought to be similar to capping of cellular mRNA, but occurs in the cytoplasm instead of the nucleus^{282,284,285}.

SARS-CoV-2 Nsp13

Nsp13 is essential for SARS-CoV viral RNA synthesis²⁸⁶, and SARS-CoV-2 Nsp13 shares 100% amino acid similarity with SARS-CoV. Nsp13 is a helicase/triphosphatase, and triphosphate cleavage initiates the first step in mRNA capping²⁸⁷. Nsp13 hydrolyses the gamma phosphate of nascent mRNA and the resulting diphosphate is then converted to a GpppN RNA by a yet to be identified guanylyl transferase.

SARS-CoV-2 Nsp13 was found to interact with 40 host proteins, from Protein Kinase A (PKA) signalling, to the Golgi apparatus, to multiple members of protein complexes associated with microtubules/centrosomes. SARS-CoV-2 Nsp13 showed a strong interaction with Giantin (GOLGB1), which has previously been shown to interact with herpes simplex virus type 1 (HSV-1) UL37²⁸⁸ and the Tick-borne encephalitis virus (TBEV) replicon²⁸⁹. Interestingly, in macaque experiments expression of the HIV protein Nef resulted in increased GOLGB1 levels and led to Golgi disruption and specific pulmonary vasculopathies²⁹⁰.

Unexpectedly, we found that SARS-CoV-2 Nsp13 pulled down both the regulatory (PRKAR2A and PRKAR2B) and the catalytic (PRKACA) subunits of PKA as well as the A-kinase anchoring protein AKAP9 and the phosphodiesterase interacting protein PDE4DIP. AKAP9 (also called AKAP450) is a large scaffolding protein that localizes to the Golgi apparatus and centrosomes^{291,292} where it assembles multiple signaling proteins (e.g., PKA and PDE4D) that control microtubule organization²⁹³, polarized secretion²⁹⁴, Golgi morphology^{294,295}, ciliogenesis²⁹⁶, directional cell migration²⁹⁷ and cell cycle progression²⁹². Importantly, the activities of PKA signaling complexes have been implicated in multiple membrane transport steps²⁹⁸⁻³⁰¹, suggestive of a role for SARS-CoV-2 Nsp13 in hijacking the host secretory pathway for viral benefit. Also notably, a pool of AKAP9 relocalizes to RNA stress granules upon treatment with arsenite where it forms a complex with G3BP and CCAR1 and regulates stress granule size and composition³⁰². PKA, being a kinase, is also targetable by small molecule inhibitors or peptides that target the AKAP-PKA binding interface.

An additional SARS-CoV-2 Nsp13 interaction partner was the endosomal transport protein ERC1. Knockout of ERC1 causes a significant decrease in dengue virus replication, and interestingly a similar phenotype was observed with additional SARS-CoV-2 Nsp13 pulldown target GOLGA2³⁰³. The NS3 protein of hepatitis C virus binds to ERC1 and may mediate the pathogenesis of HCV³⁰⁴, and knockdown of ERC1 significantly decreases human cytomegalovirus (HCMV) viral production³⁰⁵. Of particular interest, ERC1 has previously been identified as a potential drug target in dengue virus infection³⁰⁶.

SARS-CoV-2 Nsp14

Nsp14 is a bifunctional enzyme. It encodes an exonuclease (exo) domain that corrects mutations that arise during genome replication³⁰⁷. In addition, a separate domain of Nsp14 functions as a SAM dependent methyltransferase (MTase) that generates the N-7 Guanosine of the m7GpppN cap on viral mRNA. High-resolution crystal structures of Nsp10/Nsp14 suggest exo and MTase activity is stimulated by Nsp10 through an allosteric mechanism³⁰⁸. There are three host factors that copurify with Nsp14. GLA is an alpha galactosidase implicated in Fabry Disease³⁰⁹. Migalastat, a pharmacological chaperone, targets GLA through the inhibition of alpha-glucosidase and glycosylation, increasing its lysosomal activity³¹⁰. SIRT5 is a mitochondrial protein linked to metabolism and aging that removes malonyl, succinyl, acetyl, and glutaryl groups on lysines of target proteins³¹¹⁻³¹⁴. Numerous compounds target SIRT5, including HDAC inhibitors³¹⁵. IMPDH2 catalyzes the conversion of isosine 5' phosphate (IMP) to xanthine 5'-phosphate (XMP) which is then converted into guanine 5' monophosphate for *de novo* synthesis of guanine nucleotides³¹⁶. It is tempting to speculate that the copurification of Nsp14 and IMPDH2 reflects an interplay between Nsp14 activities and purine nucleotide metabolism. Merimepodib, a nucleoside analog and broad spectrum antiviral, is among the compounds targeting IMPDH2³¹⁷.

SARS-CoV Open Reading Frames

SARS-CoV-2 Orf3a

Orf3a is the largest (274 aa) group-specific Orf in the SARS-CoV-2 genome. It is thought to be non-essential but has multiple key functions in viral pathogenesis, from mediating the trafficking of SARS-CoV Spike (S protein) to inducing apoptosis and inflammation during infection³¹⁸⁻³²³. Specifically, Orf3a is a type IIIa integral membrane protein thought to induce pro-IL-1 β expression and protein maturation through the TRAF3-dependent ubiquitination of ASC and p105, ultimately activating NF- κ B and the NLRP3 inflammasome³¹⁹. Despite its clear functional significance as an accessory protein, Orf3a is not believed to be critical for the formation of viral particles³²⁰, though it has been shown to upregulate the secretion of fibrinogen in lung epithelial cells, which is responsible for the induction of cytokine storm, particularly in the respiratory tract³²⁴. Within the cell, Orf3a localizes to the perinuclear region and plasma membrane, forming punctae throughout the cytoplasm as it complexes with cellular factors^{318,325,326}. In the rER and Golgi, Orf3a has been shown to cause substantial ER stress during infection³²⁷. A Yxx Φ motif present in the C-terminal cytoplasmic domain of Orf3a is required for delivery to the plasma membrane, from which Orf3a is internalized and traffics through the endocytic pathway to lysosomes³²⁸. Orf3a can form tetramers that are proposed to act as cation-permeant ion channels³²⁹. In this study, Orf3a pulled down eight high-confidence host protein interactors (ALG5, ARL6IP6, CLCC1, HMOX1, SUN2, TRIM59, VPS11, VPS39) with functional enrichments in autophagy (HMOX1, VPS11, VPS39) and organelle localization (HMOX1, VPS11, SUN2). VPS11 and VPS39 serve as members of the HOPS and CORVET complexes, respectively, which coordinate fusion of the lysosome with the endosome and autophagosome^{330,331}.

HMOX1, a key enzyme in heme catabolism, is one of the most promising of these physical interactors. This oxygenase cleaves free heme to produce iron, biliverdin and carbon monoxide, which provides a cytoprotective effect to cells as excess free heme induces apoptosis³³². In turn, this elicits a cascade of physiological events, most notably the induction of anti-inflammatory cytokines IL-10 and IL-1RA^{333,334}. Given these features of HMOX1 and its high expression in the lungs, it has been implicated in a broad range of disease states, including diabetes, heart failure, lung carcinoma and COPD^{335,336}. In the context of infection, upregulation of HMOX1 has shown to have a protective effect against the oxidative stress of a whole host of

pathogen infections, including viruses like HIV, DENV, HCV, and IAV, as well as parasites and *Mycobacterium* species^{337,338}. Importantly, this protein is biochemically tractable, making it amenable to direct targeting with known pharmacologic agents. As severe inflammatory response in the respiratory tract is a key clinical feature of SARS-CoV-2 infection, further exploration of HMOX1 could elucidate mechanisms of SARS-CoV-2 pathogenesis and a path forward for treatments.

Another exciting protein candidate identified in this study, CLCC1, is an intracellular chloride channel that is highly expressed in the lung, heart, and a number of other tissues. We identified a very strong, high-confidence physical interaction between CLCC1 and Orf3a. Both CLCC1 and SARS-CoV Orf3a are localized to the ER membrane, where loss of *CLCC1* results in ER stress and disruption of the protein folding capacity of the ER, leading to misfolded protein accumulation and well-characterized retinal cell dysfunction in the clinic^{339,340}. In a similar vein, expression of *CLCC1* has been correlated with volume of adipose tissue in HIV-infected men³⁴¹. Given the similar roles in solute transport, similar localization in the ER, and evidence of CLCC1 interaction with NS1 of Human Respiratory Syncytial Virus (RSV), there is a high potential for not only physical but also functional interaction of CLCC1 and Orf3a in the context of SARS-CoV-2 infection³⁴². Interestingly, CLCC1 also interacts directly with SLC15A3, a druggable peptide/histidine transporter and known interferon-stimulated gene that is regulated by TLR-activation and contributes to TLR4-mediated inflammation in macrophages and epithelial cells^{343,344}. While SLC15A3 was not identified as a direct interactor of Orf3a, we identified a number of high-confidence interactions between SARS-CoV-2 proteins and members of the solute carrier superfamily such as SLC25A17 and SLC6A15, suggesting that Orf3a may play a role in modulating host innate immunity via an indirect interaction with CLCC1 or as part of a larger protein complex or pathway.

In addition to HMOX1 and CLCC1, Orf3a also interacts with known viral host factors and interactors. ALG5, an ER-localized glycosyltransferase involved in N-glycan biosynthesis, has been characterized as a cellular host factor for Influenza A virus replication in multiple genome-wide CRISPR-Cas9 knockout screening efforts, along with other ALG family proteins^{51,52}. Taken together, our data and prior studies suggest a potential role of these ER-localized glucosyltransferases in modulating viral replication and pathogenesis, potentially through manipulation of viral particle formation. Similarly, ARL6IP6, a transmembrane protein responsible for ADP ribosylation, is known to physically interact with both HPV and WNV, and was differentially expressed in CD8+ T cells from HIV+ progressors on HAART^{36,345,346}.

SARS-CoV-2 Orf3b

SARS-CoV-2 Orf3b encodes a 168 aa protein that is not well conserved (9.5% codon similarity as compared to SARS-CoV Orf3b). While Orf3b is thought to be non-essential^{1,320}, it has been shown to be an IFN antagonist in both SARS-CoV and SL-CoV (bat)^{347,348} and to subsequently be involved in pathogenesis¹. The only confident interaction partner detected for Orf3b was the mitochondrial protein STML2/STOML2. STOML2 stimulates cardiolipin biosynthesis and recruits and stabilizes prohibitin. Both STOML2 and its interactor prohibitin have been shown to be host dependency factors for Enterovirus 71 neuropathogenesis³⁴⁹. STOML2 forms large complexes with the i-AAA protease YME1L and the rhomboid protease PARL at the inner mitochondrial membrane, which regulate key proteins of the mitochondrial stress response such as PGAM5 and PINK1³⁵⁰. STOML2 may directly be involved in regulating T-cell-mediated immune responses by modulating T-cell receptor activation³⁵¹.

SARS-CoV-2 Orf6

Orf6 is not essential for the replication of SARS-CoV, but affects viral production³⁵². Orf6 may function as a type I IFN antagonist, suppressing IFN induction and IFN signalling pathways by binding to and sequestering karyopherin $\alpha 2$, which normally facilitates the nuclear import of the interferon signalling responsive transcription factor STAT1^{348,353}. In SARS-CoV infected cells, Orf6 complexes with Orf9b³⁵⁴. SARS-CoV-2 Orf6 was found to interact with three host proteins: NUP98, RAE1, and MTCH1. As described in the main text, NUP98-RAE1 is an interferon-inducible mRNA nuclear export complex that is targeted by multiple viruses including VSV, IAV, KSHV, and Polio^{355,356}.

SARS-CoV-2 Orf7a

SARS-CoV Orf7 is divided into two open reading frames, designated Orf7a and Orf7b. Orf7a (also known as U122) encodes a 122-amino-acid protein and contains a compact seven-stranded β -stack similar in structure to members of the immunoglobulin superfamily³⁵⁷. Orf7a has a well-characterized localization to different locations throughout the cell, from the perinuclear region to the cytoplasm, and even contains a type-1 transmembrane domain anchoring it in the plasma membrane³⁵⁸⁻³⁶⁰. This distribution into multiple cellular regions could help explain the various functions of Orf7 (namely regulation of cell cycle progression and apoptosis) and the diversity of its interaction partners³⁵⁷⁻³⁶⁰. The role of Orf7a in apoptosis was highlighted by an increase in caspase-3 protease activity that resulted in a significant induction of apoptosis³⁵⁸. Orf7a expression has also been shown to downregulate cyclin D3, resulting in the accumulation of retinoblastoma protein (Rb) and ultimately cell cycle arrest in G0/G1 phase³⁵⁹. Further, Orf7a has been shown to both localize in the perinuclear region and colocalize with ER and ER-Golgi intermediate compartment (ERGIC) markers during infection³⁶⁰. Interestingly, this cellular localization coincides with that of high-confidence protein interactors identified in this study, MDN1 and HEATR3, as well as a factor that was just below our MIST threshold, TNPO1. While it did not satisfy our stringent scoring criteria, TNPO1, or transportin-1, is worth mentioning due to its demonstrated role in other viral infections such as Influenza A virus, HIV-1 and Hepatitis C virus, where it plays a crucial role in mediating nuclear transport of viral proteins and protein complexes³⁶¹⁻³⁶⁴. HEATR3 has also been shown to activate the NF- κ B pathway via NOD-2, which has been implicated in a pro-inflammatory response during Crohn's disease^{365,366} and therefore Orf7a may target HEATR3 to modulate inflammatory response upon SARS-CoV-2 infection.

SARS-CoV-2 Orf8

Orf8 is an accessory protein and is not essential for virus replication *in vitro* and *in vivo*^{320,367}. It is one of the most rapidly evolving regions among SARS-CoV genomes and was previously shown to be a recombination hotspot³⁶⁸⁻³⁷⁰. Pairwise comparison of amino acid sequences showed that SARS-CoV-2 Orf8 exhibited 45.3% sequence similarity with SARS-CoV. Orf8 in human isolates from the 2003 epidemic contained a signature 29-nucleotide deletion compared to all civet and bat SARS-related CoVs, which causes the split of full-length Orf8 into two small proteins: 8a and 8b³⁷¹. Orf8 from SARS-CoV-2 encodes a single polypeptide and lacks the aggregation motif VLVVL present in SARS-CoV Orf8b, which was shown to induce ER stress and activate NLRP3 inflammasomes³⁷². Further, Orf8b protein has been shown to be modified by N-linked glycosylation on N81 residue, which protects Orf8ab protein from proteasomal degradation³⁷³. This novel Orf8 likely encodes a secreted protein and has an N-glycosylation site at N78, within the consensus sequence NYT.

We identified 47 high-confidence host protein interactions with Orf8. Several Orf8 interactors are involved in ER stress and ER-associated degradation (ERAD) pathway, including UDP-glucose/glycoprotein glucosyltransferase 2 (UGGT2), ER degradation enhancing alpha-mannosidase like protein 3 (EDEM3), OS9³⁷⁴, N-glycanase 1 (NGLY1), and FAD-dependent oxidoreductase domain-containing protein 2 (FOXRED2)³⁷⁵⁻³⁷⁸. The ERAD pathway targets unassembled glycoproteins for ubiquitylation and proteasomal degradation. EDEM3 has been shown to increase ubiquitylation of HCV envelope proteins via direct physical interaction and consequently reduce viral production³⁷⁹. OS9 and ERLEC1 proteins are also known to be targeted by other virus-encoding proteins from Dengue virus¹⁹⁰, HIV¹⁸⁹, WNV³⁶, HPV and KSHV³⁸⁰, suggesting common molecular mechanisms of infection and proliferation used by these different pathogens.

Infection with the SARS virus results in severe inflammation in the lungs, which can lead to respiratory distress and fibrosis during the late stages of infection³⁸¹. Fibroblast activation and overexpression of collagen are two important aspects of the pathogenesis of lung fibrosis. Interestingly, we identified a number of Orf8 interactors implicated in pulmonary fibrogenesis including FKBP10³⁸², GDF15³⁸³, NEU1³⁸⁴ and IL17RA³⁸⁵. In addition, the expression levels of ADAMTS1³⁸⁶ and HS6ST2³⁸⁷ are modulated during lung inflammation and fibrosis and are identified as Orf9b interactors. Growth differentiation factor 15 (GDF15) is a fibroblast-inhibiting cytokine that inhibits the growth and activation of lung fibroblasts by inactivating the TGF- β -Smad pathway, suggesting this cytokine could be a potential therapeutic for ameliorating interstitial lung

fibrosis during severe SARS infection. FK506-binding protein 10 (FKBP10) is a collagen chaperone and inhibition attenuates expression of profibrotic mediators and effectors³⁸², suggesting that this protein can be targeted to reduce virus-induced lung fibrosis. Activation of the pro-inflammatory cytokine receptor IL17RA in lung tissues is an important host defense mechanism upon fungal, bacterial and viral infections, but its overactivation increases collagen secretion and exacerbates pulmonary fibrosis³⁸⁵. Inhibition of IL17RA signaling promotes resolution of pulmonary inflammation and fibrosis in *in vivo* models³⁸⁸ and may therefore serve as a therapeutic strategy to reduce lung fibrosis during SARS infection.

Though below our stringent scoring threshold, one additional interesting protein identified in Orf8 pull-downs was the cellular guanyl transferase RINGTT/Mce1. This interaction was significant (>0.5 BFDR) but just below our MIST threshold (MIST score = 0.649). Previous studies suggest RINGTT can exist in the cytoplasm^{389,390}, it is possible that Orf8 recruits RINGTT to viral mRNA to add G to nascent mRNAs after they are acted on by Nsp13 to make GpppN mRNA that is subsequently acted on by Nsp14 and Nsp16 (see section on SARS-CoV Capping Enzymes).

SARS-CoV-2 Orf9b

Orf9b is an accessory protein synthesized from an alternative complete reading frame within the viral N gene, which encodes for a 98-aa long protein. Orf9b has been shown to be expressed in SARS-CoV-infected cells and antibodies against Orf9b were detected in the sera from convalescent-phase SARS patients^{391,392}, however the function of Orf9b is largely unknown. It is known that Orf9b can passively diffuse into the nucleus and is actively exported via Crm1-mediated nucleocytoplasmic export³⁹³. In addition, Orf9b localizes to mitochondria and causes mitochondrial elongation by inducing ubiquitination-mediated proteasomal degradation of the main pro-fission factor (DRP1) dynamin-like protein 1³⁹⁴. Orf9b targets the mitochondrial-associated adaptor molecule MAVS signalosome by utilizing PCBP2 and the HECT domain-containing E3 ligase AIP4, resulting in the degradation of MAVS and therefore limiting host cell interferon responses³⁹⁴.

We found that SARS-CoV-2 Orf9b interacts with 11 human proteins, including with a mitochondrial import receptor, translocase of outer membrane 70 (TOM70). TOM70 is known to interact with MAVS protein upon RNA virus infection and it acts as a critical adaptor linking MAVS to TBK1/IRF3, resulting in the activation of IRF-3³⁹⁵. TOM70 also makes a dynamic protein complex with HSP90/IRF3/BAX and mediates virus-induced apoptosis³⁹⁶. Though more studies need to be done to fully flesh out this interaction, it is possible SARS-CoV-2 Orf9b may target TOM70 to modulate IRF3-mediated gene expression or apoptosis upon virus infection. Another mitochondrial protein identified as interacting with Orf9b is BCL2-associated athanogene 5 (BAG5). BAG5 inhibits mitophagy of damaged mitochondria by suppressing recruitment of Parkin to the sites of damage³⁹⁷. Several viruses trigger Parkin-dependent mitophagy to promote persistent infection and impair the innate immune response³⁹⁸. SARS-CoV-2 Orf9b might act similarly by antagonizing the function of BAG5.

In addition to mitochondrial proteins, SARS-CoV-2 Orf9b was also found to interact with CHMP2A, a member of the endosomal sorting complex required for transport (ESCRT)-III machinery³⁹⁹. CHMP2A was shown to contribute to the budding of a variety of viruses, including HIV⁴⁰⁰, equine infectious anemia virus (EIAV)⁴⁰¹, and murine leukemia virus⁴⁰¹, suggesting a critical role for virus release. Other Orf9b interactors of interest include microtubule affinity-regulating kinases MARK1, MARK2, and MARK3. These proteins are involved in regulating microtubule dynamics and phosphorylation of tau⁴⁰², and MARK2 was also shown to regulate HIV trafficking through phosphorylation of FEZ1⁴⁰³.

SARS-CoV-2 Orf9c

SARS-CoV-2 Orf9c (referred to as Orf9B in Wu et. al.) encodes a short polypeptide that is 70 aa in length⁴⁰⁴. There is some debate over whether Orf9c encodes a functional protein, or what its function would be, as Orf9c is thought to be dispensable for virus replication⁴⁰⁵⁻⁴⁰⁷. Therefore it is unclear how clinically relevant molecular interactions for this bait would be in the context of coronavirus infection. Keeping that in mind, we are however able to express and purify Orf9c in HEK293T cells, identifying 26 high confidence human protein interactors of diverse functional enrichments. These functions include mitochondrial

respiratory chain complex assembly (NDUFB9, NDUFAF1, ACAD9, ECSIT, BCS1L)^{408–410}, GPI-anchor biosynthesis (PIGO, PIGS, GPAA1)⁴¹¹, and regulation of I-kappa β kinase and NF-kappa β signaling (NLRX1, F2RL1, NDFIP2).

F2RL1 is implicated in a variety of cellular processes related to the pathogenesis of respiratory viruses and pulmonary disease, including NF κ B activation, cooperativity with Toll-like receptors, innate immune recruitment and activation, and acute lung inflammation^{412–416}. In the context of IAV pathogenesis of monocytes and macrophages, F2RL1 activation protects against viral infection through an IFN-gamma-mediated mechanism^{417,418}. Importantly, F2RL1 is the target of four known pharmacologic agents AC-55541, AZ8838, GB110 and Z3451. Another interactor linked to pulmonary function is NLRX1, an attenuator of Influenza A virus-induced inflammation⁴¹⁹. During IAV infection, NLRX1 promotes type I IFN signaling and macrophage survival⁴¹⁹. It is an essential moderator of macrophage immunity, as it senses the extent of viral replication and maintains a protective balance between antiviral immunity and excessive inflammation within the lungs⁴¹⁹.

In our study, Orf9c is also shown to interact with MRP1 (encoded by *ABCC1*), a multifunctional ATP-binding cassette protein that, among other diverse functions, controls the ATP-dependent efflux of drugs from the cell. It has been implicated in multidrug resistance, viral pathogenesis, and pulmonary disease, and is directly targetable by FDA-approved pharmacologic agents daunorubicin and mitoxantrone⁴²⁰. MRP1 has a demonstrated role in both HIV and CMV biology, is found to be differentially expressed in a polarized subset of macrophages during HIV-1 infection, and is associated with CMV latency^{421–423}. Interestingly, HIV-1 protease inhibitors saquinavir, zidovudine, and zalcitabine are substrates of MRP1, though it was found that MRP1 did not affect the antiviral activity of these drugs in cell lines⁴²⁴. The role of MRP1 in determining the severity of diseases (e.g., COPD, pneumonia, and lung carcinoma) and multidrug resistance in the lung has been well-characterized, which could be particularly relevant given the clinical manifestation and treatment of ARDS and pneumonia during SARS-CoV-2 infection^{425–428}.

SARS-CoV-2 Orf10

SARS-CoV-2 Orf10 codes for a peptide only 38 aa long and does not have a homolog in SARS-CoV. There is no data yet providing evidence that the protein is expressed during SARS-CoV-2 infection, however we found that upon expression in HEK293T cells Orf10 interacts with nine host proteins. Among these are multiple members of the Cullin RING E3 ligase 2 (CRL2) complex, including CUL2, ELOB, ELOC, RBX1 and ZYG11B. Cullin RING E3 ligases play a central role in viral infections, since they are commonly hijacked by viral proteins to ubiquitinate and degrade viral restriction factors. CRL2 has been previously found to be targeted by poxviral ANK/BC via a C-terminal BC box domain resulting in potent suppression of inflammatory cytokines production, including interferon⁴²⁹. Similarly, Human Papilloma Virus protein HPV16 E7 binds to an active CRL2 complex, and the association correlates with the ability of HPV16 E7 to transform cells⁴³⁰. ZYG11B, a substrate adapter of CUL2, is the highest scoring hit in the Orf10 interactome indicating that Orf10 might bind to the assembled CUL2^{ZYG11B} complex. Interestingly, ZYG11B targets substrates with exposed N-terminal glycines for degradation⁴³¹. Orf10 contains an N-terminal glycine but does not have lysine residues, suggesting a few possible models: (1) Orf10 hijacks the CUL2^{ZYG11B} complex for ubiquitination and degradation of restriction factors, or (2) Orf10 blocks CUL2^{ZYG11B} and prevents the ubiquitination of its targets, or (3) Orf10 is targeted by CUL2^{ZYG11B} for degradation through N-terminal ubiquitination.

Supplementary Discussion References

1. Chan, J. F.-W. *et al.* Genomic characterization of the 2019 novel human-pathogenic coronavirus isolated from a patient with atypical pneumonia after visiting Wuhan. *Emerg. Microbes Infect.* **9**, 221–236 (2020).
2. Du, L. *et al.* The spike protein of SARS-CoV--a target for vaccine and therapeutic development. *Nat. Rev. Microbiol.* **7**, 226–236 (2009).
3. Xie, Y. *et al.* GPS-Lipid: a robust tool for the prediction of multiple lipid modification sites. *Sci. Rep.* **6**, 28249 (2016).
4. Ren, J. *et al.* CSS-Palm 2.0: an updated software for palmitoylation sites prediction. *Protein Eng. Des. Sel.* **21**, 639–644 (2008).
5. Petit, C. M. *et al.* Palmitoylation of the cysteine-rich endodomain of the SARS-coronavirus spike glycoprotein is important for spike-mediated cell fusion. *Virology* **360**, 264–274 (2007).
6. Ohta, E. *et al.* Identification and characterization of GCP16, a novel acylated Golgi protein that interacts with GCP170. *J. Biol. Chem.* **278**, 51957–51967 (2003).
7. Ko, P.-J. *et al.* A ZDHHC5-GOLGA7 Protein Acyltransferase Complex Promotes Nonapoptotic Cell Death. *Cell Chem Biol* **26**, 1716–1724.e9 (2019).
8. Li, Y. *et al.* DHHC5 interacts with PDZ domain 3 of post-synaptic density-95 (PSD-95) protein and plays a role in learning and memory. *J. Biol. Chem.* **285**, 13022–13031 (2010).
9. Kokkola, T. *et al.* Somatostatin receptor 5 is palmitoylated by the interacting ZDHHC5 palmitoyltransferase. *FEBS Lett.* **585**, 2665–2670 (2011).
10. Lu, Y. *et al.* Palmitoylation of NOD1 and NOD2 is required for bacterial sensing. *Science* **366**, 460–467 (2019).
11. Swarthout, J. T. *et al.* DHHC9 and GCP16 constitute a human protein fatty acyltransferase with specificity for H- and N-Ras. *J. Biol. Chem.* **280**, 31141–31148 (2005).
12. Burkard, C. *et al.* ATP1A1-mediated Src signaling inhibits coronavirus entry into host cells. *J. Virol.* **89**, 4434–4448 (2015).

13. Lingemann, M. *et al.* The alpha-1 subunit of the Na⁺,K⁺-ATPase (ATP1A1) is required for macropinocytic entry of respiratory syncytial virus (RSV) in human respiratory epithelial cells. *PLoS Pathog.* **15**, e1007963 (2019).
14. García-Dorival, I. *et al.* Elucidation of the Ebola virus VP24 cellular interactome and disruption of virus biology through targeted inhibition of host-cell protein function. *J. Proteome Res.* **13**, 5120–5135 (2014).
15. Iwasaki, M. *et al.* Interactome analysis of the lymphocytic choriomeningitis virus nucleoprotein in infected cells reveals ATPase Na⁺/K⁺ transporting subunit Alpha 1 and prohibitin as host-cell factors involved in the life cycle of mammarenaviruses. *PLoS Pathog.* **14**, e1006892 (2018).
16. Tan, Y.-J., Lim, S. G. & Hong, W. Characterization of viral proteins encoded by the SARS-coronavirus genome. *Antiviral Res.* **65**, 69–78 (2005).
17. DeDiego, M. L. *et al.* Coronavirus virulence genes with main focus on SARS-CoV envelope gene. *Virus Res.* **194**, 124–137 (2014).
18. Schoeman, D. & Fielding, B. C. Coronavirus envelope protein: current knowledge. *Viol. J.* **16**, 69 (2019).
19. Du, Y., Zuckermann, F. A. & Yoo, D. Myristoylation of the small envelope protein of porcine reproductive and respiratory syndrome virus is non-essential for virus infectivity but promotes its growth. *Virus Res.* **147**, 294–299 (2010).
20. Li, Y., Surya, W., Claudine, S. & Torres, J. Structure of a conserved Golgi complex-targeting signal in coronavirus envelope proteins. *J. Biol. Chem.* **289**, 12535–12549 (2014).
21. Jimenez-Guardeño, J. M. *et al.* Identification of the Mechanisms Causing Reversion to Virulence in an Attenuated SARS-CoV for the Design of a Genetically Stable Vaccine. *PLoS Pathog.* **11**, e1005215 (2015).
22. Venkatagopalan, P., Daskalova, S. M., Lopez, L. A., Dolezal, K. A. & Hogue, B. G. Coronavirus envelope (E) protein remains at the site of assembly. *Virology* **478**, 75–85 (2015).
23. Tang, X. *et al.* BET bromodomain proteins mediate downstream signaling events following growth factor stimulation in human lung fibroblasts and are involved in bleomycin-induced pulmonary fibrosis. *Mol. Pharmacol.* **83**, 283–293 (2013).

24. Huang, B., Yang, X.-D., Zhou, M.-M., Ozato, K. & Chen, L.-F. Brd4 coactivates transcriptional activation of NF-kappaB via specific binding to acetylated RelA. *Mol. Cell. Biol.* **29**, 1375–1387 (2009).
25. Tian, B. *et al.* Selective Antagonists of the Bronchiolar Epithelial NF-κB-Bromodomain-Containing Protein 4 Pathway in Viral-Induced Airway Inflammation. *Cell Rep.* **23**, 1138–1151 (2018).
26. You, J., Croyle, J. L., Nishimura, A., Ozato, K. & Howley, P. M. Interaction of the bovine papillomavirus E2 protein with Brd4 tethers the viral DNA to host mitotic chromosomes. *Cell* **117**, 349–360 (2004).
27. Taniguchi, Y. The Bromodomain and Extra-Terminal Domain (BET) Family: Functional Anatomy of BET Paralogous Proteins. *Int. J. Mol. Sci.* **17**, (2016).
28. LeRoy, G., Rickards, B. & Flint, S. J. The double bromodomain proteins Brd2 and Brd3 couple histone acetylation to transcription. *Mol. Cell* **30**, 51–60 (2008).
29. Hsu, S. C. *et al.* The BET Protein BRD2 Cooperates with CTCF to Enforce Transcriptional and Architectural Boundaries. *Mol. Cell* **66**, 102–116.e7 (2017).
30. Faivre, E. J. *et al.* Selective inhibition of the BD2 bromodomain of BET proteins in prostate cancer. *Nature* **578**, 306–310 (2020).
31. Boehm, D., Conrad, R. J. & Ott, M. Bromodomain proteins in HIV infection. *Viruses* **5**, 1571–1586 (2013).
32. McBride, A. A. & Jang, M. K. Current understanding of the role of the Brd4 protein in the papillomavirus lifecycle. *Viruses* **5**, 1374–1394 (2013).
33. Robinson, M. S. & Bonifacino, J. S. Adaptor-related proteins. *Curr. Opin. Cell Biol.* **13**, 444–453 (2001).
34. Liu, L. *et al.* Defective HIV-1 particle assembly in AP-3-deficient cells derived from patients with Hermansky-Pudlak syndrome type 2. *J. Virol.* **86**, 11242–11253 (2012).
35. Jung, J. *et al.* Identification of a homozygous deletion in the AP3B1 gene causing Hermansky-Pudlak syndrome, type 2. *Blood* **108**, 362–369 (2006).
36. Li, M. *et al.* Identification of antiviral roles for the exon-junction complex and nonsense-mediated decay in flaviviral infection. *Nat Microbiol* **4**, 985–995 (2019).
37. Arndt, A. L., Larson, B. J. & Hogue, B. G. A conserved domain in the coronavirus membrane protein tail is important for virus assembly. *J. Virol.* **84**, 11418–11428 (2010).

38. Neuman, B. W. *et al.* A structural analysis of M protein in coronavirus assembly and morphology. *J. Struct. Biol.* **174**, 11–22 (2011).
39. Perrier, A. *et al.* The C-terminal domain of the MERS coronavirus M protein contains a trans-Golgi network localization signal. *J. Biol. Chem.* **294**, 14406–14421 (2019).
40. Pacciarini, F. *et al.* Persistent replication of severe acute respiratory syndrome coronavirus in human tubular kidney cells selects for adaptive mutations in the membrane protein. *J. Virol.* **82**, 5137–5144 (2008).
41. Fang, X. *et al.* The membrane protein of SARS-CoV suppresses NF-kappaB activation. *J. Med. Virol.* **79**, 1431–1439 (2007).
42. Siu, K.-L. *et al.* Severe acute respiratory syndrome coronavirus M protein inhibits type I interferon production by impeding the formation of TRAF3.TANK.TBK1/IKKepsilon complex. *J. Biol. Chem.* **284**, 16202–16209 (2009).
43. Chan, C.-M., Ma, C.-W., Chan, W.-Y. & Chan, H. Y. E. The SARS-Coronavirus Membrane protein induces apoptosis through modulating the Akt survival pathway. *Arch. Biochem. Biophys.* **459**, 197–207 (2007).
44. Tsoi, H. *et al.* The SARS-coronavirus membrane protein induces apoptosis via interfering with PDK1-PKB/Akt signalling. *Biochem. J* **464**, 439–447 (2014).
45. Tan, Y.-J., Lim, S. G. & Hong, W. Regulation of cell death during infection by the severe acute respiratory syndrome coronavirus and other coronaviruses. *Cell. Microbiol.* **9**, 2552–2561 (2007).
46. Appenzeller-Herzog, C. & Hauri, H.-P. The ER-Golgi intermediate compartment (ERGIC): in search of its identity and function. *J. Cell Sci.* **119**, 2173–2183 (2006).
47. Krishnan, M. N. *et al.* RNA interference screen for human genes associated with West Nile virus infection. *Nature* **455**, 242–245 (2008).
48. Karlas, A. *et al.* Genome-wide RNAi screen identifies human host factors crucial for influenza virus replication. *Nature* **463**, 818–822 (2010).
49. Orvedahl, A. *et al.* Image-based genome-wide siRNA screen identifies selective autophagy factors. *Nature* **480**, 113–117 (2011).

50. Ooi, Y. S., Stiles, K. M., Liu, C. Y., Taylor, G. M. & Kielian, M. Genome-wide RNAi screen identifies novel host proteins required for alphavirus entry. *PLoS Pathog.* **9**, e1003835 (2013).
51. Han, J. *et al.* Genome-wide CRISPR/Cas9 Screen Identifies Host Factors Essential for Influenza Virus Replication. *Cell Rep.* **23**, 596–607 (2018).
52. Li, B. *et al.* Genome-wide CRISPR screen identifies host dependency factors for influenza A virus infection. *Nat. Commun.* **11**, 164 (2020).
53. Wang, S., Tukachinsky, H., Romano, F. B. & Rapoport, T. A. Cooperation of the ER-shaping proteins atlastin, lunapark, and reticulons to generate a tubular membrane network. *Elife* **5**, (2016).
54. Yamamoto, Y., Yoshida, A., Miyazaki, N., Iwasaki, K. & Sakisaka, T. Arl6IP1 has the ability to shape the mammalian ER membrane in a reticulon-like fashion. *Biochem. J* **458**, 69–79 (2014).
55. Diaz, A., Wang, X. & Ahlquist, P. Membrane-shaping host reticulon proteins play crucial roles in viral RNA replication compartment formation and function. *Proc. Natl. Acad. Sci. U. S. A.* **107**, 16291–16296 (2010).
56. Chen, Y.-J., Williams, J. M., Arvan, P. & Tsai, B. Reticulon protects the integrity of the ER membrane during ER escape of large macromolecular protein complexes. *J. Cell Biol.* **219**, (2020).
57. Haenssler, E., Ramabhadran, V., Murphy, C. S., Heidtman, M. I. & Isberg, R. R. Endoplasmic Reticulum Tubule Protein Reticulon 4 Associates with the Legionella pneumophila Vacuole and with Translocated Substrate Ceg9. *Infect. Immun.* **83**, 3479–3489 (2015).
58. Hafirassou, M. L. *et al.* A Global Interactome Map of the Dengue Virus NS1 Identifies Virus Restriction and Dependency Host Factors. *Cell Rep.* **21**, 3900–3913 (2017).
59. Singh, C. R. *et al.* Mechanisms of translational regulation by a human eIF5-mimic protein. *Nucleic Acids Res.* **39**, 8314–8328 (2011).
60. Cheng, D.-D. *et al.* Downregulation of BZW2 inhibits osteosarcoma cell growth by inactivating the Akt/mTOR signaling pathway. *Oncol. Rep.* **38**, 2116–2122 (2017).
61. Jin, X., Liao, M., Zhang, L., Yang, M. & Zhao, J. Role of the novel gene BZW2 in the development of hepatocellular carcinoma. *J. Cell. Physiol.* (2019) doi:10.1002/jcp.28331.
62. Sato, K. *et al.* Novel oncogene 5MP1 reprograms c-Myc translation initiation to drive malignant

- phenotypes in colorectal cancer. *EBioMedicine* **44**, 387–402 (2019).
63. Wang, S., Bai, W., Huang, J., Lv, F. & Bai, H. Prognostic significance of BZW2 expression in lung adenocarcinoma patients. *Int. J. Clin. Exp. Pathol.* **12**, 4289–4296 (2019).
64. Gao, H. *et al.* BZW2 gene knockdown induces cell growth inhibition, G1 arrest and apoptosis in muscle-invasive bladder cancers: A microarray pathway analysis. *J. Cell. Mol. Med.* **23**, 3905–3915 (2019).
65. Park, C. R. *et al.* The accessory proteins REEP5 and REEP6 refine CXCR1-mediated cellular responses and lung cancer progression. *Sci. Rep.* **6**, 39041 (2016).
66. Warner, N., Burberry, A., Pliakas, M., McDonald, C. & Núñez, G. A genome-wide small interfering RNA (siRNA) screen reveals nuclear factor- κ B (NF- κ B)-independent regulators of NOD2-induced interleukin-8 (IL-8) secretion. *J. Biol. Chem.* **289**, 28213–28224 (2014).
67. Strieter, R. M., Kunkel, S. L., Keane, M. P. & Standiford, T. J. Chemokines in lung injury: Thomas A. Neff Lecture. *Chest* **116**, 103S–110S (1999).
68. Hu, Y. *et al.* Scramblase TMEM16F terminates T cell receptor signaling to restrict T cell exhaustion. *J. Exp. Med.* **213**, 2759–2772 (2016).
69. Wang, H. *et al.* SARS coronavirus entry into host cells through a novel clathrin- and caveolae-independent endocytic pathway. *Cell Res.* **18**, 290–301 (2008).
70. Ehlen, H. W. A. *et al.* Inactivation of anoctamin-6/Tmem16f, a regulator of phosphatidylserine scrambling in osteoblasts, leads to decreased mineral deposition in skeletal tissues. *J. Bone Miner. Res.* **28**, 246–259 (2013).
71. He, R. *et al.* Analysis of multimerization of the SARS coronavirus nucleocapsid protein. *Biochem. Biophys. Res. Commun.* **316**, 476–483 (2004).
72. Nelson, G. W., Stohlman, S. A. & Tahara, S. M. High affinity interaction between nucleocapsid protein and leader/intergenic sequence of mouse hepatitis virus RNA. *J. Gen. Virol.* **81**, 181–188 (2000).
73. Baric, R. S. *et al.* Interactions between coronavirus nucleocapsid protein and viral RNAs: implications for viral transcription. *J. Virol.* **62**, 4280–4287 (1988).

74. Raaben, M., Groot Koerkamp, M. J. A., Rottier, P. J. M. & de Haan, C. A. M. Mouse hepatitis coronavirus replication induces host translational shutoff and mRNA decay, with concomitant formation of stress granules and processing bodies. *Cell. Microbiol.* **9**, 2218–2229 (2007).
75. Wada, M., Lokugamage, K. G., Nakagawa, K., Narayanan, K. & Makino, S. Interplay between coronavirus, a cytoplasmic RNA virus, and nonsense-mediated mRNA decay pathway. *Proc. Natl. Acad. Sci. U. S. A.* **115**, E10157–E10166 (2018).
76. Surjit, M. *et al.* The severe acute respiratory syndrome coronavirus nucleocapsid protein is phosphorylated and localizes in the cytoplasm by 14-3-3-mediated translocation. *J. Virol.* **79**, 11476–11486 (2005).
77. V'kovski, P. *et al.* Determination of host proteins composing the microenvironment of coronavirus replicase complexes by proximity-labeling. *Elife* **8**, (2019).
78. Emmott, E. *et al.* The cellular interactome of the coronavirus infectious bronchitis virus nucleocapsid protein and functional implications for virus biology. *J. Virol.* **87**, 9486–9500 (2013).
79. Sun, N. *et al.* Proteomics Analysis of Cellular Proteins Co-Immunoprecipitated with Nucleoprotein of Influenza A Virus (H7N9). *Int. J. Mol. Sci.* **16**, 25982–25998 (2015).
80. White, J. P. & Lloyd, R. E. Poliovirus unlinks TIA1 aggregation and mRNA stress granule formation. *J. Virol.* **85**, 12442–12454 (2011).
81. Visser, L. J. *et al.* Foot-and-Mouth Disease Virus Leader Protease Cleaves G3BP1 and G3BP2 and Inhibits Stress Granule Formation. *J. Virol.* **93**, (2019).
82. Panas, M. D. *et al.* Sequestration of G3BP coupled with efficient translation inhibits stress granules in Semliki Forest virus infection. *Mol. Biol. Cell* **23**, 4701–4712 (2012).
83. Katsafanas, G. C. & Moss, B. Colocalization of transcription and translation within cytoplasmic poxvirus factories coordinates viral expression and subjugates host functions. *Cell Host Microbe* **2**, 221–228 (2007).
84. Borghese, F. & Michiels, T. The leader protein of cardioviruses inhibits stress granule assembly. *J. Virol.* **85**, 9614–9622 (2011).

85. Ward, A. M. *et al.* Quantitative mass spectrometry of DENV-2 RNA-interacting proteins reveals that the DEAD-box RNA helicase DDX6 binds the DB1 and DB2 3' UTR structures. *RNA Biol.* **8**, 1173–1186 (2011).
86. Bidet, K., Dadlani, D. & Garcia-Blanco, M. A. G3BP1, G3BP2 and CAPRIN1 are required for translation of interferon stimulated mRNAs and are targeted by a dengue virus non-coding RNA. *PLoS Pathog.* **10**, e1004242 (2014).
87. Kato, H. *et al.* Japanese encephalitis virus core protein inhibits stress granule formation through an interaction with Caprin-1 and facilitates viral propagation. *J. Virol.* **87**, 489–502 (2013).
88. Nelson, E. V. *et al.* Ebola Virus Does Not Induce Stress Granule Formation during Infection and Sequesters Stress Granule Proteins within Viral Inclusions. *J. Virol.* **90**, 7268–7284 (2016).
89. Nakagawa, K., Narayanan, K., Wada, M. & Makino, S. Inhibition of Stress Granule Formation by Middle East Respiratory Syndrome Coronavirus 4a Accessory Protein Facilitates Viral Translation, Leading to Efficient Virus Replication. *J. Virol.* **92**, (2018).
90. Brownsword, M. J., Doyle, N., Brocard, M., Locker, N. & Maier, H. J. Infectious bronchitis virus regulates cellular stress granule signaling. *bioRxiv* 819482 (2019) doi:10.1101/819482.
91. Chen, H. *et al.* Mass spectroscopic characterization of the coronavirus infectious bronchitis virus nucleoprotein and elucidation of the role of phosphorylation in RNA binding by using surface plasmon resonance. *J. Virol.* **79**, 1164–1179 (2005).
92. Reineke, L. C. *et al.* Casein Kinase 2 Is Linked to Stress Granule Dynamics through Phosphorylation of the Stress Granule Nucleating Protein G3BP1. *Mol. Cell. Biol.* **37**, (2017).
93. de Wilde, A. H. *et al.* A Kinome-Wide Small Interfering RNA Screen Identifies Proviral and Antiviral Host Factors in Severe Acute Respiratory Syndrome Coronavirus Replication, Including Double-Stranded RNA-Activated Protein Kinase and Early Secretory Pathway Proteins. *J. Virol.* **89**, 8318–8333 (2015).
94. Siddiqui-Jain, A. *et al.* CX-4945, an orally bioavailable selective inhibitor of protein kinase CK2, inhibits prosurvival and angiogenic signaling and exhibits antitumor efficacy. *Cancer Res.* **70**, 10288–10298 (2010).

95. Taiaroa, G. *et al.* Direct RNA sequencing and early evolution of SARS-CoV-2. *bioRxiv* 2020.03.05.976167 (2020) doi:10.1101/2020.03.05.976167.
96. Culbertson, M. R., Underbrink, K. M. & Fink, G. R. Frameshift suppression *Saccharomyces cerevisiae*. II. Genetic properties of group II suppressors. *Genetics* **95**, 833–853 (1980).
97. Philippe, L., van den Elzen, A. M. G., Watson, M. J. & Thoreen, C. C. Global analysis of LARP1 translation targets reveals tunable and dynamic features of 5' TOP motifs. *Proc. Natl. Acad. Sci. U. S. A.* **117**, 5319–5328 (2020).
98. McKinney, C., Yu, D. & Mohr, I. A new role for the cellular PABP repressor Paip2 as an innate restriction factor capable of limiting productive cytomegalovirus replication. *Genes Dev.* **27**, 1809–1820 (2013).
99. Le Sage, V., Cinti, A., Amorim, R. & Mouland, A. J. Adapting the Stress Response: Viral Subversion of the mTOR Signaling Pathway. *Viruses* **8**, (2016).
100. Dyal, J. *et al.* Middle East Respiratory Syndrome and Severe Acute Respiratory Syndrome: Current Therapeutic Options and Potential Targets for Novel Therapies. *Drugs* **77**, 1935–1966 (2017).
101. Kindrachuk, J. *et al.* Antiviral potential of ERK/MAPK and PI3K/AKT/mTOR signaling modulation for Middle East respiratory syndrome coronavirus infection as identified by temporal kinome analysis. *Antimicrob. Agents Chemother.* **59**, 1088–1099 (2015).
102. Wang, C.-H. *et al.* Adjuvant treatment with a mammalian target of rapamycin inhibitor, sirolimus, and steroids improves outcomes in patients with severe H1N1 pneumonia and acute respiratory failure. *Crit. Care Med.* **42**, 313–321 (2014).
103. Kumar, G. R. & Glaunsinger, B. A. Nuclear import of cytoplasmic poly(A) binding protein restricts gene expression via hyperadenylation and nuclear retention of mRNA. *Mol. Cell. Biol.* **30**, 4996–5008 (2010).
104. Suzuki, Y. *et al.* Characterization of RyDEN (C19orf66) as an Interferon-Stimulated Cellular Inhibitor against Dengue Virus Replication. *PLoS Pathog.* **12**, e1005357 (2016).
105. Hsu, C.-H. *et al.* Identification and Characterization of Potential Biomarkers by Quantitative Tissue Proteomics of Primary Lung Adenocarcinoma. *Mol. Cell. Proteomics* **15**, 2396–2410 (2016).
106. Gregersen, L. H. *et al.* MOV10 Is a 5' to 3' RNA helicase contributing to UPF1 mRNA target degradation

- by translocation along 3' UTRs. *Mol. Cell* **54**, 573–585 (2014).
107. Cuevas, R. A. *et al.* MOV10 Provides Antiviral Activity against RNA Viruses by Enhancing RIG-I-MAVS-Independent IFN Induction. *J. Immunol.* **196**, 3877–3886 (2016).
108. Balinsky, C. A. *et al.* IRAV (FLJ11286), an Interferon-Stimulated Gene with Antiviral Activity against Dengue Virus, Interacts with MOV10. *J. Virol.* **91**, (2017).
109. Zhao, K. *et al.* MOV10 inhibits replication of porcine reproductive and respiratory syndrome virus by retaining viral nucleocapsid protein in the cytoplasm of Marc-145 cells. *Biochem. Biophys. Res. Commun.* **504**, 157–163 (2018).
110. Li, J. *et al.* MOV10 sequesters the RNP of influenza A virus in the cytoplasm and is antagonized by viral NS1 protein. *Biochem. J* **476**, 467–481 (2019).
111. Ziebuhr, J. The coronavirus replicase. *Curr. Top. Microbiol. Immunol.* **287**, 57–94 (2005).
112. Wathelet, M. G., Orr, M., Frieman, M. B. & Baric, R. S. Severe acute respiratory syndrome coronavirus evades antiviral signaling: role of nsp1 and rational design of an attenuated strain. *J. Virol.* **81**, 11620–11633 (2007).
113. Law, A. H. Y., Lee, D. C. W., Cheung, B. K. W., Yim, H. C. H. & Lau, A. S. Y. Role for nonstructural protein 1 of severe acute respiratory syndrome coronavirus in chemokine dysregulation. *J. Virol.* **81**, 416–422 (2007).
114. Starokadomskyy, P. *et al.* DNA polymerase- α regulates the activation of type I interferons through cytosolic RNA:DNA synthesis. *Nat. Immunol.* **17**, 495–504 (2016).
115. Xu, L. H., Huang, M., Fang, S. G. & Liu, D. X. Coronavirus infection induces DNA replication stress partly through interaction of its nonstructural protein 13 with the p125 subunit of DNA polymerase δ . *J. Biol. Chem.* **286**, 39546–39559 (2011).
116. Wang, L. *et al.* Comparative influenza protein interactomes identify the role of plakophilin 2 in virus restriction. *Nat. Commun.* **8**, 13876 (2017).
117. Graham, R. L., Sims, A. C., Brockway, S. M., Baric, R. S. & Denison, M. R. The nsp2 replicase proteins of murine hepatitis virus and severe acute respiratory syndrome coronavirus are dispensable for viral

- replication. *J. Virol.* **79**, 13399–13411 (2005).
118. Graham, R. L., Sims, A. C., Baric, R. S. & Denison, M. R. The nsp2 proteins of mouse hepatitis virus and SARS coronavirus are dispensable for viral replication. *Adv. Exp. Med. Biol.* **581**, 67–72 (2006).
119. Viklund, I.-M. *et al.* WAFL, a new protein involved in regulation of early endocytic transport at the intersection of actin and microtubule dynamics. *Exp. Cell Res.* **315**, 1040–1052 (2009).
120. Derivery, E. *et al.* The Arp2/3 activator WASH controls the fission of endosomes through a large multiprotein complex. *Dev. Cell* **17**, 712–723 (2009).
121. Jia, D. *et al.* WASH and WAVE actin regulators of the Wiskott-Aldrich syndrome protein (WASP) family are controlled by analogous structurally related complexes. *Proc. Natl. Acad. Sci. U. S. A.* **107**, 10442–10447 (2010).
122. Morita, M. *et al.* A novel 4EHP-GIGYF2 translational repressor complex is essential for mammalian development. *Mol. Cell. Biol.* **32**, 3585–3593 (2012).
123. Fusco, D. N. *et al.* HELZ2 Is an IFN Effector Mediating Suppression of Dengue Virus. *Front. Microbiol.* **8**, 240 (2017).
124. Sakai, Y. *et al.* Two-amino acids change in the nsp4 of SARS coronavirus abolishes viral replication. *Virology* **510**, 165–174 (2017).
125. Oudshoorn, D. *et al.* Expression and Cleavage of Middle East Respiratory Syndrome Coronavirus nsp3-4 Polyprotein Induce the Formation of Double-Membrane Vesicles That Mimic Those Associated with Coronaviral RNA Replication. *MBio* **8**, (2017).
126. Beachboard, D. C., Anderson-Daniels, J. M. & Denison, M. R. Mutations across murine hepatitis virus nsp4 alter virus fitness and membrane modifications. *J. Virol.* **89**, 2080–2089 (2015).
127. Affholter, J. A., Hsieh, C. L., Francke, U. & Roth, R. A. Insulin-degrading enzyme: stable expression of the human complementary DNA, characterization of its protein product, and chromosomal mapping of the human and mouse genes. *Mol. Endocrinol.* **4**, 1125–1135 (1990).
128. Vekrellis, K. *et al.* Neurons regulate extracellular levels of amyloid beta-protein via proteolysis by insulin-degrading enzyme. *J. Neurosci.* **20**, 1657–1665 (2000).

129. Parmentier, N. *et al.* Production of an antigenic peptide by insulin-degrading enzyme. *Nat. Immunol.* **11**, 449–454 (2010).
130. Li, Q., Ali, M. A. & Cohen, J. I. Insulin degrading enzyme is a cellular receptor mediating varicella-zoster virus infection and cell-to-cell spread. *Cell* **127**, 305–316 (2006).
131. Li, Q., Krogmann, T., Ali, M. A., Tang, W.-J. & Cohen, J. I. The amino terminus of varicella-zoster virus (VZV) glycoprotein E is required for binding to insulin-degrading enzyme, a VZV receptor. *J. Virol.* **81**, 8525–8532 (2007).
132. Mühlenbein, N., Hofmann, S., Rothbauer, U. & Bauer, M. F. Organization and function of the small Tim complexes acting along the import pathway of metabolite carriers into mammalian mitochondria. *J. Biol. Chem.* **279**, 13540–13546 (2004).
133. Ioakeimidis, F. *et al.* A splicing mutation in the novel mitochondrial protein DNAJC11 causes motor neuron pathology associated with cristae disorganization, and lymphoid abnormalities in mice. *PLoS One* **9**, e104237 (2014).
134. Rind, N. *et al.* A severe human metabolic disease caused by deficiency of the endoplasmic mannosyltransferase hALG11 leads to congenital disorder of glycosylation-Ip. *Hum. Mol. Genet.* **19**, 1413–1424 (2010).
135. Thiel, C. *et al.* Improved diagnostics lead to identification of three new patients with congenital disorder of glycosylation-Ip. *Hum. Mutat.* **33**, 485–487 (2012).
136. Cohen, M., Feinstein, N., Wilson, K. L. & Gruenbaum, Y. Nuclear pore protein gp210 is essential for viability in HeLa cells and *Caenorhabditis elegans*. *Mol. Biol. Cell* **14**, 4230–4237 (2003).
137. Borlido, J. *et al.* Nuclear pore complex-mediated modulation of TCR signaling is required for naïve CD4⁺ T cell homeostasis. *Nat. Immunol.* **19**, 594–605 (2018).
138. Neuman, B. W., Chamberlain, P., Bowden, F. & Joseph, J. Atlas of coronavirus replicase structure. *Virus Res.* **194**, 49–66 (2014).
139. Ziebuhr, J., Snijder, E. J. & Gorbalenya, A. E. Virus-encoded proteinases and proteolytic processing in the Nidovirales. *J. Gen. Virol.* **81**, 853–879 (2000).

140. Barnes, P. J. Role of HDAC2 in the pathophysiology of COPD. *Annu. Rev. Physiol.* **71**, 451–464 (2009).
141. Angelini, M. M., Akhlaghpour, M., Neuman, B. W. & Buchmeier, M. J. Severe acute respiratory syndrome coronavirus nonstructural proteins 3, 4, and 6 induce double-membrane vesicles. *MBio* **4**, (2013).
142. Oostra, M. *et al.* Topology and membrane anchoring of the coronavirus replication complex: not all hydrophobic domains of nsp3 and nsp6 are membrane spanning. *J. Virol.* **82**, 12392–12405 (2008).
143. Lundin, A. *et al.* Targeting membrane-bound viral RNA synthesis reveals potent inhibition of diverse coronaviruses including the middle East respiratory syndrome virus. *PLoS Pathog.* **10**, e1004166 (2014).
144. Perlman, S. & Netland, J. Coronaviruses post-SARS: update on replication and pathogenesis. *Nat. Rev. Microbiol.* **7**, 439–450 (2009).
145. Hagemeyer, M. C., Rottier, P. J. M. & de Haan, C. A. M. Biogenesis and dynamics of the coronavirus replicative structures. *Viruses* **4**, 3245–3269 (2012).
146. Neuman, B. W. How the double spherules of infectious bronchitis virus impact our understanding of RNA virus replicative organelles. *mBio* vol. 4 e00987–13 (2013).
147. Knoops, K. *et al.* SARS-coronavirus replication is supported by a reticulovesicular network of modified endoplasmic reticulum. *PLoS Biol.* **6**, e226 (2008).
148. Cottam, E. M., Whelband, M. C. & Wileman, T. Coronavirus NSP6 restricts autophagosome expansion. *Autophagy* **10**, 1426–1441 (2014).
149. Munger, J., Bajad, S. U., Coller, H. A., Shenk, T. & Rabinowitz, J. D. Dynamics of the cellular metabolome during human cytomegalovirus infection. *PLoS Pathog.* **2**, e132 (2006).
150. Anand, S. K. & Tikoo, S. K. Viruses as modulators of mitochondrial functions. *Adv. Virol.* **2013**, 738794 (2013).
151. Baratta, M. G. Virus-mediated hijack of one-carbon metabolism. *Nature reviews. Cancer* vol. 19 486 (2019).
152. Fontaine, K. A., Sanchez, E. L., Camarda, R. & Lagunoff, M. Dengue virus induces and requires glycolysis for optimal replication. *J. Virol.* **89**, 2358–2366 (2015).
153. Garrus, J. E. *et al.* Tsg101 and the vacuolar protein sorting pathway are essential for HIV-1 budding. *Cell*

- 107**, 55–65 (2001).
- 154.Licata, J. M. *et al.* Overlapping motifs (PTAP and PPEY) within the Ebola virus VP40 protein function independently as late budding domains: involvement of host proteins TSG101 and VPS-4. *J. Virol.* **77**, 1812–1819 (2003).
- 155.Gorai, T. *et al.* F₁F_o-ATPase, F-type proton-translocating ATPase, at the plasma membrane is critical for efficient influenza virus budding. *Proc. Natl. Acad. Sci. U. S. A.* **109**, 4615–4620 (2012).
- 156.Forgac, M. Vacuolar ATPases: rotary proton pumps in physiology and pathophysiology. *Nat. Rev. Mol. Cell Biol.* **8**, 917–929 (2007).
- 157.König, R. *et al.* Human host factors required for influenza virus replication. *Nature* **463**, 813–817 (2010).
- 158.Banerjee, I., Yamauchi, Y., Helenius, A. & Horvath, P. High-content analysis of sequential events during the early phase of influenza A virus infection. *PLoS One* **8**, e68450 (2013).
- 159.Ochiai, H., Sakai, S., Hirabayashi, T., Shimizu, Y. & Terasawa, K. Inhibitory effect of bafilomycin A1, a specific inhibitor of vacuolar-type proton pump, on the growth of influenza A and B viruses in MDCK cells. *Antiviral Res.* **27**, 425–430 (1995).
- 160.Brass, A. L. *et al.* The IFITM proteins mediate cellular resistance to influenza A H1N1 virus, West Nile virus, and dengue virus. *Cell* **139**, 1243–1254 (2009).
- 161.Sessions, O. M. *et al.* Discovery of insect and human dengue virus host factors. *Nature* **458**, 1047–1050 (2009).
- 162.Jansen, E. J. R. *et al.* ATP6AP1 deficiency causes an immunodeficiency with hepatopathy, cognitive impairment and abnormal protein glycosylation. *Nat. Commun.* **7**, 11600 (2016).
- 163.Pareja, F. *et al.* Loss-of-function mutations in ATP6AP1 and ATP6AP2 in granular cell tumors. *Nat. Commun.* **9**, 3533 (2018).
- 164.Soh, T. K. *et al.* Herpes simplex virus-1 pUL56 degrades GOPC to alter the plasma membrane proteome. *bioRxiv* 729343 (2019) doi:10.1101/729343.
- 165.Matheson, N. J. *et al.* Cell Surface Proteomic Map of HIV Infection Reveals Antagonism of Amino Acid Metabolism by Vpu and Nef. *Cell Host Microbe* **18**, 409–423 (2015).

166. Lee, M. N. *et al.* Common genetic variants modulate pathogen-sensing responses in human dendritic cells. *Science* **343**, 1246980 (2014).
167. Gräf, S. *et al.* Identification of rare sequence variation underlying heritable pulmonary arterial hypertension. *Nat. Commun.* **9**, 1416 (2018).
168. Liu Bin *et al.* Abstract 14378: ATP13A3 Loss of Function Disrupts Polyamine Homeostasis in Pulmonary Arterial Endothelial Cells. *Circulation* **140**, A14378–A14378 (2019).
169. Subissi, L. *et al.* One severe acute respiratory syndrome coronavirus protein complex integrates processive RNA polymerase and exonuclease activities. *Proc. Natl. Acad. Sci. U. S. A.* **111**, E3900–9 (2014).
170. Kirchdoerfer, R. N. & Ward, A. B. Structure of the SARS-CoV nsp12 polymerase bound to nsp7 and nsp8 co-factors. *Nat. Commun.* **10**, 2342 (2019).
171. Zhai, Y. *et al.* Insights into SARS-CoV transcription and replication from the structure of the nsp7-nsp8 hexadecamer. *Nat. Struct. Mol. Biol.* **12**, 980–986 (2005).
172. te Velthuis, A. J. W., Arnold, J. J., Cameron, C. E., van den Worm, S. H. E. & Snijder, E. J. The RNA polymerase activity of SARS-coronavirus nsp12 is primer dependent. *Nucleic Acids Res.* **38**, 203–214 (2010).
173. te Velthuis, A. J. W., van den Worm, S. H. E. & Snijder, E. J. The SARS-coronavirus nsp7+nsp8 complex is a unique multimeric RNA polymerase capable of both de novo initiation and primer extension. *Nucleic Acids Res.* **40**, 1737–1747 (2012).
174. Gorbalenya, A. E. *et al.* The palm subdomain-based active site is internally permuted in viral RNA-dependent RNA polymerases of an ancient lineage. *J. Mol. Biol.* **324**, 47–62 (2002).
175. Lehmann, K. C. *et al.* Discovery of an essential nucleotidylating activity associated with a newly delineated conserved domain in the RNA polymerase-containing protein of all nidoviruses. *Nucleic Acids Res.* **43**, 8416–8434 (2015).
176. Brockway, S. M., Clay, C. T., Lu, X. T. & Denison, M. R. Characterization of the expression, intracellular localization, and replication complex association of the putative mouse hepatitis virus RNA-dependent

- RNA polymerase. *J. Virol.* **77**, 10515–10527 (2003).
177. Gao, Y. *et al.* Structure of RNA-dependent RNA polymerase from 2019-nCoV, a major antiviral drug target. *bioRxiv* 2020.03.16.993386 (2020) doi:10.1101/2020.03.16.993386.
178. Gurkan, C. *et al.* Large-scale profiling of Rab GTPase trafficking networks: the membrane. *Mol. Biol. Cell* **16**, 3847–3864 (2005).
179. Linford, A. *et al.* Rab14 and its exchange factor FAM116 link endocytic recycling and adherens junction stability in migrating cells. *Dev. Cell* **22**, 952–966 (2012).
180. Qi, M. *et al.* Rab11-FIP1C and Rab14 direct plasma membrane sorting and particle incorporation of the HIV-1 envelope glycoprotein complex. *PLoS Pathog.* **9**, e1003278 (2013).
181. Pechenick Jowers, T. *et al.* RAB1A promotes Vaccinia virus replication by facilitating the production of intracellular enveloped virions. *Virology* **475**, 66–73 (2015).
182. Lin, J. *et al.* Rab1A is required for assembly of classical swine fever virus particle. *Virology* **514**, 18–29 (2018).
183. Macovei, A., Petrareanu, C., Lazar, C., Florian, P. & Branza-Nichita, N. Regulation of hepatitis B virus infection by Rab5, Rab7, and the endolysosomal compartment. *J. Virol.* **87**, 6415–6427 (2013).
184. Inoue, J. *et al.* HBV secretion is regulated through the activation of endocytic and autophagic compartments mediated by Rab7 stimulation. *J. Cell Sci.* **128**, 1696–1706 (2015).
185. Bayliss, R., Wheeldon, J., Caucheteux, S. M., Niessen, C. M. & Piguet, V. Identification of host trafficking genes required for HIV-1 virological synapse formation in dendritic cells. *J. Virol.* (2020) doi:10.1128/JVI.01597-19.
186. Padanad, M. S. *et al.* Fatty Acid Oxidation Mediated by Acyl-CoA Synthetase Long Chain 3 Is Required for Mutant KRAS Lung Tumorigenesis. *Cell Rep.* **16**, 1614–1628 (2016).
187. Saliakoura, M. *et al.* The ACSL3-LPIAT1 signaling drives prostaglandin synthesis in non-small cell lung cancer. *Oncogene* (2020) doi:10.1038/s41388-020-1196-5.
188. Nchoutmboube, J. A. *et al.* Increased long chain acyl-Coa synthetase activity and fatty acid import is linked to membrane synthesis for development of picornavirus replication organelles. *PLoS Pathog.* **9**,

- e1003401 (2013).
189. Jäger, S. *et al.* Global landscape of HIV-human protein complexes. *Nature* **481**, 365–370 (2011).
190. Shah, P. S. *et al.* Comparative Flavivirus-Host Protein Interaction Mapping Reveals Mechanisms of Dengue and Zika Virus Pathogenesis. *Cell* **175**, 1931–1945.e18 (2018).
191. Ramage, H. R. *et al.* A combined proteomics/genomics approach links hepatitis C virus infection with nonsense-mediated mRNA decay. *Mol. Cell* **57**, 329–340 (2015).
192. Penn, B. H. *et al.* An Mtb-Human Protein-Protein Interaction Map Identifies a Switch between Host Antiviral and Antibacterial Responses. *Mol. Cell* **71**, 637–648.e5 (2018).
193. Sadat, M. A. *et al.* Glycosylation, hypogammaglobulinemia, and resistance to viral infections. *N. Engl. J. Med.* **370**, 1615–1625 (2014).
194. Huang, K.-H., Wang, C.-H., Lin, C.-H. & Kuo, H.-P. NF- κ B repressing factor downregulates basal expression and mycobacterium tuberculosis induced IP-10 and IL-8 synthesis via interference with NF- κ B in monocytes. *J. Biomed. Sci.* **21**, 71 (2014).
195. Huang, K.-H. *et al.* NF- κ B repressing factor inhibits chemokine synthesis by peripheral blood mononuclear cells and alveolar macrophages in active pulmonary tuberculosis. *PLoS One* **8**, e77789 (2013).
196. Sawicki, S. G. & Sawicki, D. L. Coronaviruses use discontinuous extension for synthesis of subgenome-length negative strands. *Adv. Exp. Med. Biol.* **380**, 499–506 (1995).
197. Hu, J. *et al.* AKAP95 regulates splicing through scaffolding RNAs and RNA processing factors. *Nat. Commun.* **7**, 13347 (2016).
198. Chua, K. & Reed, R. Human step II splicing factor hSlu7 functions in restructuring the spliceosome between the catalytic steps of splicing. *Genes Dev.* **13**, 841–850 (1999).
199. König, R. *et al.* Global analysis of host-pathogen interactions that regulate early-stage HIV-1 replication. *Cell* **135**, 49–60 (2008).
200. Schäffler, K. *et al.* A stimulatory role for the La-related protein 4B in translation. *RNA* **16**, 1488–1499 (2010).

201. Lin, Y. J., Liao, C. L. & Lai, M. M. Identification of the cis-acting signal for minus-strand RNA synthesis of a murine coronavirus: implications for the role of minus-strand RNA in RNA replication and transcription. *J. Virol.* **68**, 8131–8140 (1994).
202. Spagnolo, J. F. & Hogue, B. G. Host protein interactions with the 3' end of bovine coronavirus RNA and the requirement of the poly(A) tail for coronavirus defective genome replication. *J. Virol.* **74**, 5053–5065 (2000).
203. Cirillo, L. *et al.* UBAP2L Forms Distinct Cores that Act in Nucleating Stress Granules Upstream of G3BP1. *Curr. Biol.* **30**, 698–707.e6 (2020).
204. Kedersha, N. *et al.* Stress granules and processing bodies are dynamically linked sites of mRNP remodeling. *J. Cell Biol.* **169**, 871–884 (2005).
205. Jiang, H. *et al.* Regulation of transcription by the MLL2 complex and MLL complex-associated AKAP95. *Nat. Struct. Mol. Biol.* **20**, 1156–1163 (2013).
206. Cho, Y. S. *et al.* Phosphorylation-driven assembly of the RIP1-RIP3 complex regulates programmed necrosis and virus-induced inflammation. *Cell* **137**, 1112–1123 (2009).
207. Holler, N. *et al.* Fas triggers an alternative, caspase-8-independent cell death pathway using the kinase RIP as effector molecule. *Nat. Immunol.* **1**, 489–495 (2000).
208. Weinlich, R. & Green, D. R. The two faces of receptor interacting protein kinase-1. *Mol. Cell* **56**, 469–480 (2014).
209. Chaudhary, P. M., Jasmin, A., Eby, M. T. & Hood, L. Modulation of the NF-kappa B pathway by virally encoded death effector domains-containing proteins. *Oncogene* **18**, 5738–5746 (1999).
210. Dondelinger, Y. *et al.* Serine 25 phosphorylation inhibits RIPK1 kinase-dependent cell death in models of infection and inflammation. *Nat. Commun.* **10**, 1729 (2019).
211. Wagner, R. N., Reed, J. C. & Chanda, S. K. HIV-1 protease cleaves the serine-threonine kinases RIPK1 and RIPK2. *Retrovirology* **12**, 74 (2015).
212. Sheridan, C. Death by inflammation: drug makers chase the master controller. *Nat. Biotechnol.* **37**, 111–113 (2019).

213. Kamada, S., Kikkawa, U., Tsujimoto, Y. & Hunter, T. A-kinase-anchoring protein 95 functions as a potential carrier for the nuclear translocation of active caspase 3 through an enzyme-substrate-like association. *Mol. Cell. Biol.* **25**, 9469–9477 (2005).
214. Almazán, F., DeDiego, M. L., Galán, C., Alvarez, E. & Enjuanes, L. Identification of essential genes as a strategy to select a SARS candidate vaccine using a SARS-CoV infectious cDNA. *Adv. Exp. Med. Biol.* **581**, 579–583 (2006).
215. Xu, X. *et al.* New antiviral target revealed by the hexameric structure of mouse hepatitis virus nonstructural protein nsp15. *J. Virol.* **80**, 7909–7917 (2006).
216. Deng, X. *et al.* Coronavirus nonstructural protein 15 mediates evasion of dsRNA sensors and limits apoptosis in macrophages. *Proc. Natl. Acad. Sci. U. S. A.* **114**, E4251–E4260 (2017).
217. Paschal, B. M. & Gerace, L. Identification of NTF2, a cytosolic factor for nuclear import that interacts with nuclear pore complex protein p62. *J. Cell Biol.* **129**, 925–937 (1995).
218. Steggerda, S. M., Black, B. E. & Paschal, B. M. Monoclonal antibodies to NTF2 inhibit nuclear protein import by preventing nuclear translocation of the GTPase Ran. *Mol. Biol. Cell* **11**, 703–719 (2000).
219. Pasqualato, S., Ménétrey, J., Franco, M. & Cherfils, J. The structural GDP/GTP cycle of human Arf6. *EMBO Rep.* **2**, 234–238 (2001).
220. Selyunin, A. S. *et al.* The assembly of a GTPase-kinase signalling complex by a bacterial catalytic scaffold. *Nature* **469**, 107–111 (2011).
221. Ha, V. L. *et al.* ASAP3 is a focal adhesion-associated Arf GAP that functions in cell migration and invasion. *J. Biol. Chem.* **283**, 14915–14926 (2008).
222. D'Souza-Schorey, C. & Stahl, P. D. Myristoylation is required for the intracellular localization and endocytic function of ARF6. *Exp. Cell Res.* **221**, 153–159 (1995).
223. Fang, Z. *et al.* Proteomic identification and functional characterization of a novel ARF6 GTPase-activating protein, ACAP4. *Mol. Cell. Proteomics* **5**, 1437–1449 (2006).
224. O'Neal, C. J., Jobling, M. G., Holmes, R. K. & Hol, W. G. J. Structural basis for the activation of cholera toxin by human ARF6-GTP. *Science* **309**, 1093–1096 (2005).

225. Wang, C. *et al.* The E3 ubiquitin ligase Nrdp1 'preferentially' promotes TLR-mediated production of type I interferon. *Nat. Immunol.* **10**, 744–752 (2009).
226. Miknis, Z. J. *et al.* Severe acute respiratory syndrome coronavirus nsp9 dimerization is essential for efficient viral growth. *J. Virol.* **83**, 3007–3018 (2009).
227. Egloff, M.-P. *et al.* The severe acute respiratory syndrome-coronavirus replicative protein nsp9 is a single-stranded RNA-binding subunit unique in the RNA virus world. *Proc. Natl. Acad. Sci. U. S. A.* **101**, 3792–3796 (2004).
228. Ponnusamy, R., Moll, R., Weimar, T., Mesters, J. R. & Hilgenfeld, R. Variable oligomerization modes in coronavirus non-structural protein 9. *J. Mol. Biol.* **383**, 1081–1096 (2008).
229. Sutton, G. *et al.* The nsp9 replicase protein of SARS-coronavirus, structure and functional insights. *Structure* **12**, 341–353 (2004).
230. von Brunn, A. *et al.* Analysis of intraviral protein-protein interactions of the SARS coronavirus ORFome. *PLoS One* **2**, e459 (2007).
231. Sharma, A., Solmaz, S. R., Blobel, G. & Melčák, I. Ordered Regions of Channel Nucleoporins Nup62, Nup54, and Nup58 Form Dynamic Complexes in Solution. *J. Biol. Chem.* **290**, 18370–18378 (2015).
232. Dewangan, P. S., Sonawane, P. J., Chouksey, A. R. & Chauhan, R. The Nup62 Coiled-Coil Motif Provides Plasticity for Triple-Helix Bundle Formation. *Biochemistry* **56**, 2803–2811 (2017).
233. Ulrich, A., Partridge, J. R. & Schwartz, T. U. The stoichiometry of the nucleoporin 62 subcomplex of the nuclear pore in solution. *Mol. Biol. Cell* **25**, 1484–1492 (2014).
234. Solmaz, S. R., Blobel, G. & Melčák, I. Ring cycle for dilating and constricting the nuclear pore. *Proc. Natl. Acad. Sci. U. S. A.* **110**, 5858–5863 (2013).
235. Chug, H., Trakhanov, S., Hülsmann, B. B., Pleiner, T. & Görlich, D. Crystal structure of the metazoan Nup62•Nup58•Nup54 nucleoporin complex. *Science* **350**, 106–110 (2015).
236. Beck, M. & Hurt, E. The nuclear pore complex: understanding its function through structural insight. *Nat. Rev. Mol. Cell Biol.* **18**, 73–89 (2017).
237. Wang, B., Zhang, X. & Zhao, Z. Validation-based insertional mutagenesis for identification of Nup214 as a

- host factor for EV71 replication in RD cells. *Biochem. Biophys. Res. Commun.* **437**, 452–456 (2013).
238. Di Nunzio, F. *et al.* Human nucleoporins promote HIV-1 docking at the nuclear pore, nuclear import and integration. *PLoS One* **7**, e46037 (2012).
239. Malik, P. *et al.* Herpes simplex virus ICP27 protein directly interacts with the nuclear pore complex through Nup62, inhibiting host nucleocytoplasmic transport pathways. *J. Biol. Chem.* **287**, 12277–12292 (2012).
240. Park, N., Skern, T. & Gustin, K. E. Specific cleavage of the nuclear pore complex protein Nup62 by a viral protease. *J. Biol. Chem.* **285**, 28796–28805 (2010).
241. Watters, K. *et al.* Differential Disruption of Nucleocytoplasmic Trafficking Pathways by Rhinovirus 2A Proteases. *J. Virol.* **91**, (2017).
242. Zhang Y.-Z. *et al.* [The 2A protease of enterovirus 71 cleaves nup62 to inhibit nuclear transport]. *Bing Du Xue Bao* **29**, 421–425 (2013).
243. Watters, K. & Palmenberg, A. C. Differential processing of nuclear pore complex proteins by rhinovirus 2A proteases from different species and serotypes. *J. Virol.* **85**, 10874–10883 (2011).
244. Walker, E. J. *et al.* Rhinovirus 3C protease facilitates specific nucleoporin cleavage and mislocalisation of nuclear proteins in infected host cells. *PLoS One* **8**, e71316 (2013).
245. Castelló, A., Izquierdo, J. M., Welnowska, E. & Carrasco, L. RNA nuclear export is blocked by poliovirus 2A protease and is concomitant with nucleoporin cleavage. *J. Cell Sci.* **122**, 3799–3809 (2009).
246. Park, N., Katikaneni, P., Skern, T. & Gustin, K. E. Differential targeting of nuclear pore complex proteins in poliovirus-infected cells. *J. Virol.* **82**, 1647–1655 (2008).
247. Porter, F. W. & Palmenberg, A. C. Leader-induced phosphorylation of nucleoporins correlates with nuclear trafficking inhibition by cardioviruses. *J. Virol.* **83**, 1941–1951 (2009).
248. Bardina, M. V. *et al.* Mengovirus-induced rearrangement of the nuclear pore complex: hijacking cellular phosphorylation machinery. *J. Virol.* **83**, 3150–3161 (2009).
249. Porter, F. W., Brown, B. & Palmenberg, A. C. Nucleoporin phosphorylation triggered by the encephalomyocarditis virus leader protein is mediated by mitogen-activated protein kinases. *J. Virol.* **84**,

- 12538–12548 (2010).
250. Khuperkar, D. *et al.* Selective recruitment of nucleoporins on vaccinia virus factories and the role of Nup358 in viral infection. *Virology* **512**, 151–160 (2017).
251. Chang, C.-W. *et al.* Epstein-Barr virus protein kinase BGLF4 targets the nucleus through interaction with nucleoporins. *J. Virol.* **86**, 8072–8085 (2012).
252. Eberhard, J., Onder, Z. & Moroianu, J. Nuclear import of high risk HPV16 E7 oncoprotein is mediated by its zinc-binding domain via hydrophobic interactions with Nup62. *Virology* **446**, 334–345 (2013).
253. Onder, Z. & Moroianu, J. Nuclear import of cutaneous beta genus HPV8 E7 oncoprotein is mediated by hydrophobic interactions between its zinc-binding domain and FG nucleoporins. *Virology* **449**, 150–162 (2014).
254. Ao, Z. *et al.* Contribution of host nucleoporin 62 in HIV-1 integrase chromatin association and viral DNA integration. *J. Biol. Chem.* **287**, 10544–10555 (2012).
255. Tafforeau, L. *et al.* Generation and comprehensive analysis of an influenza virus polymerase cellular interaction network. *J. Virol.* **85**, 13010–13018 (2011).
256. Bauer, M. *et al.* The E3 Ubiquitin Ligase Mind Bomb 1 Controls Adenovirus Genome Release at the Nuclear Pore Complex. *Cell Rep.* **29**, 3785–3795.e8 (2019).
257. Fry, A. M., O'Regan, L., Sabir, S. R. & Bayliss, R. Cell cycle regulation by the NEK family of protein kinases. *J. Cell Sci.* **125**, 4423–4433 (2012).
258. Jung, R., Radko, S. & Pelka, P. The Dual Nature of Nek9 in Adenovirus Replication. *J. Virol.* **90**, 1931–1943 (2016).
259. Jin, J., Arias, E. E., Chen, J., Harper, J. W. & Walter, J. C. A family of diverse Cul4-Ddb1-interacting proteins includes Cdt2, which is required for S phase destruction of the replication factor Cdt1. *Mol. Cell* **23**, 709–721 (2006).
260. Zemke, N. R. & Berk, A. J. The Adenovirus E1A C Terminus Suppresses a Delayed Antiviral Response and Modulates RAS Signaling. *Cell Host Microbe* **22**, 789–800.e5 (2017).
261. Feng, P., Everly, D. N., Jr & Read, G. S. mRNA decay during herpes simplex virus (HSV) infections:

- protein-protein interactions involving the HSV virion host shutoff protein and translation factors eIF4H and eIF4A. *J. Virol.* **79**, 9651–9664 (2005).
262. Doepker, R. C., Hsu, W.-L., Saffran, H. A. & Smiley, J. R. Herpes simplex virus virion host shutoff protein is stimulated by translation initiation factors eIF4B and eIF4H. *J. Virol.* **78**, 4684–4699 (2004).
263. Sarma, N., Agarwal, D., Shiflett, L. A. & Read, G. S. Small interfering RNAs that deplete the cellular translation factor eIF4H impede mRNA degradation by the virion host shutoff protein of herpes simplex virus. *J. Virol.* **82**, 6600–6609 (2008).
264. Teo, C. S. H. & O'Hare, P. A bimodal switch in global protein translation coupled to eIF4H relocalisation during advancing cell-cell transmission of herpes simplex virus. *PLoS Pathog.* **14**, e1007196 (2018).
265. Yin, W. *et al.* Fibrillin-2 is a key mediator of smooth muscle extracellular matrix homeostasis during mouse tracheal tubulogenesis. *Eur. Respir. J.* **53**, (2019).
266. Uriarte, J. J. *et al.* Early Impairment of Lung Mechanics in a Murine Model of Marfan Syndrome. *PLoS One* **11**, e0152124 (2016).
267. Kuang, P.-P. *et al.* Coordinate expression of fibulin-5/DANCE and elastin during lung injury repair. *Am. J. Physiol. Lung Cell. Mol. Physiol.* **285**, L1147–52 (2003).
268. Jean, J.-C., Eruchalu, I., Cao, Y. X. & Joyce-Brady, M. DANCE in developing and injured lung. *Am. J. Physiol. Lung Cell. Mol. Physiol.* **282**, L75–82 (2002).
269. Dabovic, B. *et al.* Function of latent TGF β binding protein 4 and fibulin 5 in elastogenesis and lung development. *J. Cell. Physiol.* **230**, 226–236 (2015).
270. Brandsma, C.-A. *et al.* A large lung gene expression study identifying fibulin-5 as a novel player in tissue repair in COPD. *Thorax* **70**, 21–32 (2015).
271. Albig, A. R. & Schiemann, W. P. Fibulin-5 antagonizes vascular endothelial growth factor (VEGF) signaling and angiogenic sprouting by endothelial cells. *DNA Cell Biol.* **23**, 367–379 (2004).
272. Chen, X. *et al.* Fibulin-5 inhibits Wnt/ β -catenin signaling in lung cancer. *Oncotarget* **6**, 15022–15034 (2015).
273. Joseph, J. S. *et al.* Crystal structure of nonstructural protein 10 from the severe acute respiratory

- syndrome coronavirus reveals a novel fold with two zinc-binding motifs. *J. Virol.* **80**, 7894–7901 (2006).
274. Siddell, S., Sawicki, D., Meyer, Y., Thiel, V. & Sawicki, S. Identification of the mutations responsible for the phenotype of three MHV RNA-negative ts mutants. *Adv. Exp. Med. Biol.* **494**, 453–458 (2001).
275. Chen, Y. *et al.* Biochemical and structural insights into the mechanisms of SARS coronavirus RNA ribose 2'-O-methylation by nsp16/nsp10 protein complex. *PLoS Pathog.* **7**, e1002294 (2011).
276. Su, D. *et al.* Dodecamer structure of severe acute respiratory syndrome coronavirus nonstructural protein nsp10. *J. Virol.* **80**, 7902–7908 (2006).
277. Buffalo, C. Z. *et al.* Structural Basis for Tetherin Antagonism as a Barrier to Zoonotic Lentiviral Transmission. *Cell Host Microbe* **26**, 359–368.e8 (2019).
278. Buffalo, C. Z., Iwamoto, Y., Hurley, J. H. & Ren, X. How HIV Nef Proteins Hijack Membrane Traffic To Promote Infection. *J. Virol.* **93**, (2019).
279. Breuza, L. *et al.* Proteomics of endoplasmic reticulum-Golgi intermediate compartment (ERGIC) membranes from brefeldin A-treated HepG2 cells identifies ERGIC-32, a new cycling protein that interacts with human Erv46. *J. Biol. Chem.* **279**, 47242–47253 (2004).
280. Choglay, A. A., Chapple, J. P., Blatch, G. L. & Cheetham, M. E. Identification and characterization of a human mitochondrial homologue of the bacterial co-chaperone GrpE. *Gene* **267**, 125–134 (2001).
281. Magnuson, B. *et al.* ERp29 triggers a conformational change in polyomavirus to stimulate membrane binding. *Mol. Cell* **20**, 289–300 (2005).
282. Sevajol, M., Subissi, L., Decroly, E., Canard, B. & Imbert, I. Insights into RNA synthesis, capping, and proofreading mechanisms of SARS-coronavirus. *Virus Res.* **194**, 90–99 (2014).
283. Chen, Y. & Guo, D. Molecular mechanisms of coronavirus RNA capping and methylation. *Virol. Sin.* **31**, 3–11 (2016).
284. Gu, M. & Lima, C. D. Processing the message: structural insights into capping and decapping mRNA. *Curr. Opin. Struct. Biol.* **15**, 99–106 (2005).
285. Ramanathan, A., Robb, G. B. & Chan, S.-H. mRNA capping: biological functions and applications. *Nucleic Acids Res.* **44**, 7511–7526 (2016).

286. Enjuanes, L., Almazán, F., Sola, I. & Zuñiga, S. Biochemical aspects of coronavirus replication and virus-host interaction. *Annu. Rev. Microbiol.* **60**, 211–230 (2006).
287. Menachery, V. D., Debbink, K. & Baric, R. S. Coronavirus non-structural protein 16: evasion, attenuation, and possible treatments. *Virus Res.* **194**, 191–199 (2014).
288. Desai, P., Sexton, G. L., Huang, E. & Person, S. Localization of herpes simplex virus type 1 UL37 in the Golgi complex requires UL36 but not capsid structures. *J. Virol.* **82**, 11354–11361 (2008).
289. Miorin, L., Maiuri, P., Hoenninger, V. M., Mandl, C. W. & Marcello, A. Spatial and temporal organization of tick-borne encephalitis flavivirus replicated RNA in living cells. *Virology* **379**, 64–77 (2008).
290. Sehgal, P. B. *et al.* Golgi dysfunction is a common feature in idiopathic human pulmonary hypertension and vascular lesions in SHIV-nef-infected macaques. *Am. J. Physiol. Lung Cell. Mol. Physiol.* **297**, L729–37 (2009).
291. Rivero, S., Cardenas, J., Bornens, M. & Rios, R. M. Microtubule nucleation at the cis-side of the Golgi apparatus requires AKAP450 and GM130. *EMBO J.* **28**, 1016–1028 (2009).
292. Terrin, A. *et al.* PKA and PDE4D3 anchoring to AKAP9 provides distinct regulation of cAMP signals at the centrosome. *J. Cell Biol.* **198**, 607–621 (2012).
293. Wu, J. *et al.* Molecular Pathway of Microtubule Organization at the Golgi Apparatus. *Dev. Cell* **39**, 44–60 (2016).
294. Wang, Z., Zhang, C. & Qi, R. Z. A newly identified myomegalin isoform functions in Golgi microtubule organization and ER-Golgi transport. *J. Cell Sci.* **127**, 4904–4917 (2014).
295. Witczak, O. *et al.* Cloning and characterization of a cDNA encoding an A-kinase anchoring protein located in the centrosome, AKAP450. *EMBO J.* **18**, 1858–1868 (1999).
296. Greer, Y. E. *et al.* Casein kinase 1δ functions at the centrosome and Golgi to promote ciliogenesis. *Mol. Biol. Cell* **25**, 1629–1640 (2014).
297. Hurtado, L. *et al.* Disconnecting the Golgi ribbon from the centrosome prevents directional cell migration and ciliogenesis. *J. Cell Biol.* **193**, 917–933 (2011).
298. Subramanian, A. *et al.* Auto-regulation of Secretory Flux by Sensing and Responding to the Folded Cargo

- Protein Load in the Endoplasmic Reticulum. *Cell* **176**, 1461–1476.e23 (2019).
- 299.Tenorio, M. J., Luchsinger, C. & Mardones, G. A. Protein kinase A activity is necessary for fission and fusion of Golgi to endoplasmic reticulum retrograde tubules. *PLoS One* **10**, e0135260 (2015).
- 300.Huang, Z.-X., Wang, H., Wang, Y.-M. & Wang, Y. Novel mechanism coupling cyclic AMP-protein kinase A signaling and golgi trafficking via Gyp1 phosphorylation in polarized growth. *Eukaryot. Cell* **13**, 1548–1556 (2014).
- 301.Cancino, J. *et al.* Control systems of membrane transport at the interface between the endoplasmic reticulum and the Golgi. *Dev. Cell* **30**, 280–294 (2014).
- 302.Kolobova, E. *et al.* Microtubule-dependent association of AKAP350A and CCAR1 with RNA stress granules. *Exp. Cell Res.* **315**, 542–555 (2009).
- 303.Khadka, S. *et al.* A physical interaction network of dengue virus and human proteins. *Mol. Cell. Proteomics* **10**, M111.012187 (2011).
- 304.Hidajat, R. *et al.* Hepatitis C virus NS3 protein interacts with ELKS- δ and ELKS- α , members of a novel protein family involved in intracellular transport and secretory pathways. *J. Gen. Virol.* **86**, 2197–2208 (2005).
- 305.McCormick, D., Lin, Y.-T. & Grey, F. Identification of Host Factors Involved in Human Cytomegalovirus Replication, Assembly, and Egress Using a Two-Step Small Interfering RNA Screen. *MBio* **9**, (2018).
- 306.Amemiya, T., Gromiha, M. M., Horimoto, K. & Fukui, K. Drug repositioning for dengue haemorrhagic fever by integrating multiple omics analyses. *Sci. Rep.* **9**, 523 (2019).
- 307.Eckerle, L. D. *et al.* Infidelity of SARS-CoV Nsp14-exonuclease mutant virus replication is revealed by complete genome sequencing. *PLoS Pathog.* **6**, e1000896 (2010).
- 308.Ma, Y. *et al.* Structural basis and functional analysis of the SARS coronavirus nsp14-nsp10 complex. *Proc. Natl. Acad. Sci. U. S. A.* **112**, 9436–9441 (2015).
- 309.Lukas, J. *et al.* Functional and Clinical Consequences of Novel α -Galactosidase A Mutations in Fabry Disease. *Hum. Mutat.* **37**, 43–51 (2016).
- 310.McCafferty, E. H. & Scott, L. J. Migalastat: A Review in Fabry Disease. *Drugs* **79**, 543–554 (2019).

311. Peng, C. *et al.* The first identification of lysine malonylation substrates and its regulatory enzyme. *Mol. Cell. Proteomics* **10**, M111.012658 (2011).
312. Du, J. *et al.* Sirt5 is a NAD-dependent protein lysine demalonylase and desuccinylase. *Science* **334**, 806–809 (2011).
313. Tan, M. *et al.* Lysine glutarylation is a protein posttranslational modification regulated by SIRT5. *Cell Metab.* **19**, 605–617 (2014).
314. Yang, X. *et al.* SHMT2 Desuccinylation by SIRT5 Drives Cancer Cell Proliferation. *Cancer Res.* **78**, 372–386 (2018).
315. Fischer, F. *et al.* Sirt5 deacylation activities show differential sensitivities to nicotinamide inhibition. *PLoS One* **7**, e45098 (2012).
316. Carr, S. F., Papp, E., Wu, J. C. & Natsumeda, Y. Characterization of human type I and type II IMP dehydrogenases. *J. Biol. Chem.* **268**, 27286–27290 (1993).
317. Hedstrom, L., Liechti, G., Goldberg, J. B. & Gollapalli, D. R. The antibiotic potential of prokaryotic IMP dehydrogenase inhibitors. *Curr. Med. Chem.* **18**, 1909–1918 (2011).
318. Tan, Y.-J. *et al.* A novel severe acute respiratory syndrome coronavirus protein, U274, is transported to the cell surface and undergoes endocytosis. *J. Virol.* **78**, 6723–6734 (2004).
319. Siu, K.-L. *et al.* Severe acute respiratory syndrome coronavirus ORF3a protein activates the NLRP3 inflammasome by promoting TRAF3-dependent ubiquitination of ASC. *FASEB J.* **33**, 8865–8877 (2019).
320. Yount, B. *et al.* Severe acute respiratory syndrome coronavirus group-specific open reading frames encode nonessential functions for replication in cell cultures and mice. *J. Virol.* **79**, 14909–14922 (2005).
321. McBride, R. & Fielding, B. C. The role of severe acute respiratory syndrome (SARS)-coronavirus accessory proteins in virus pathogenesis. *Viruses* **4**, 2902–2923 (2012).
322. Padhan, K., Minakshi, R., Towheed, M. A. B. & Jameel, S. Severe acute respiratory syndrome coronavirus 3a protein activates the mitochondrial death pathway through p38 MAP kinase activation. *J. Gen. Virol.* **89**, 1960–1969 (2008).
323. Yue, Y. *et al.* SARS-Coronavirus Open Reading Frame-3a drives multimodal necrotic cell death. *Cell*

- Death Dis.* **9**, 904 (2018).
324. Tan, Y.-J. *et al.* The severe acute respiratory syndrome coronavirus 3a protein up-regulates expression of fibrinogen in lung epithelial cells. *J. Virol.* **79**, 10083–10087 (2005).
325. Narayanan, K., Huang, C. & Makino, S. SARS coronavirus accessory proteins. *Virus Res.* **133**, 113–121 (2008).
326. Ito, N. *et al.* Severe acute respiratory syndrome coronavirus 3a protein is a viral structural protein. *J. Virol.* **79**, 3182–3186 (2005).
327. Minakshi, R. *et al.* The SARS Coronavirus 3a protein causes endoplasmic reticulum stress and induces ligand-independent downregulation of the type 1 interferon receptor. *PLoS One* **4**, e8342 (2009).
328. Minakshi, R. & Padhan, K. The YXXΦ motif within the severe acute respiratory syndrome coronavirus (SARS-CoV) 3a protein is crucial for its intracellular transport. *Viol. J.* **11**, 75 (2014).
329. Lu, W. *et al.* Severe acute respiratory syndrome-associated coronavirus 3a protein forms an ion channel and modulates virus release. *Proc. Natl. Acad. Sci. U. S. A.* **103**, 12540–12545 (2006).
330. Balderhaar, H. J. K. & Ungermann, C. CORVET and HOPS tethering complexes - coordinators of endosome and lysosome fusion. *J. Cell Sci.* **126**, 1307–1316 (2013).
331. Jiang, P. *et al.* The HOPS complex mediates autophagosome-lysosome fusion through interaction with syntaxin 17. *Mol. Biol. Cell* **25**, 1327–1337 (2014).
332. Dunn, L. L. *et al.* New insights into intracellular locations and functions of heme oxygenase-1. *Antioxid. Redox Signal.* **20**, 1723–1742 (2014).
333. Lee, T.-S. & Chau, L.-Y. Heme oxygenase-1 mediates the anti-inflammatory effect of interleukin-10 in mice. *Nat. Med.* **8**, 240–246 (2002).
334. Piantadosi, C. A. *et al.* Heme oxygenase-1 couples activation of mitochondrial biogenesis to anti-inflammatory cytokine expression. *J. Biol. Chem.* **286**, 16374–16385 (2011).
335. Skrzypek, K. *et al.* Interplay between heme oxygenase-1 and miR-378 affects non-small cell lung carcinoma growth, vascularization, and metastasis. *Antioxid. Redox Signal.* **19**, 644–660 (2013).
336. Chen, L.-H., Liao, C.-Y., Lai, L.-C., Tsai, M.-H. & Chuang, E. Y. Semaphorin 6A Attenuates the Migration

- Capability of Lung Cancer Cells via the NRF2/HMOX1 Axis. *Sci. Rep.* **9**, 13302 (2019).
337. Singh, N., Ahmad, Z., Baid, N. & Kumar, A. Host heme oxygenase-1: Friend or foe in tackling pathogens? *IUBMB Life* **70**, 869–880 (2018).
338. Kumar, A. *et al.* Heme oxygenase-1-derived carbon monoxide induces the Mycobacterium tuberculosis dormancy regulon. *J. Biol. Chem.* **283**, 18032–18039 (2008).
339. Jia, Y., Jucius, T. J., Cook, S. A. & Ackerman, S. L. Loss of Clcc1 results in ER stress, misfolded protein accumulation, and neurodegeneration. *J. Neurosci.* **35**, 3001–3009 (2015).
340. Chu, Q. *et al.* Regulation of the ER stress response by a mitochondrial microprotein. *Nat. Commun.* **10**, 4883 (2019).
341. Irvin, M. R. *et al.* Genes linked to energy metabolism and immunoregulatory mechanisms are associated with subcutaneous adipose tissue distribution in HIV-infected men. *Pharmacogenet. Genomics* **21**, 798–807 (2011).
342. Wu, W. *et al.* The interactome of the human respiratory syncytial virus NS1 protein highlights multiple effects on host cell biology. *J. Virol.* **86**, 7777–7789 (2012).
343. Hubel, P. *et al.* A protein-interaction network of interferon-stimulated genes extends the innate immune system landscape. *Nat. Immunol.* **20**, 493–502 (2019).
344. Song, F. *et al.* Regulation and biological role of the peptide/histidine transporter SLC15A3 in Toll-like receptor-mediated inflammatory responses in macrophage. *Cell Death Dis.* **9**, 770 (2018).
345. Eckhardt, M. *et al.* Multiple Routes to Oncogenesis Are Promoted by the Human Papillomavirus-Host Protein Network. *Cancer Discov.* **8**, 1474–1489 (2018).
346. Wu, J. Q. *et al.* Transcriptional profiles in CD8+ T cells from HIV+ progressors on HAART are characterized by coordinated up-regulation of oxidative phosphorylation enzymes and interferon responses. *Virology* **380**, 124–135 (2008).
347. Zhou, P., Li, H., Wang, H., Wang, L.-F. & Shi, Z. Bat severe acute respiratory syndrome-like coronavirus ORF3b homologues display different interferon antagonist activities. *J. Gen. Virol.* **93**, 275–281 (2012).
348. Kopecky-Bromberg, S. A., Martínez-Sobrido, L., Frieman, M., Baric, R. A. & Palese, P. Severe acute

- respiratory syndrome coronavirus open reading frame (ORF) 3b, ORF 6, and nucleocapsid proteins function as interferon antagonists. *J. Virol.* **81**, 548–557 (2007).
349. Too, I. H. K., Bonne, I., Tan, E. L., Chu, J. J. H. & Alonso, S. Prohibitin plays a critical role in Enterovirus 71 neuropathogenesis. *PLoS Pathog.* **14**, e1006778 (2018).
350. Wai, T. *et al.* The membrane scaffold SLP2 anchors a proteolytic hub in mitochondria containing PARL and the i-AAA protease YME1L. *EMBO Rep.* **17**, 1844–1856 (2016).
351. Kirchhof, M. G. *et al.* Modulation of T cell activation by stomatin-like protein 2. *J. Immunol.* **181**, 1927–1936 (2008).
352. Zhao, J. *et al.* Severe acute respiratory syndrome coronavirus protein 6 is required for optimal replication. *J. Virol.* **83**, 2368–2373 (2009).
353. Zhou, H. *et al.* The N-terminal region of severe acute respiratory syndrome coronavirus protein 6 induces membrane rearrangement and enhances virus replication. *J. Virol.* **84**, 3542–3551 (2010).
354. Calvo, E. *et al.* Severe acute respiratory syndrome coronavirus accessory proteins 6 and 9b interact in vivo. *Virus Res.* **169**, 282–288 (2012).
355. Quan, B., Seo, H.-S., Blobel, G. & Ren, Y. Vesiculoviral matrix (M) protein occupies nucleic acid binding site at nucleoporin pair (Rae1 • Nup98). *Proc. Natl. Acad. Sci. U. S. A.* **111**, 9127–9132 (2014).
356. Faria, P. A. *et al.* VSV disrupts the Rae1/mrnp41 mRNA nuclear export pathway. *Mol. Cell* **17**, 93–102 (2005).
357. Nelson, C. A., Pekosz, A., Lee, C. A., Diamond, M. S. & Fremont, D. H. Structure and intracellular targeting of the SARS-coronavirus Orf7a accessory protein. *Structure* **13**, 75–85 (2005).
358. Tan, Y.-J. *et al.* Overexpression of 7a, a protein specifically encoded by the severe acute respiratory syndrome coronavirus, induces apoptosis via a caspase-dependent pathway. *J. Virol.* **78**, 14043–14047 (2004).
359. Yuan, X. *et al.* SARS coronavirus 7a protein blocks cell cycle progression at G0/G1 phase via the cyclin D3/pRb pathway. *Virology* **346**, 74–85 (2006).
360. Fielding, B. C. *et al.* Characterization of a unique group-specific protein (U122) of the severe acute

- respiratory syndrome coronavirus. *J. Virol.* **78**, 7311–7318 (2004).
361. Barraud, P., Banerjee, S., Mohamed, W. I., Jantsch, M. F. & Allain, F. H.-T. A bimodular nuclear localization signal assembled via an extended double-stranded RNA-binding domain acts as an RNA-sensing signal for transportin 1. *Proc. Natl. Acad. Sci. U. S. A.* **111**, E1852–61 (2014).
362. Arnold, M., Nath, A., Hauber, J. & Kehlenbach, R. H. Multiple importins function as nuclear transport receptors for the Rev protein of human immunodeficiency virus type 1. *J. Biol. Chem.* **281**, 20883–20890 (2006).
363. Miyake, Y. *et al.* Influenza virus uses transportin 1 for vRNP debundling during cell entry. *Nat Microbiol* **4**, 578–586 (2019).
364. Gagné, B., Tremblay, N., Park, A. Y., Baril, M. & Lamarre, D. Importin β 1 targeting by hepatitis C virus NS3/4A protein restricts IRF3 and NF- κ B signaling of IFNB1 antiviral response. *Traffic* **18**, 362–377 (2017).
365. Zhang, W. *et al.* Extended haplotype association study in Crohn's disease identifies a novel, Ashkenazi Jewish-specific missense mutation in the NF- κ B pathway gene, HEATR3. *Genes Immun.* **14**, 310–316 (2013).
366. Caruso, R., Warner, N., Inohara, N. & Núñez, G. NOD1 and NOD2: signaling, host defense, and inflammatory disease. *Immunity* **41**, 898–908 (2014).
367. Dediego, M. L. *et al.* Pathogenicity of severe acute respiratory coronavirus deletion mutants in hACE-2 transgenic mice. *Virology* **376**, 379–389 (2008).
368. Lau, S. K. P. *et al.* Severe acute respiratory syndrome coronavirus-like virus in Chinese horseshoe bats. *Proc. Natl. Acad. Sci. U. S. A.* **102**, 14040–14045 (2005).
369. Song, H.-D. *et al.* Cross-host evolution of severe acute respiratory syndrome coronavirus in palm civet and human. *Proc. Natl. Acad. Sci. U. S. A.* **102**, 2430–2435 (2005).
370. Lau, S. K. P. *et al.* Severe Acute Respiratory Syndrome (SARS) Coronavirus ORF8 Protein Is Acquired from SARS-Related Coronavirus from Greater Horseshoe Bats through Recombination. *J. Virol.* **89**, 10532–10547 (2015).

371. Oostra, M., de Haan, C. A. M. & Rottier, P. J. M. The 29-nucleotide deletion present in human but not in animal severe acute respiratory syndrome coronaviruses disrupts the functional expression of open reading frame 8. *J. Virol.* **81**, 13876–13888 (2007).
372. Shi, C.-S., Nabar, N. R., Huang, N.-N. & Kehrl, J. H. SARS-Coronavirus Open Reading Frame-8b triggers intracellular stress pathways and activates NLRP3 inflammasomes. *Cell Death Discov* **5**, 101 (2019).
373. Le, T. M. *et al.* Expression, post-translational modification and biochemical characterization of proteins encoded by subgenomic mRNA8 of the severe acute respiratory syndrome coronavirus. *FEBS J.* **274**, 4211–4222 (2007).
374. Hosokawa, N., Kamiya, Y., Kamiya, D., Kato, K. & Nagata, K. Human OS-9, a lectin required for glycoprotein endoplasmic reticulum-associated degradation, recognizes mannose-trimmed N-glycans. *J. Biol. Chem.* **284**, 17061–17068 (2009).
375. Suzuki, T., Huang, C. & Fujihira, H. The cytoplasmic peptide:N-glycanase (NGLY1) - Structure, expression and cellular functions. *Gene* **577**, 1–7 (2016).
376. Hirao, K. *et al.* EDEM3, a soluble EDEM homolog, enhances glycoprotein endoplasmic reticulum-associated degradation and mannose trimming. *J. Biol. Chem.* **281**, 9650–9658 (2006).
377. Arnold, S. M. & Kaufman, R. J. The noncatalytic portion of human UDP-glucose: glycoprotein glucosyltransferase I confers UDP-glucose binding and transferase function to the catalytic domain. *J. Biol. Chem.* **278**, 43320–43328 (2003).
378. Riemer, J. *et al.* A luminal flavoprotein in endoplasmic reticulum-associated degradation. *Proc. Natl. Acad. Sci. U. S. A.* **106**, 14831–14836 (2009).
379. Saeed, M. *et al.* Role of the endoplasmic reticulum-associated degradation (ERAD) pathway in degradation of hepatitis C virus envelope proteins and production of virus particles. *J. Biol. Chem.* **286**, 37264–37273 (2011).
380. Davis, Z. H. *et al.* Global mapping of herpesvirus-host protein complexes reveals a transcription strategy for late genes. *Mol. Cell* **57**, 349–360 (2015).
381. Ye, J. *et al.* Molecular pathology in the lungs of severe acute respiratory syndrome patients. *Am. J.*

- Pathol.* **170**, 538–545 (2007).
382. Staab-Weijnitz, C. A. *et al.* FK506-Binding Protein 10, a Potential Novel Drug Target for Idiopathic Pulmonary Fibrosis. *Am. J. Respir. Crit. Care Med.* **192**, 455–467 (2015).
383. Kim, Y.-I. *et al.* Epithelial cell-derived cytokines CST3 and GDF15 as potential therapeutics for pulmonary fibrosis. *Cell Death Dis.* **9**, 506 (2018).
384. Luzina, I. G. *et al.* Elevated expression of NEU1 sialidase in idiopathic pulmonary fibrosis provokes pulmonary collagen deposition, lymphocytosis, and fibrosis. *Am. J. Physiol. Lung Cell. Mol. Physiol.* **310**, L940–54 (2016).
385. Gurczynski, S. J. & Moore, B. B. IL-17 in the lung: the good, the bad, and the ugly. *Am. J. Physiol. Lung Cell. Mol. Physiol.* **314**, L6–L16 (2018).
386. Liu L. *et al.* [miR-21 promotes pulmonary fibrosis in rats via down-regulating the expression of ADAMTS-1]. *Xi Bao Yu Fen Zi Mian Yi Xue Za Zhi* **32**, 1636–1640 (2016).
387. Lu, J., Auduong, L., White, E. S. & Yue, X. Up-regulation of heparan sulfate 6-O-sulfation in idiopathic pulmonary fibrosis. *Am. J. Respir. Cell Mol. Biol.* **50**, 106–114 (2014).
388. Mi, S. *et al.* Blocking IL-17A promotes the resolution of pulmonary inflammation and fibrosis via TGF-beta1-dependent and -independent mechanisms. *J. Immunol.* **187**, 3003–3014 (2011).
389. Otsuka, Y., Kedersha, N. L. & Schoenberg, D. R. Identification of a cytoplasmic complex that adds a cap onto 5'-monophosphate RNA. *Mol. Cell. Biol.* **29**, 2155–2167 (2009).
390. Trotman, J. B. & Schoenberg, D. R. A recap of RNA recapping. *Wiley Interdiscip. Rev. RNA* **10**, e1504 (2019).
391. Qiu, M. *et al.* Antibody responses to individual proteins of SARS coronavirus and their neutralization activities. *Microbes Infect.* **7**, 882–889 (2005).
392. Chan, W. S. *et al.* Coronaviral hypothetical and structural proteins were found in the intestinal surface enterocytes and pneumocytes of severe acute respiratory syndrome (SARS). *Mod. Pathol.* **18**, 1432–1439 (2005).
393. Sharma, K. *et al.* SARS-CoV 9b protein diffuses into nucleus, undergoes active Crm1 mediated

- nucleocytoplasmic export and triggers apoptosis when retained in the nucleus. *PLoS One* **6**, e19436 (2011).
394. Shi, C.-S. *et al.* SARS-coronavirus open reading frame-9b suppresses innate immunity by targeting mitochondria and the MAVS/TRAF3/TRAF6 signalosome. *J. Immunol.* **193**, 3080–3089 (2014).
395. Liu, X.-Y., Wei, B., Shi, H.-X., Shan, Y.-F. & Wang, C. Tom70 mediates activation of interferon regulatory factor 3 on mitochondria. *Cell Res.* **20**, 994–1011 (2010).
396. Wei, B. *et al.* Tom70 mediates Sendai virus-induced apoptosis on mitochondria. *J. Virol.* **89**, 3804–3818 (2015).
397. De Snoo, M. L. *et al.* Bcl-2-associated athanogene 5 (BAG5) regulates Parkin-dependent mitophagy and cell death. *Cell Death Dis.* **10**, 907 (2019).
398. Zhang, L., Qin, Y. & Chen, M. Viral strategies for triggering and manipulating mitophagy. *Autophagy* **14**, 1665–1673 (2018).
399. Vietri, M. *et al.* Spastin and ESCRT-III coordinate mitotic spindle disassembly and nuclear envelope sealing. *Nature* **522**, 231–235 (2015).
400. Morita, E. *et al.* ESCRT-III protein requirements for HIV-1 budding. *Cell Host Microbe* **9**, 235–242 (2011).
401. Bartusch, C. & Prange, R. ESCRT Requirements for Murine Leukemia Virus Release. *Viruses* **8**, 103 (2016).
402. Gu, G. J. *et al.* Role of individual MARK isoforms in phosphorylation of tau at Ser²⁶² in Alzheimer's disease. *Neuromolecular Med.* **15**, 458–469 (2013).
403. Malikov, V. & Naghavi, M. H. Localized Phosphorylation of a Kinesin-1 Adaptor by a Capsid-Associated Kinase Regulates HIV-1 Motility and Uncoating. *Cell Rep.* **20**, 2792–2799 (2017).
404. Wu, F. *et al.* A new coronavirus associated with human respiratory disease in China. *Nature* (2020) doi:10.1038/s41586-020-2008-3.
405. Inberg, A. & Linial, M. Evolutional insights on uncharacterized SARS coronavirus genes. *FEBS Lett.* **577**, 159–164 (2004).
406. Shukla, A. & Hilgenfeld, R. Acquisition of new protein domains by coronaviruses: analysis of overlapping

- genes coding for proteins N and 9b in SARS coronavirus. *Virus Genes* **50**, 29–38 (2015).
407. Marra, M. A. *et al.* The Genome sequence of the SARS-associated coronavirus. *Science* **300**, 1399–1404 (2003).
408. Stroud, D. A. *et al.* Accessory subunits are integral for assembly and function of human mitochondrial complex I. *Nature* **538**, 123–126 (2016).
409. Dunning, C. J. R. *et al.* Human CIA30 is involved in the early assembly of mitochondrial complex I and mutations in its gene cause disease. *EMBO J.* **26**, 3227–3237 (2007).
410. Nouws, J. *et al.* Acyl-CoA dehydrogenase 9 is required for the biogenesis of oxidative phosphorylation complex I. *Cell Metab.* **12**, 283–294 (2010).
411. Ohishi, K., Inoue, N. & Kinoshita, T. PIG-S and PIG-T, essential for GPI anchor attachment to proteins, form a complex with GAA1 and GPI8. *EMBO J.* **20**, 4088–4098 (2001).
412. Csernok, E. *et al.* Wegener autoantigen induces maturation of dendritic cells and licenses them for Th1 priming via the protease-activated receptor-2 pathway. *Blood* **107**, 4440–4448 (2006).
413. Chiu, L.-L., Perng, D.-W., Yu, C.-H., Su, S.-N. & Chow, L.-P. Mold allergen, pen C 13, induces IL-8 expression in human airway epithelial cells by activating protease-activated receptor 1 and 2. *J. Immunol.* **178**, 5237–5244 (2007).
414. Goon Goh, F. *et al.* G-protein-dependent and -independent pathways regulate proteinase-activated receptor-2 mediated p65 NFkappaB serine 536 phosphorylation in human keratinocytes. *Cell. Signal.* **20**, 1267–1274 (2008).
415. Rallabhandi, P. *et al.* Analysis of proteinase-activated receptor 2 and TLR4 signal transduction: a novel paradigm for receptor cooperativity. *J. Biol. Chem.* **283**, 24314–24325 (2008).
416. Su, X., Camerer, E., Hamilton, J. R., Coughlin, S. R. & Matthay, M. A. Protease-activated receptor-2 activation induces acute lung inflammation by neuropeptide-dependent mechanisms. *J. Immunol.* **175**, 2598–2605 (2005).
417. Feld, M. *et al.* Agonists of proteinase-activated receptor-2 enhance IFN-gamma-inducible effects on human monocytes: role in influenza A infection. *J. Immunol.* **180**, 6903–6910 (2008).

418. Antoniak, S. & Mackman, N. Multiple roles of the coagulation protease cascade during virus infection. *Blood* **123**, 2605–2613 (2014).
419. Allen, I. C. *et al.* NLRX1 protein attenuates inflammatory responses to infection by interfering with the RIG-I-MAVS and TRAF6-NF- κ B signaling pathways. *Immunity* **34**, 854–865 (2011).
420. Cole, S. P. C. Multidrug resistance protein 1 (MRP1, ABCC1), a ‘multitasking’ ATP-binding cassette (ABC) transporter. *J. Biol. Chem.* **289**, 30880–30888 (2014).
421. Jorajuria, S., Dereuddre-Bosquet, N., Naissant-Storck, K., Dormont, D. & Clayette, P. Differential expression levels of MRP1, MRP4, and MRP5 in response to human immunodeficiency virus infection in human macrophages. *Antimicrob. Agents Chemother.* **48**, 1889–1891 (2004).
422. He, H. *et al.* Polarized macrophage subsets differentially express the drug efflux transporters MRP1 and BCRP, resulting in altered HIV production. *Antivir. Chem. Chemother.* **26**, 2040206617745168 (2018).
423. Weekes, M. P. *et al.* Latency-associated degradation of the MRP1 drug transporter during latent human cytomegalovirus infection. *Science* **340**, 199–202 (2013).
424. Srinivas, R. V., Middlemas, D., Flynn, P. & Fridland, A. Human immunodeficiency virus protease inhibitors serve as substrates for multidrug transporter proteins MDR1 and MRP1 but retain antiviral efficacy in cell lines expressing these transporters. *Antimicrob. Agents Chemother.* **42**, 3157–3162 (1998).
425. Young, L. C., Campling, B. G., Cole, S. P., Deeley, R. G. & Gerlach, J. H. Multidrug resistance proteins MRP3, MRP1, and MRP2 in lung cancer: correlation of protein levels with drug response and messenger RNA levels. *Clin. Cancer Res.* **7**, 1798–1804 (2001).
426. Okamura, T., Kikuchi, T., Okada, M., Wakizaka, H. & Zhang, M.-R. Imaging of activity of multidrug resistance-associated protein 1 in the lungs. *Am. J. Respir. Cell Mol. Biol.* **49**, 335–340 (2013).
427. Budulac, S. E. *et al.* Multidrug resistance-associated protein-1 (MRP1) genetic variants, MRP1 protein levels and severity of COPD. *Respir. Res.* **11**, 60 (2010).
428. Zukauskas, A. *et al.* Transporters MRP1 and MRP2 Regulate Opposing Inflammatory Signals To Control Transepithelial Neutrophil Migration during *Streptococcus pneumoniae* Lung Infection. *mSphere* **3**, (2018).

429. Odon, V., Georgana, I., Holley, J., Morata, J. & Maluquer de Motes, C. Novel Class of Viral Ankyrin Proteins Targeting the Host E3 Ubiquitin Ligase Cullin-2. *J. Virol.* **92**, (2018).
430. Westrich, J. A. *et al.* Human Papillomavirus 16 E7 Stabilizes APOBEC3A Protein by Inhibiting Cullin 2-Dependent Protein Degradation. *J. Virol.* **92**, (2018).
431. Timms, R. T. *et al.* A glycine-specific N-degron pathway mediates the quality control of protein N-myristoylation. *Science* **365**, (2019).

Supplemental methods

Supplemental Figure 1 Method: All MS runs were compared and clustered using standard artMS (<https://github.com/biodavidjm/artMS>) procedures on observed feature intensities computed by MaxQuant. Supplemental Figure 1 shows all Pearson's pairwise correlations between MS runs, and are clustered according to similar correlation patterns.

Supplemental Figure 2 Method: See main text.

Supplemental Figure 3 Method: PFAM domain enrichment analysis. The enrichment of individual PFAM domains (or PFAM clans)(El-Gebali et al. 2019) was calculated with a hypergeometric test where success is defined as number of domains, and the number of trials is the number of individual preys pulled-down with each viral bait. The population values were the numbers of individual PFAM domains and clans in the human proteome. To make sure that the p-values that signify enrichment were meaningful, we only considered PFAM domains that have been pulled-down at least three times with any SARS-CoV-2 protein, and which occur in the human proteome at least five times. In SI Figure 3 we show PFAM domains/clans with the lowest p-value for a given viral bait protein.

Supplemental Figure 4 and 5 Method: Expression analysis of interacting genes. We used GTEx (version 8, median gene-level transcripts per million (TPM) by tissue), which consisted of 17382 samples (578 lung samples)(Melé et al. 2015) to examine the mRNA expression of all interacting proteins (n=323). The comparison gene group was all RefSeq genes (n=24,491). The lung expression values represent the median expression of each gene across the GTEx lung samples. The lung enrichment values are calculated by dividing the median expression of each gene in lung tissue by the median expression of each gene across all tissues (including lung). A value of greater than one indicates that the gene expression is enriched in lung tissue. Values were plotted on a log₁₀ scale. All figures and statistics were produced in Python3 and code and reference tables can be found at: (https://github.com/stephaniewanko/Fraser_Lab/tree/master/QCRG_COVID19).

Supplemental Figure 6 Method: Conservation analysis of interacting genes. We used gnomAD version 2.1(Karczewski et al. 2019), which consists of 125,748 exomes and 15,708 genomes, to determine human genetic variation observed in the interacting proteins (n=323) versus all Refseq genes (n=24,491). Briefly the observed/expected ratio per gene indicates the number of observed variants of that type divided by the number of expected mutations of that type, with a lower observed/expected ratio indicating strong intolerance toward mutation. The number of expected variants were estimated based on the number of CpG and non-CpG transitions observed across the genome(Karczewski et al. 2019). All figures and statistics were produced in Python3 and code and reference tables can be found at: (https://github.com/stephaniewanko/Fraser_Lab/tree/master/QCRG_COVID19).

Supplemental Figure 7 Method: Nsp5 main protease (3Clpro) cleavage prediction. We used sequence specificity data for SARS nsp5(Goetz et al. 2007) (98.7% identical to SARS-CoV-2 nsp5) and NetCorona(Kiemer et al. 2004) to predict cleavage sites within interacting factors. PDB ID: 1UJ1 served as template for peptide docking which was performed using the predicted P4-P1 residues (BioLuminate, Schrödinger, LLC). Illustration of the docked model was generated in PyMol (Schrödinger, LLC).

Supplemental Figure 8 Method: Orf6 consensus sequence analysis. Orf6 sequence homologs were identified using the BLAST tool(Johnson et al. 2008) (accession number YP_009724394.1), run with the default settings: gap opening and extension costs of 11 and 1, respectively, BLOSUM62 as the scoring matrix, and an e-value threshold of 10. The search yielded 34 homologous sequences. The multiple sequence alignment was visualized using the MView web server: <https://www.ebi.ac.uk/Tools/msa/mview/> (Brown, Leroy, and Sander 1998) and the WebLogo server (<https://weblogo.berkeley.edu/logo.cgi>)(Crooks et al. 2004).

Supplemental Table 1 Method: See main text.

Supplemental Table 2 Method: See main text.

Supplementary Methods References

- Brown, N. P., C. Leroy, and C. Sander. 1998. "MView: A Web-Compatible Database Search or Multiple Alignment Viewer." *Bioinformatics* 14 (4): 380–81. <https://doi.org/10.1093/bioinformatics/14.4.380>.
- Crooks, Gavin E., Gary Hon, John-Marc Chandonia, and Steven E. Brenner. 2004. "WebLogo: A Sequence Logo Generator." *Genome Research* 14 (6): 1188–90. <https://doi.org/10.1101/gr.849004>.
- El-Gebali, Sara, Jaina Mistry, Alex Bateman, Sean R. Eddy, Aurélien Luciani, Simon C. Potter, Matloob Qureshi, et al. 2019. "The Pfam Protein Families Database in 2019." *Nucleic Acids Research* 47 (D1): D427–32. <https://doi.org/10.1093/nar/gky995>.
- Goetz, D. H., Y. Choe, E. Hansell, Y. T. Chen, M. McDowell, C. B. Jonsson, W. R. Roush, J. McKerrow, and C. S. Craik. 2007. "Substrate Specificity Profiling and Identification of a New Class of Inhibitor for the Major Protease of the SARS Coronavirus." *Biochemistry* 46 (30): 8744–52. <https://doi.org/10.1021/bi0621415>.
- Johnson, Mark, Irena Zaretskaya, Yan Raytselis, Yuri Merezuk, Scott McGinnis, and Thomas L. Madden. 2008. "NCBI BLAST: A Better Web Interface." *Nucleic Acids Research* 36 (Web Server issue): W5–9. <https://doi.org/10.1093/nar/gkn201>.
- Karczewski, Konrad J., Laurent C. Francioli, Grace Tiao, Beryl B. Cummings, Jessica Alfoldi, Qingbo Wang, Ryan L. Collins, et al. 2019. "Variation across 141,456 Human Exomes and Genomes Reveals the Spectrum of Loss-of-Function Intolerance across Human Protein-Coding Genes." *bioRxiv*. <https://doi.org/10.1101/531210>.
- Kiemer, Lars, Ole Lund, Søren Brunak, and Nikolaj Blom. 2004. "Coronavirus 3CLpro Proteinase Cleavage Sites: Possible Relevance to SARS Virus Pathology." *BMC Bioinformatics* 5 (June): 72. <https://doi.org/10.1186/1471-2105-5-72>.
- Melé, Marta, Pedro G. Ferreira, Ferran Reverter, David S. DeLuca, Jean Monlong, Michael Sammeth, Taylor R. Young, et al. 2015. "Human Genomics. The Human Transcriptome across Tissues and Individuals." *Science* 348 (6235): 660–65. <https://doi.org/10.1126/science.aaa0355>.